UNIVERSITÀ DI PARMA

UNIVERSITA' DEGLI STUDI DI PARMA

DOTTORATO DI RICERCA IN

"Scienze del Farmaco, delle Biomoloecole e dei Prodotti per la Salute"

Ciclo XXXIII

Synthesis of new potential inhibitors for the enzyme *N*-Acylethanolamine Acid Amidase and investigation of substrate specificity

Coordinatore

Chiar.mo Prof. Marco Mor

Tutor

Chiar.mo Prof. Daniele Piomelli

Dottorando: Andrea Ghidini

Anni Accademici 2017/2018 – 2019/2020

Acknowledgement

First of all, I want to express my deepest gratitude to Professor Daniele Piomelli. Working in his lab with him has been an incredible experience and a great occasion of improvement for me. I really appreciated every lesson that I could learn, and I wish I'll reach the same level of enthusiasm he showed everyday.

Along with him, I want to show my greatest appreciation to the coordinator Professor Marco Mor for the constant presence in my education, helping me to develop my attitude and ability in scientific research.

I then want to thank Professor Silvia Rivara and Professor Alessio Lodola, for their constant support during my years as a Ph.D. student in Parma.

A big thank goes to Dr. Riccardo Castelli, constantly involved in the synthetic part of the project. I'm grateful for all the knowledge that he shared with me about his experience in chemistry and laboratory techniques.

I want to show my deep appreciation to Dr. Laura Scalvini, for the infinite patience demonstrated in helping me during these years. With her, I want to thank Dr. Donatella Callegari, Dr. Martina Maccesi, Dr. Francesca Ferlenghi, Dr. Nicole Bozza, Dr. Giuseppe Marseglia, and the tomorrow doctors Gianmarco Elisi and Lorenzo Guidetti, later inserted in the group. I'm grateful for the time I spent with all of you in and out of the lab, and I wish the best to all of you.

My deepest gratitude goes to Dr. Kwang-Mook Jung, for being a constant positive figure during my time in Piomelli's Lab, and Dr. Faizy Ahmed for the time and the patience dedicated to my education in analytical techniques.

I want to reserve special thanks to Dr. Francesca Palese for the big help in the development of biochemical analyses, and for taking care of the biological part of NAAA project with me.
Big thanks also to Dr. Lin Lin, Dr. Yannik Fotio, Dr. Hyelim Lee and Dr. Alex Mabou Tagne and Alexa Torrens for the time they spent with me, making me feel at home, while I was on the other side of the world; an extra thank goes to Alexa for managing my lab orders.
In the end I want to say thanks to all the students that were involved on my projects: Alessia Di Domizio, Jennifer Ferrara, Rossella Urselli and Marina Cisquella Serra, and to the students that I met during these 3 years.

Table of contents

1. Fatty Acid Ethanolamides

Starting from the discovery of anandamide (arachidonoylethanolamide) in 1992[1] as prime ligand of Cannabinoid Receptors, the interest in this class of molecules and lipidic signaling has grown fast. This led to the disclosure of an entire family of bioactive molecules, ubiquitously produced and released in the body of all mammals,[2] each one with its peculiar cellular target and effect on the body homeostasis.

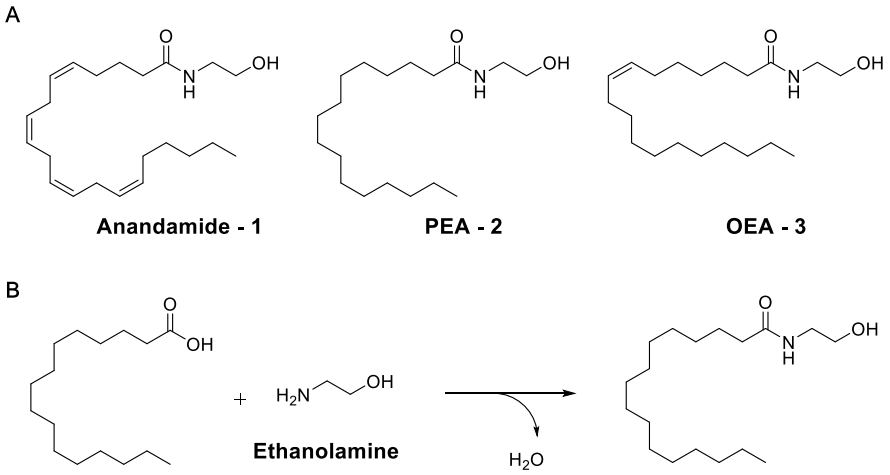

Figure 1: *A) Representation of the structures of the three most important FAEs B) the ideal condensation between palmitic acid and ethanolamine to obtain PEA.*

To the molecules included in this class of lipidic signals was given the name of fatty acid ethanolamides (**FAEs**, also known as N-acylethanolamines, **NAEs**):[3] the name of the family is due to the common structure of these compounds, that can be described as the product of a condensation between a molecule of a fatty acid and a molecule of ethanolamine (2-aminoethanol) by an amide bond. In Figure 1 are shown the chemical

structures of the most known and abundant FAEs in human body, that are the endocannabinoid Anandamide (arachidonoylethanolamide or **AEA**, compound **1**),[1] the analgesic and anti-inflammatory Palmitoylethanolamide (**PEA,** compound **2**)[4,5] and the feeding regulator Oleoylethanolamide (**OEA**, compound **3**).[6,7,8] The FAEs family is part of a wider group of fatty acid amides, in which the fatty acid moiety remains almost unaltered, while the polar head is peculiar of each class: examples of these molecules are *N*-acyltaurines (**NATs**), where the fatty acid is condensed with a taurine (2-aminoethansulfonic acid), involved in skin wound healing[9] and glucose homeostasis,[10,11] and *N*-acylglycines, with the amino acid glycine that replace the ethanolamine portion, involved in vasorelaxation[12] and modulation of electrical signals, acting on T-channel currents.[13,14]

1.1.Anandamide

Anandamide was discovered and characterized by Mechoulam and co-workers from porcine brain in 1992,[1] and today is the most known and the most studied molecule from the FAEs family. The name "Anandamide" comes from the Sanskrit word "Ananda" that literally means "internal bliss", to underline the inhibitory effects on pain processes[4,15,16] due to the activity of this substance. **AEA** is part of a group of polyunsaturated fatty acid derivatives called "endocannabinoids", named after their ability to bind and to activate the same receptors activated by ∆-9-Tetrahydrocannabinol (**THC**)[17], that is one of the most known bioactive compounds from *Cannabis sativa*, along with Cannabidiol (**CBD**) (Figure 2).

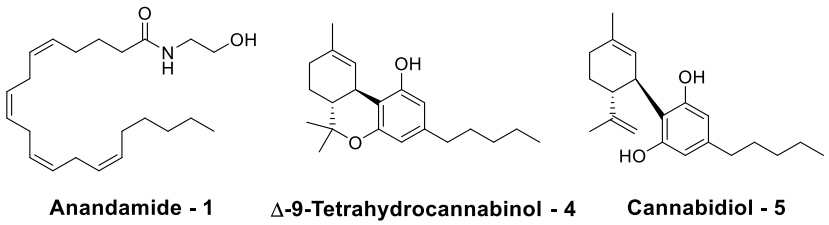

Figure 2: *The endocannabinoid AEA, and the active compounds of Cannabis s.*

Cannabinoid receptor-1 (CB-1)[18] and cannabinoid receptor-2 (CB-2)[19] are both pre-synaptic G protein-coupled receptors widely expressed in the whole body. The activation of these receptors may result in different biological effect, based on the tissue where the activation occurs. In particular, CB-1 receptor is highly expressed in the brain and in the spinal cord,[18,20] and in a lower amount in peripheral tissues, such as the skeletal muscle,[21,22] the liver and the pancreatic islet.[23] On the other hand CB-2

receptor is mostly expressed in the immune system cells and lymphoid organs[19,23,24], and in a little amount in the central nervous system.[25] AEA is a partial agonist for both CB-1 and CB-2[26] and is mainly responsible for the analgesic response mediated by the activation of CB-1 receptors expressed in CNS areas involved in the transmission of pain stimuli. The activation of pre-synaptic CB receptors by AEA results in the blockage of the pain stimuli progression along the neuronal fiber.[4] Other important effects concern physiological processes like the regulation food intake, and the embryo implantation in the womb at the beginning of pregnancy.[27,28] In the central nervous system, the inhibition of AEA signaling deactivation is related to an increased and stable level of the endocannabinoid, with good results for the treatment of neuropathic pain in a mouse model.[29,30]

1.2.Palmitoylethanolamide

Palmitoylethanolamide (PEA) was identified for the first time as a lipid extracted from various natural products (soybeans, peanuts and egg yolk),[31,32] and then found in mammalian tissues.[33] Its activity in the reduction of inflammation and allergic responses were clarified in preclinical tests in animal models during the first 20 years from the chemical characterization.[34,35,36] Few studies went beyond the animal models, proving PEA antinflammatory efficacy in the treatment of the inflammatory symptoms related to pulmonary infections in humans.[37,38] Deeper studies in the Nineties brought new information about PEA analgesic[4,5] and neuroprotective[39] effects, followed by the discovery of the site of PEA activity: even if structurally related to AEA, PEA is not active at all on CB receptors, and for this reason it is not considered as part of the endocannabinoid family.[40] PEA exerts its effects through the activation of an intracellular receptor known as peroxisome proliferator-activated receptor-α (**PPAR-α**).[41,42,43,44] The binding of PEA provokes the activation of PPAR-α, that recruits a cofactor known as PGC-1α,[45] and forms a heterodimer with the retinoid receptor RXR.[46] The active dimer recognizes the DNA promoter sequence for anti-inflammatory cytokines, blocking the Nf-κb mediated pro-inflammatory signaling pathway.[47] In white blood cells, like macrophages and monocytes, PEA is constantly released and hydrolyzed, in order to maintain the required level for the activation of PPAR-α.

***Figure 3**: the hydrolysis of PEA. The reaction can be performed by two different enzyme: Fatty Acid Amide Hydrolase (FAAH) or N-Acylethanolamine Acid Amidase (NAAA).*

The physiological deactivation of PEA occurs when a pro-inflammatory signal reaches the cell. The immediate response of the activated cell is to lower the levels of PEA, following two synergistic steps: the inhibition of the biosynthesis of PEA,[48] together with the increase of the expression and the activity of the enzyme responsible for PEA hydrolysis. In this way, the level of PEA falls, leading to the inactivation of PPAR-α and thus blocking the release of anti-inflammatory cytokines. Furthermore palmitic acid, that is the direct product of PEA hydrolysis (Figure 3), is able to bind to PGC-1α coactivator, contributing to the inactivation of PPAR-α, in a synergism with PEA low levels.[49] The main consequence of PPAR-α inactivation is the activation of the transcriptional factor known as Nf-κb, which stimulates the pro-inflammatory response promoting the synthesis of cytokines (IL-1, IL-6, TNF-α) and enzymes (like the inducible Nitric Oxide Synthase - iNOS), that activate the immune response (Fig. 4).[49]

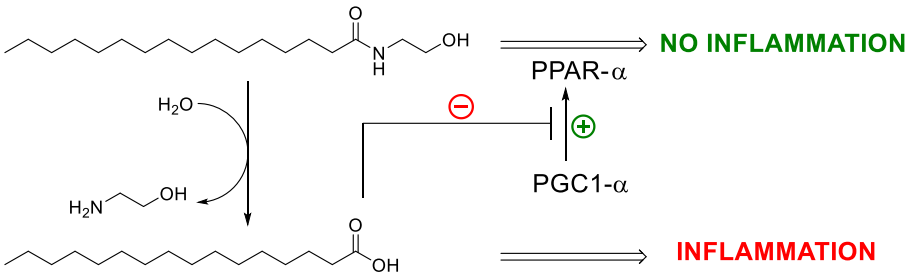

Figure 4: *In homeostatic conditions, PEA is released to activate PPAR-α receptor. To start of the inflammatory process, PEA is hydrolyzed to palmitic acid, that acts as an inhibitor of PGC1-α coactivator recruitment. As a consequence, PPAR-α is not activated, and pro-inflammatory cytokines are released.*

1.3.Metabolism of FAEs

1.3.1. Biosynthesis of fatty acid ethanolamides

The most important biosynthetic pathway for the production of FAEs consists of two steps catalyzed by two different enzymes that take place on the cell membrane (Figure 5).

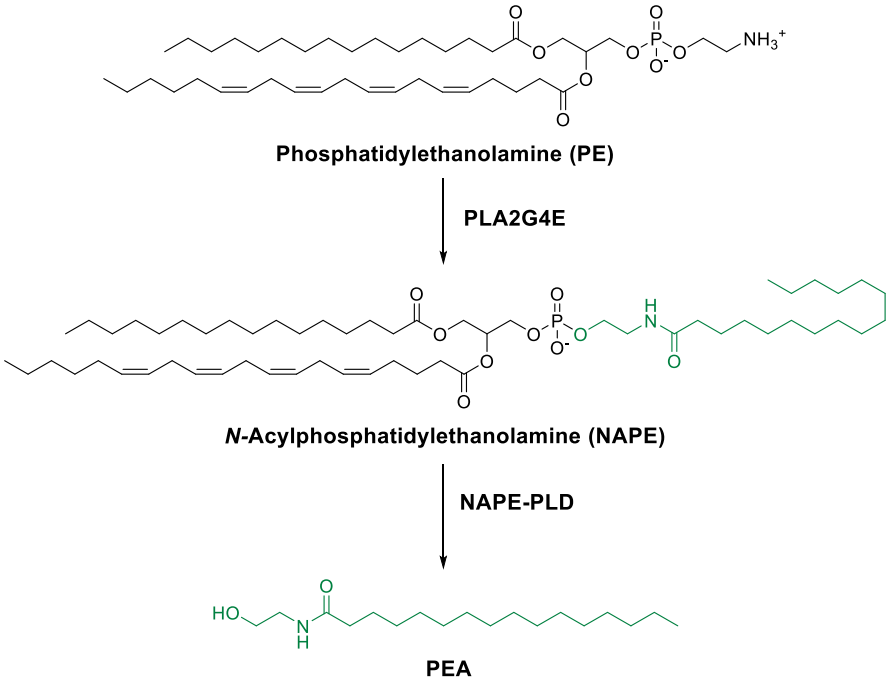

Figure 5: *The most relevant biosynthetic pathway for PEA release. The Ca^{2+} sensitive PLA2 transfer a palmitoyl chain from a phosphatidylcholine to a free phosphatidylethanolamine. The following NAPE-PLD mediated hydrolysis releases PEA.*

The first step is the transfer of a fatty acid acyl chain from the *sn*-1 position of a molecule of phosphatidylcholine to the free terminal amine of a molecule of phosphatidylethanolamine. This reaction is catalyzed by a calcium-dependent phospholipase A,[50] known as PLA2G4E. The product of

this reaction is a member of a family of phospholipids known as *N*-acylphosphatidylethanolamines (NAPEs), that are stored in the cell membrane. The release of the FAEs is made either constitutively (as for PEA) or on demand (in the case of AEA)[51] by the activation of a NAPE-specific hydrolytic enzyme called *N*-acylphosphatidylethanolamines-phospholipase D (NAPE-PLD).[52,53,48]

The enzymes from the family of the phospholipases are classified by a letter that identify their specific site of action (Figure 6):

- Phospholipases **A1**: catalyzes the hydrolysis of the bond between the glycerol residue and the fatty acid in position *sn*-1;
- Phospholipases **A2**: catalyzes the release of the fatty acid in position *sn*-2 on glycerol;
- Phospholipase **C**: hydrolyzes the phosphoester bond between the phosphate and the glycerol residue;
- Phospholipase **D**: attacks the glycerophospholipid on the distal phosphoester bond, producing phosphatidic acid and, in the case of NAPE-PLD, a molecule of FAE.

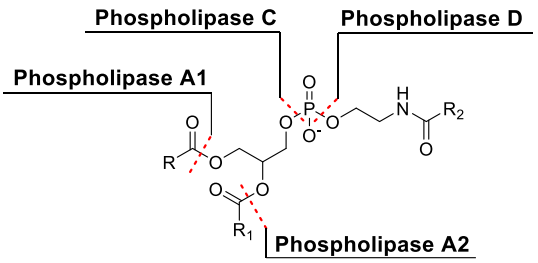

***Figure 6**: the phospholipase enzyme family sites of action.*

Alternative NAPE-PLD-independent pathways for PEA biosynthesis had been reported:[54] these are multi-steps pathways that involve other enzymes from

the Phospholipase family. Phospholipases A1 and A2, that remove the acyl chains from the glycerol residue, or Phospholipase C, that breaks the bond between the phosphate and the glycerol. Further reactions are required to release the active PEA (Figure 7).

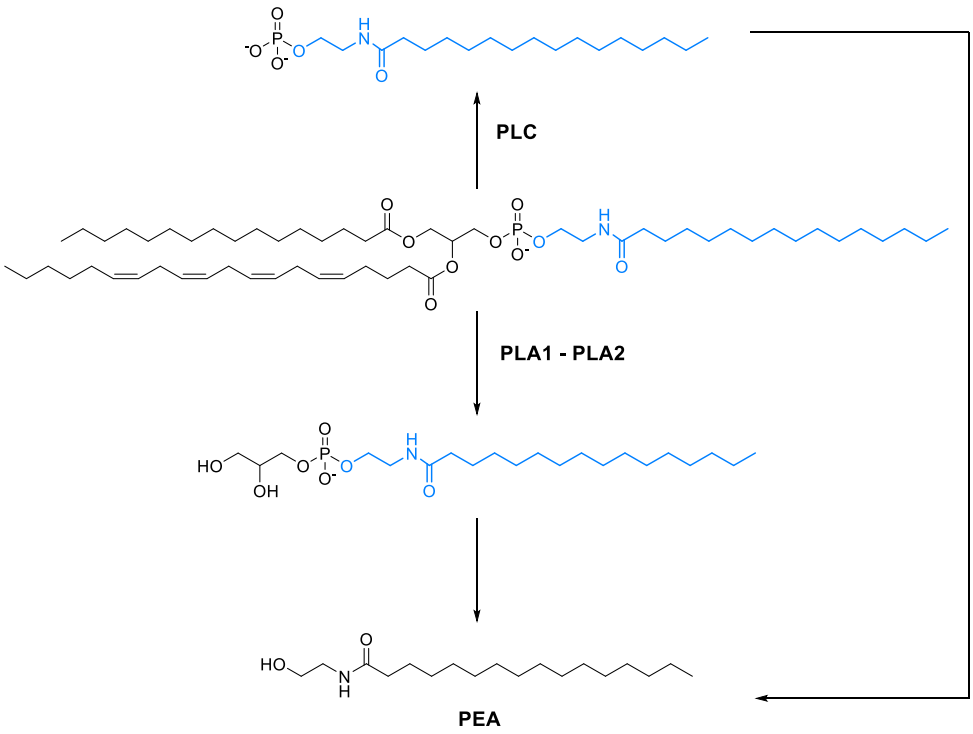

Figure 7: *NAPE-PLD-independent pathways for PEA synthesis. From the NAPE molecules in the center, the upper road shows the Phospholipase C – mediated synthesis; while the lower is the phospholipase A pathway.*

Given the important role that these molecules exert in the body, and the wide range of effects related to the activation of their receptors, the activation and the block of these signals must be precisely regulated. FAEs are usually released by increasing the activity of NAPE-PLD, and on the other hand, the quenching of these signals is obtained by reducing the activity of

this phospholipase, helped by the contemporary activation of two different enzymes, that hydrolyze those signals: fatty acid amide hydrolase (FAAH) and *N*-acylethanolamine acid amidase (NAAA).

2. *N*-Acylethanolamine Acid Amidase

2.1.Structure and catalysis

N-acylethanolamine acid amidase (NAAA) is a hydrolytic enzyme member of the *N*-terminal nucleophile (Ntn) enzyme superfamily. All the enzymes belonging to this family are characterized by an *N*-terminal nucleophile (a serine, a threonine or a cysteine), which is released upon an autocatalytic activation, and which is responsible for the cleavage of an amidic bond.[55,56] Among the enzymes from the Ntn family, only Acid Ceramidase (ASAH1) shares significant sequence homology with NAAA (35% identity).[57] As for the other Ntn proteins, NAAA is synthesized as a single-chain inactive proenzyme, that is activated in a second moment by self-cleavage of an internal peptide bond, resulting in two subunits, usually called α and β, that remain physically attached; this process of activation involves the same amino acid residue that is responsible for the catalysis in the mature enzyme.[55,56] In the specific case of NAAA, self-cleavage gives a heterodimer in which a smaller α-subunit is strictly associated with a larger β-subunit that starts with the nucleophilic residue, Cys126 for human NAAA, or Cys131 for mouse and rat NAAA.[58,59]

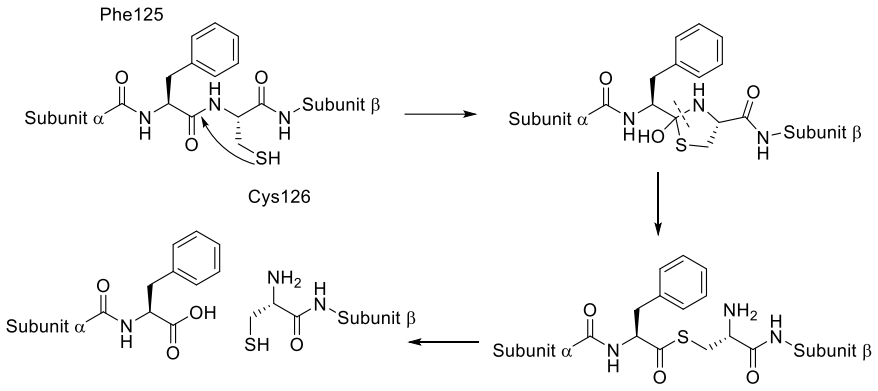

Figure 8: *simplified mechanism for NAAA self-cleavage. The first step regards the attack of the thiol on the carbonyl group, and further acyl substitution. The release of the amine produces a thioester that is subsequently hydrolyzed to obtain the two subunits.*

The cleavage is possible only in acidic environment, that is consistent with its subcellular localization in the lysosomes and other acidic compartments (not fully proven yet),[60],[61] where the pH is able to reach value around 4.5 – 5,[62] a perfect value not only for the cleavage, but also for PEA hydrolysis.[58] The process of activation starts with the attack of the side-chain thiol of Cys126 to the carbonyl group, followed by the release of Phe125 free carboxylate. After the synthesis, inactive NAAA is *N*-glycosylated at two different sites on each subunit.[58,59,63] These sites are highly preserved, and the post-translational modifications are probably required to achieve the right subcellular localization, where NAAA remains in its inactive form until the activation is triggered. Inflammatory signals are probably involved in the activation process, but this hypothesis remains to be tested. [64] Association with the lipid bilayer was clarified by structural studies: NAAA is a soluble protein that is characterized by two α-helix motives, rich of hydrophobic and positive residues, that are probably involved in the binding to lysosomal membrane phospholipids.[59] It looks like that binding to the membrane is a

key step for NAAA to expose the substrate binding site and to catalyze its reaction at its optimal velocity, and this hypothesis is supported from experimental data that show that in vitro NAAA activity is stimulated by the presence of phospholipids in the test wells, like phosphatidylethanolamine or sphingomyelin.[65]

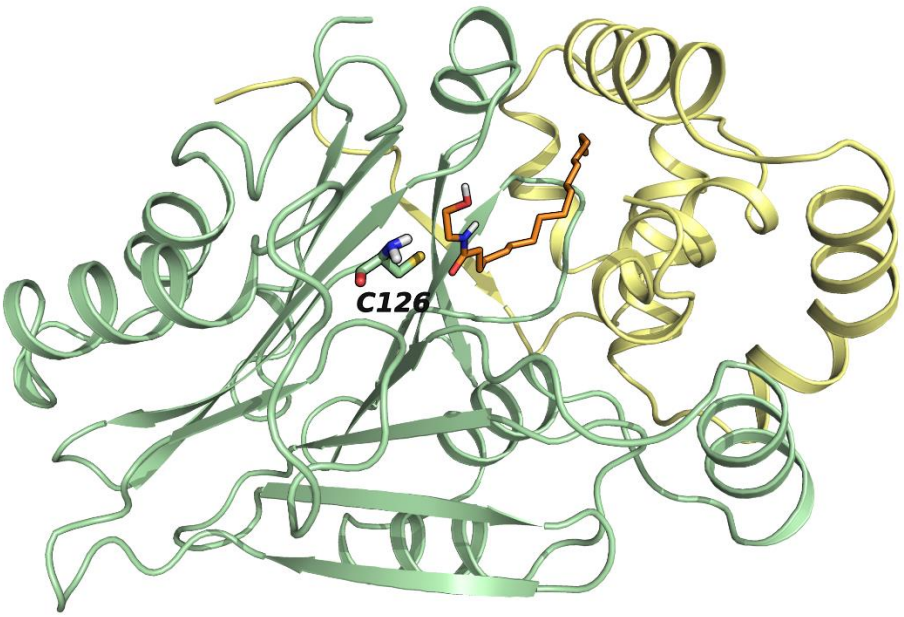

Figure 9: *X-ray structure of human NAAA. The two subunits are highlighted in two different colors, yellow for the α-subunit, green for the β. PEA is colored in orange and is located at the interface of the two subunits, close to the catalytic C126.*

Recently, different X-ray structures of the enzyme have been disclosed, providing important insights into the structure of NAAA binding site. In particular, the X-ray of the rabbit form of NAAA in complex with a molecule of myristate strongly suggests that the 16-carbon atoms acyl chain of PEA may accommodate within the narrow lipophilic pocket that is formed at the interface between the α- and β-subunits, while the hydroxyethyl moiety

would be placed in a cavity open to the solvent, closer to the catalytic residue. Considerations made from the enzyme structure, along with the comparison with acid ceramidase, brought to hypothesize a catalysis mechanism made by four steps:[66]

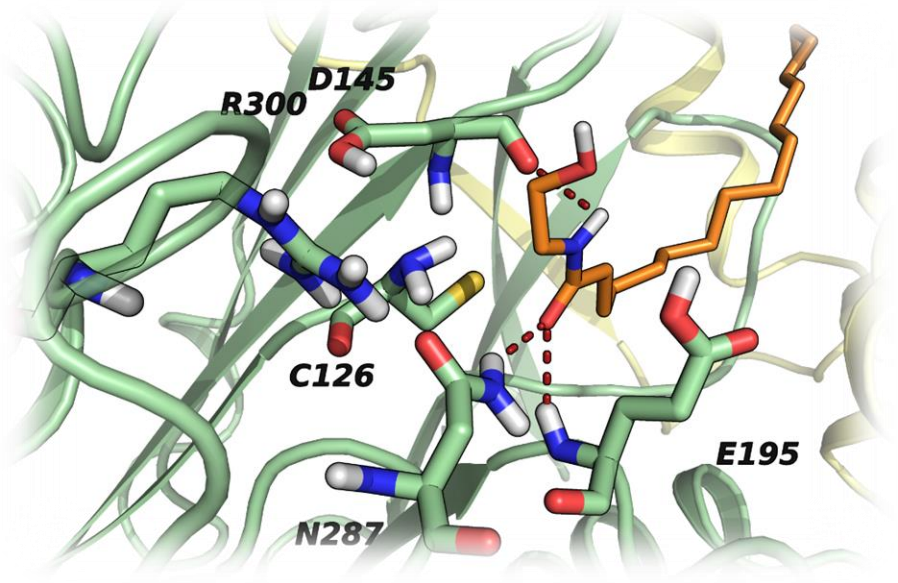

Figure 10: *a close up of NAAA active site: the two subunits are colored in yellow (α) and green (β), while the substrate PEA is orange. The interactions between the substrate and the relevant residues in the active site are highlighted: while the sulfide of the Cys126 is pointed at the amide carbon, the oxygen is stabilized in the oxyanion hole made by the side chain of Asn287 and the backbone amide group of Glu195.*

1. The free amine of Cys126 backbone gets the acidic proton from the thiol of the same residue, generating a transient zwitterionic form, that results in the activation of the reactive thiolate anion;

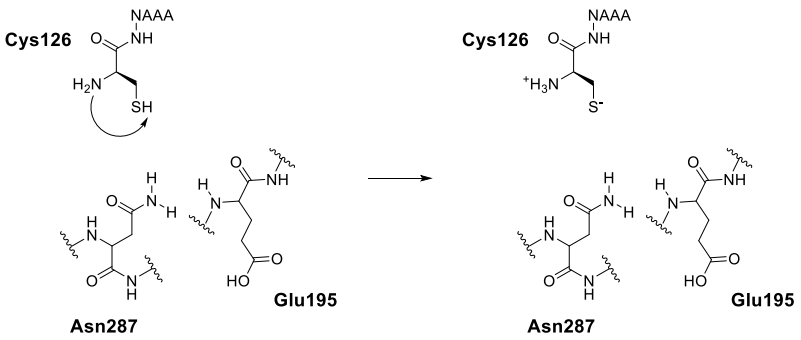

Scheme 1: *the catalytic mechanism of NAAA starts with the proton exchange between the thiol and the amine of the catalytic cysteine.*

2. The thiolate attacks the carbonyl carbon of PEA and the resulting tetrahedral adduct is stabilized in an oxyanion hole formed by the backbone nitrogen of Glu195 and the amide on the side chain of Asn287;

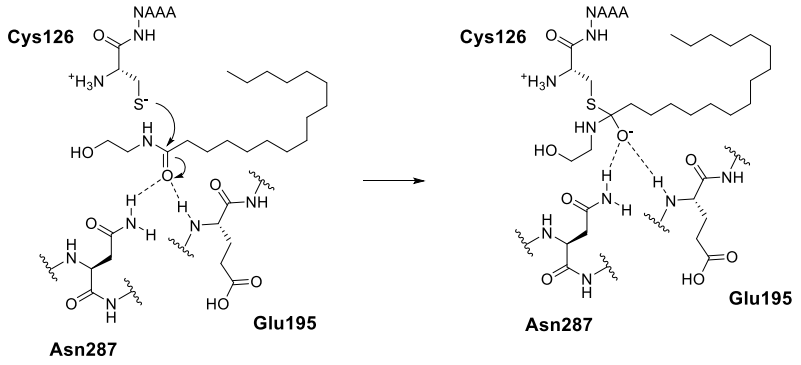

Scheme 2: *the substrate takes place in the binding site, and the thiolate attacks the carbonyl. The resulting tetrahedric anion is stabilized in the oxyanion hole, made by the side chain amide of Asn287 and the backbone NH of Glu195.*

3. The nitrogen of the ethanolamine moiety is protonated, and the ethanolamine is forced to abandon the enzyme site. At this time the

thiol is forming a thioester bond with palmitic acid, so the enzyme is acylated;

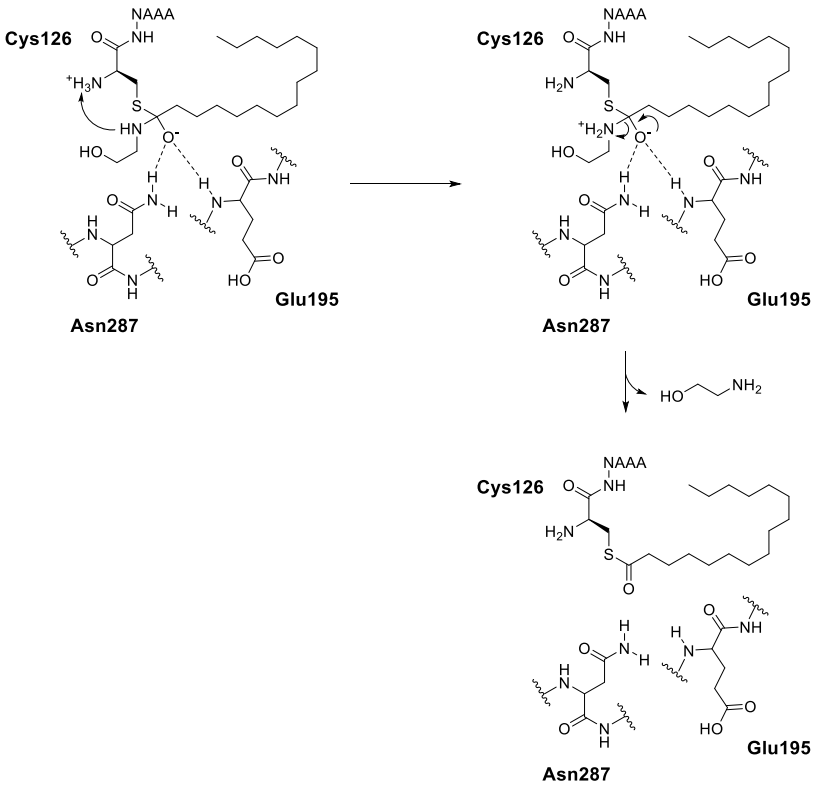

Scheme 3: *the thiolate attack is followed by a proton exchange between the ammonium on cys126 and the ethanolamine moiety. The release of the ethanolamine yield the acylenzyme.*

4. A molecule of water enters the active site, leading to the hydrolysis of the thioester and regenerating the initial state of the enzyme.

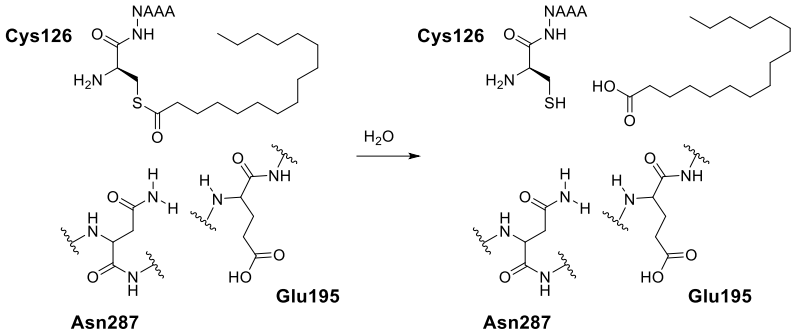

Scheme 4: *the acylenzyme is hydrolized by the addition of a molecule of water, releasing the free fatty acid and restoring the initial state of NAAA.*

2.2.FAAH and NAAA

Starting from 1995, when it was firstly characterized, the enzyme FAAH has been intensively studied for its role in the control of the endocannabinoid system by AEA hydrolysis.[67,68,69] For this activity, FAAH is now under investigation and evaluation for the therapy of social anxiety, post-traumatic stress disorder (PTSD), and peripheral neuropathies. Despite they basically perform the same hydrolytic reaction, FAAH and NAAA show differences in many aspects of their structures and activities:

- FAAH is widely distributed in the whole body, especially in the brain, where it reaches the highest concentrations, and in the liver. This enzyme is a homodimer protein, strictly associated with the membranes thanks to its transmembrane domains (1 α-helix in each subunit). Inside the cells, it is distributed on different subcellular structures: it can be found on the membranes of the nucleus and on the rough endoplasmic reticulum, where the physiologic pH of 7.4 is close to the value found for the highest FAAH in-vitro activity (between 8.5 and 10).[70] The catalytic mechanism of this enzyme is built on the activity of a serine-serine-lysine triad. The substrate-binding site is wide and able to easily allocate arachidonic acid derivatives, as well as other saturated and unsaturated substrates. In facts, a wide range of molecules are hydrolyzed by FAAH: not only AEA and other members of the endocannabinoid family, like 2-Arachinodoylglycerol (2-AG), but also other FAEs, like OEA and PEA, *N*-acyltaurines (with chains that may be even longer than the 20-carbons tail of AEA) and *N*-acylglycines.[71]

- NAAA is almost exclusively expressed in immune cells such as monocytes and tissue macrophages (especially in lungs and spleen). It is a cysteine hydrolase localized in acidic vesicles, such as the lysosomes, where the acidic environment provides the ideal conditions required for the activation and catalytic activity of the enzyme.[58] NAAA is known to be a hydrolase specific for PEA and, with a lower affinity, for OEA, while it doesn't recognize AEA at all.[61] No other relevant classes of fatty acid amide derivatives were investigated until today. Probably for the reason that NAAA is not involved in the regulation of the endocannabinoid system, this enzyme was not investigated as deep as its counterpart, but the increasing importance of PEA in the control of inflammatory processes and pain is bringing new interest on this enzyme.[64]

	FAAH	**NAAA**
Family	The amidase signature family	The choloylglycine hydrolase family
Enzyme structure	579 aminoacids, a homodimer	359 aminoacids, a heterodimer
pH optimum	8.5 – 10	4.5 – 5.0
cell localization	Membranes of nucleus and endoplasmic reticulum	Internal membrane of lysosomes and endosomes
Reactivity with FAEs	AEA > OEA > PEA	PEA > OEA, no activity on AEA
Reactivity with other substrates	2-Arachidonoylglycerol, *N*-acyltaurines and *N*-acylglycines	No data

Table 1: *a summary of the differencies between NAAA and FAAH.*

2.3.A novel target for inflammation and pain

Deficits in PEA disposability related to inflammatory diseases are supported only for arthritis and ulcerative colitis, while information about other pathologies remains insufficient. It is reported that topical administration of the covalent inhibitor ARN077 (also reported as URB913, **6**, Fig. 11) is able to suppress inflammatory reactions on the skin provoked by exposure to phorbol esters or UV-B radiation in rodent models; in particular, compound **6** reverses edema and redness, and reinstates the homeostatic levels of circulating interleukin-4 (IL-4) and immunoglobulin-E (Ig-E). These effects produced by NAAA inhibition are strictly correlated to PPAR-α activation due to the restoration of normal PEA concentration in the tissues. These results offer few expectations on the possibility of using NAAA inhibition in the treatment of chronic inflammatory phenomena.

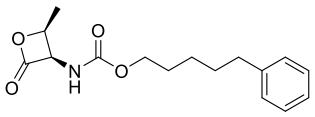

ARN077 - 6

Figure 11: *chemical structure of the lactone-based covalent NAAA-inhibitor ARN077.*

The selectivity and the safety profile of ARN077 in preclinical and clinical tests, its effects on mediators of the allergic response, like IL-4 and Ig-E, and the efficacy showed by PEA as an adjuvant treatment for eczema, push the evaluation of NAAA as a target for both topically or systemically active drugs to treat disorders characterized by an allergic component.

In addition to peripheral inflammation, new evidences brought the idea that NAAA inhibition could be helpful in the improvement of neural inflammation and chronic pain situations, as proven by the systemic administration of noncovalent inhibitor ARN19702,[72] able to mitigate the symptoms of neuroinflammation in a mouse model of multiple sclerosis; Nevertheless, ARN077 demonstrated analgesic activity in rodent models of inflammation and nerve injury.

3. NAAA Inhibition

3.1.First steps

Years before the disclosure of the X-ray crystallographic data of NAAA, early investigation on NAAA-targeting compounds already produced remarkable results. These studies either concerned chemical modulation of PEA structure or made an attempt to selectively bind to the catalytic cysteine. Systematic changes to the ethanolamine moiety of PEA allowed the identification of *N*-pentadecylcyclohexanecarboxamide, which was initially reported to inhibit rat NAAA with a median Inhibitory Concentration (IC50) around 4.5 µM,[73] but subsequent works proved that the responsible for the inhibitory activity was pentadecylamine (Figure 12, compound **7**, IC50 = 5.7 µM on rat NAAA), an intermediate in the synthesis of the previous compound. This result was then confirmed by the discovery of another long chain-amine inhibitor, with a comparable potency: tridecyl-2-aminoacetate (**8**, IC50 = 11.8 µM).[74]

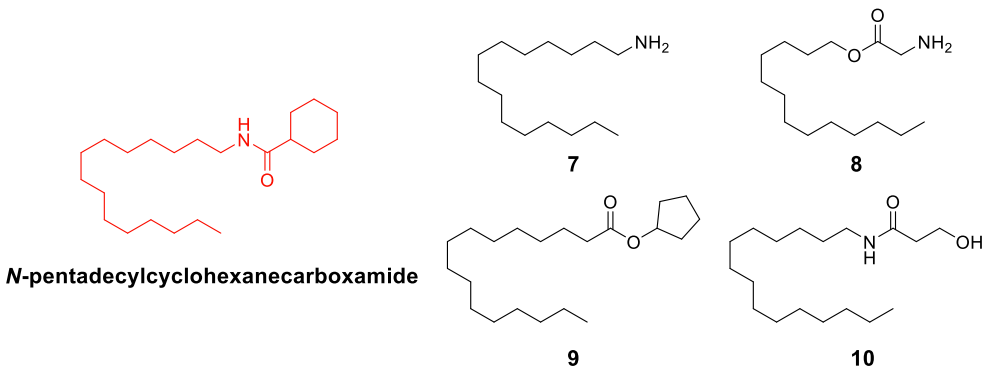

Figure 12: *First steps in the discovery of NAAA inhibitors. Common feature of these structures is the long chain that mimic PEA acyl chain.*

Later on, cyclopentylpalmitate (**9**, IC50 = 10 µM on human NAAA)[75] and *N*-pentadecyl-3-hydroxypropanamide (**10**, IC50 = 34 µM on human NAAA) were reported to have inhibitory activity comparable to the previous compounds.[76] The main features of PEA were retained in all these compounds (the polar head and the long carbon chain) in order to maintain the ability of these molecules to compete with PEA for NAAA's binding hydrophobic pocket, but with low productive interactions with other components of the substrate-binding site, that resulted in a low potency.

3.2.Covalent Inhibitors

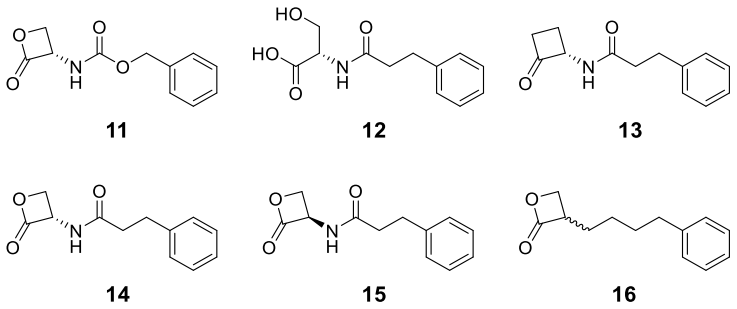

Figure 13: *NAAA inhibitors derived from the β-lactone 11: first information on the SAR revealed the importance of the lactone moiety and the amide on the side chain for the activity on the target. The geometry of the stereocenter plays a role to maintain the activity: compound **14** is more active than its enantiomer **15**.*

Solorzano and collaborators, using a computational model of NAAA built on the crystallographic structure of Conjugated Bile Acid Hydrolases (CBAH),[77] another enzyme from Ntn family, identified the β-lactone **11** from a library of cysteine-traps, discovering a compound with a good inhibitory potency on rat NAAA (IC50 = 3 μM).[78] The importance of the β-lactone ring for the inhibition was proven by the fact that the replacement of this group with an hydrolyzed lactone moiety (**12**), or with a cyclobutanone (**13**) led to the complete loss of activity (both IC50 > 100 μM).[79] Successive steps led to *N*-[(3S)-2-oxo-3-oxetanyl]-3-phenylpropan-amide (**S-OOPP**, **14**), that inhibits rat NAAA with a sub-micromolar potency (IC50 = 420 nM);[78] S-OOPP showed a good selectivity for NAAA compared to related enzymes (functionally and structurally related), while its enantiomer **15** resulted to be less active (IC50 = 6 μM on rat NAAA). S-OOPP normalized PEA levels in macrophages stimulated with bacterial endotoxin and its subdermal application prevented

carrageenan-induced inflammatory response in mice: this response was mimicked by the administration of exogenous PEA or PPAR-α agonists, but it was not observed in PPAR-α KO mice.

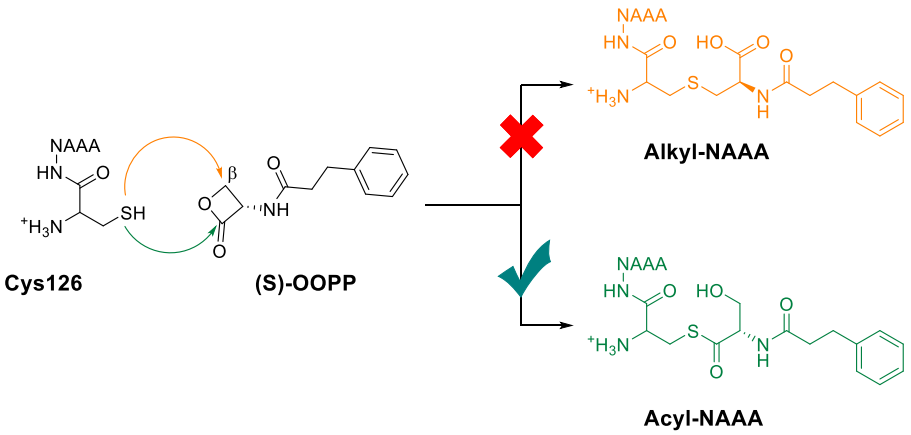

Figure 14: *two possible routes for NAAA inhibition due to a covalent engagement of the catalytic cysteine by the inhibitor (S)-OOPP. Orange-stained is the irreversible thioether, in green the reversible thioester. Experimental studies proved that the S-acylation is the right inhibition mechanism.*

Initial theories on the inhibition mechanism mediated by **14** concerned that NAAA's catalytic residue, as hypothesized for other cysteine hydrolases,[80,81,82] could attack the lactone ring on two distinct electrophile positions: the carbonyl carbon, resulting in a labile thioester, or the β-carbon of the ring, yielding a hydrolysis-resistant thioether (Figure 14). The answer for which of these product was responsible for the inhibition came out from mass spectrometry experiment,[83] together with an assay consisting in a dialysis of the enzyme-inhibitor complex, that resulted in a partial reversibility of the complex, that brought the idea that NAAA inhibition by β-lactones was due to the cysteine acylation rather than alkylation.[78] Driven by these preliminary results, Solorzano and coworkers explored the

Structure-Activity Relationships (SAR) towards the β-lactone and the side chain linked to the ring in α-position. The importance of the amide on the side chain was first rationalized by computational studies on NAAA homology model built on CBAH, and successively confirmed by the low potency for 3-(4-phenylbutyl)oxetan-2-one **16** (IC50 = 11 μM on rat NAAA),[79] that lacks of the amide group.

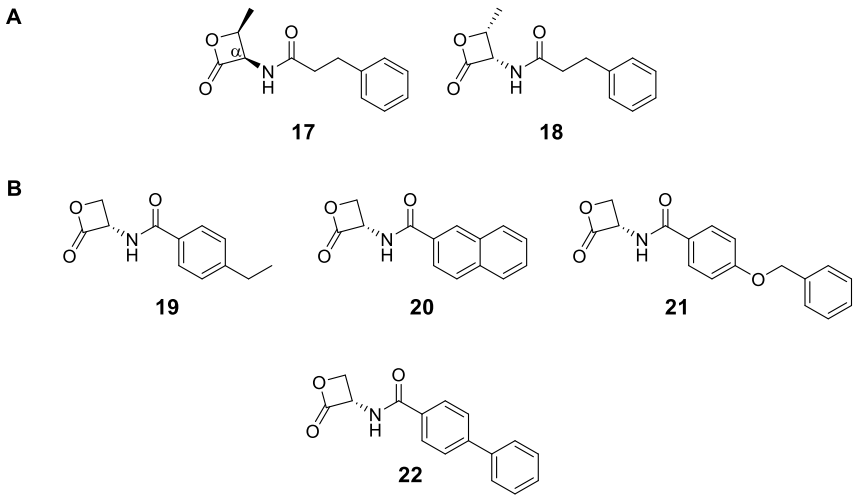

Figure 15: *A) methylated derivatives of compound S-OOPP; the insertion of a methyl on the β-carbon of the cycle brought to less potent compounds, with an inverted stereoselectivity (**17** has a better activity than **18**). B) Investigation of the effect of the side chain: **19** IC50 = 102 nM, **20** IC50 = 160 nM, **21** IC50 = 90 nM, **22** IC50 = 115 nM.*

Successive studies on the crystallographic coordinates of NAAA suggested that the importance of the amide moiety on the side chain was related to the position assumed by the inhibitor in the active site of the enzyme, with the carbonyl of the side chain in the oxyanion hole, making reliable interaction to promote the inhibition.[79]

The introduction of a second stereocenter on the β-carbon of the lactone ring brought new information partially explained by the computational model; in particular, β-lactones with a syn configuration of the two substituents (Figure 15) resulted more stable, but poorly active (**17**, IC50 = 3.2 μM on rat NAAA) or completely inactive (**18**, IC50 > 100 μM). Interestingly, the more active of the two enantiomers has a configuration of the stereocenter on carbon-α that is the opposite than the one on non-methylated compounds, as seen for compounds **14** and **15**.[79]

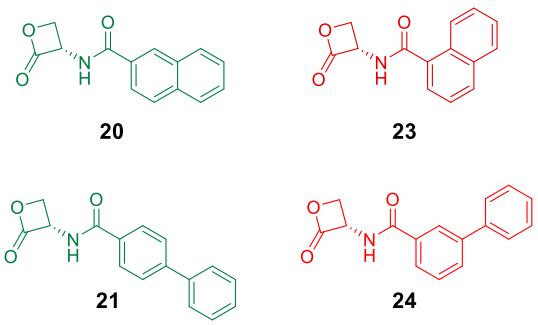

Figure 16: *the effect of the orientation of the side chain: compounds **23** (IC50 = 50 μM) and **24** (IC50 = 4.4 μM) are way less potent than their relative isomers.*

The influence of the lipophilic side-chain linked to the amide moiety had been investigated too. Both the dimension and the flexibility were explored, introducing longer chain, aromatic ring alone or coupled as a naphthyl residue or as a biphenyl pattern. Great results were given from compound with a certain rigidity and planarity (Figure 15, compounds **19** – **22**). The orientation of the side chain plays a significant role, as seen for isomers in Figure 16: compound **20** (IC50 = 160 nM) and **21** (IC50 = 115 nM) are more potent than their relative isomer **23** and **24** (IC50 = 50 μM and 4.4 μM,

respectively), indicating that the geometry of the side chain plays a role in the ligand recognition process.[79]

Investigation on the β-lactone surroundings revealed that the replacement of the amide group with a carbamate, together with the β-methyl substituent improves the stability of the ring, while retains the inhibitory potency: one of these threonine-β-lactones, named ARN077 (**6**, IC50 = 50 nM on rat NAAA and 7 nM on human NAAA) showed a great inhibitory potency, along with an improved chemical stability;[84] successive steps led to the biphenyl derivative **25** (IC50 = 7 nM on both rat and human enzymes)[85] whose structure confirmed the target recognition is improved by the presence of rigid lipophilic tails. A study for potential off-target of ARN077 was assessed, finding that this lactone is selective for NAAA, proven its safety in preclinical studies.[86,87,88]

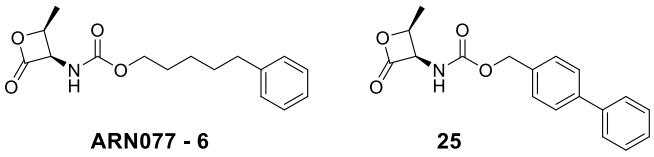

Figure 17: *Chemical structure of* ***ARN077*** *and compound* ***25.***

Even if the modifications introduced by Duranti on the β-lactone improved the stability of the ring, the overall effect was not enough to allow a systemic administration of these compounds, whose half-lives remain too short to make this class of compounds interesting for clinical use: **ARN077** half-life is 190 min in vitro at pH 5.0, but it is shorter than 10 min in rat plasma.[84]

To overcome the problem of the stability a new class of inhibitors was developed replacing the lactone with a β-lactam ring.[89] This modification

improved the biological stability. On the other hand, similarly to what observed for lactones, the methylation on carbon β produced an inversion of the stereoselectivity for the side chain, from S- to R-, and the methyl, along with the carbamate replacement results in compound with a long half-life and great potency. Noteworthy, compounds from these class, are active by systemic administration. The most noticeable from this class is ARN726, compound **26** (IC50 = 27 nM on human NAAA)[90] that is able to inhibit NAAA in peripheral tissues, although the penetration in the central nervous system was limited,[72] and the elimination in vivo was too fast, as seen from pharmacokinetics studies. Compound **27** (IC50 = 85 nM on human NAAA) came out from further SAR exploration on the side chain, with a lower potency and an increased stability compared to ARN726.[91]

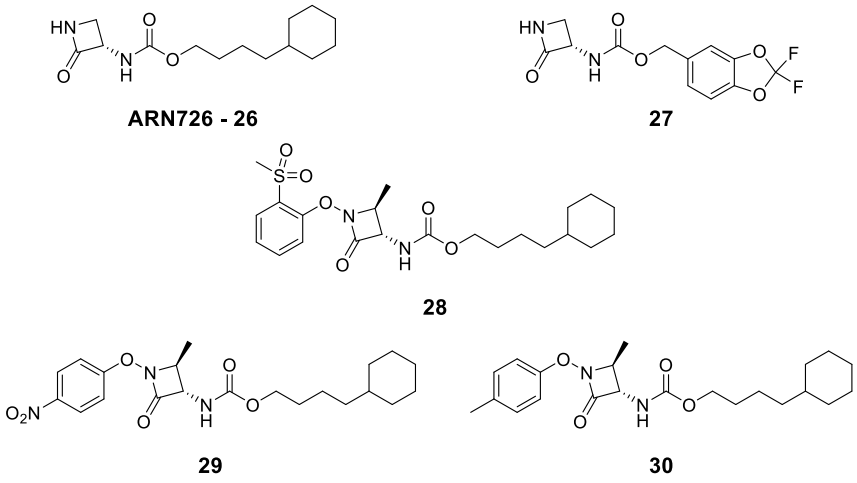

***Figure 18**: β-lactam **ARN726** and its derivatives.*

The discovery of the β-lactam class brought successive investigation possibilities: a new class of *N*-substituted derivatives was studied, leading to

the introduction of N-O-aryl and N-O-alkyl β-lactams: compound **28** – **30** demonstrates nanomolar potency (IC50 = 6 nM, 17 nM and 31 nM for **28**, **29** and **30** respectively) and good stability.[92]

Noteworthy, the introduction of the second stereocenter on *N*-O-Aryl substituted β-lactam brought to unexpected results: the favorite stereoisomer is the one with the two substituents in anti (absolute stereochemistry 2S,3S), and the stereocenter on C-α is maintained, opposite to all previous results, in which the active compounds present syn-stereochemistry.

Compounds from these new classes of β-lactams brought new tools to the investigation of NAAA; probes like **ARN14686** (compound **31**), carrying a terminal alkyne, used as a reaction site to attach a fluorescent probe in the biological medium (click chemistry reaction, Scheme 5),[93] or compounds directly linked to a fluorescent residue,[92] were developed to study active NAAA from cell lysates, live cell cultures, or even animals: potency and selectivity of **31** make this compound useful for the quantification of NAAA activity in animal models of inflammation.[94]

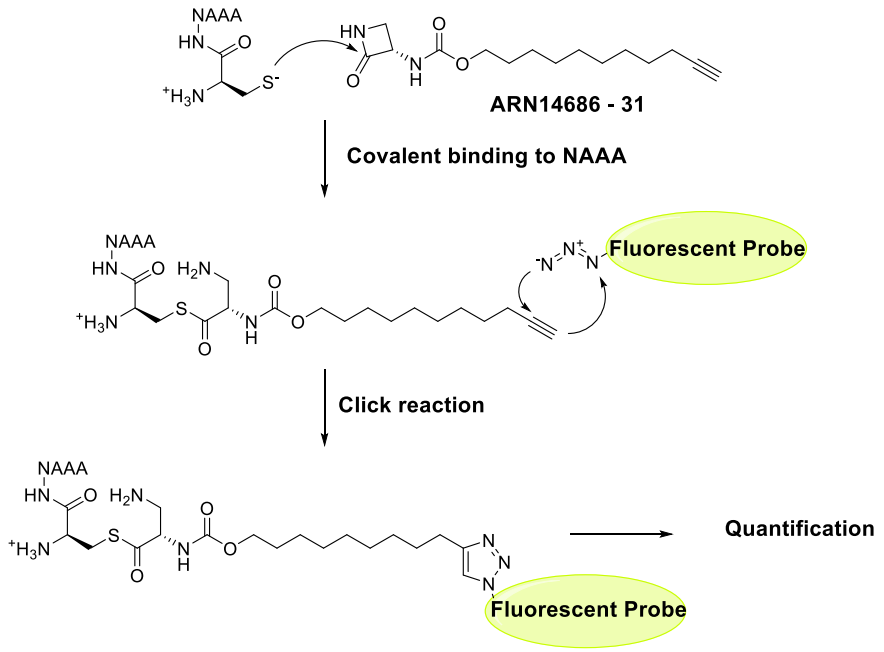

Scheme 5: *NAAA probe ARN14686 is used to quantify NAAA activity by fluorogenic assays. It binds to the catalytic cysteine, then in a second step, the terminal alkyne is used to attack a fluorescent probe. The intensity of the fluorescence is proportional to the amount of active NAAA.*

Other cysteine-trap moieties were investigated, producing a series of compounds bearing an isothiocyanate warhead. Starting from pentadecylisothiocyanate **32**, that inhibits NAAA in a reversible way, compound **33** (**AM9053**, IC50 = 30nM on human NAAA)[95] was found to be selective for NAAA, and active in a mouse model of colitis.[96]

The next step in the investigation of new warheads led to the discovery of the latest class of inhibitors, that share the cyanamide warhead (known to be thiol-binding moiety from a previous study on the reversible inhibition of cathepsin K).[97] Cyanamide-cysteine traps were found to be stable in plasma ($t_{1/2}$ > 2 h both in rat and human), but it is rapidly inactivated ($t_{1/2}$ = 5 – 15

min) when incubated with microsomal enzymes preparations ($t_{1/2}$ values ranging from 5 to 15 min). Nanomolar inhibitor **34** is one of the most potent NAAA inhibitors (IC50 = 3 nM):[98] as for lactones and lactams, the result of the cysteine reaction with cyanamides is an acylation of the enzyme (an isothiourea is formed). To prevent the microsomal oxidation, the most promising strategy involved the introduction of bulky substituent near the cyanamide moiety; compound **35** showed an improved subnanomolar potency, but no selectivity towards FAAH (IC50 = 0.3 nM on NAAA, 1nM on FAAH). Selectivity was finally obtained by the introduction of a methoxy substituent on the meta-position on the distal benzene ring, as in compound **36**, that preserved the potency against NAAA (IC50 = 1.6 nM on human NAAA), while resulted 100 times more selective.[99]

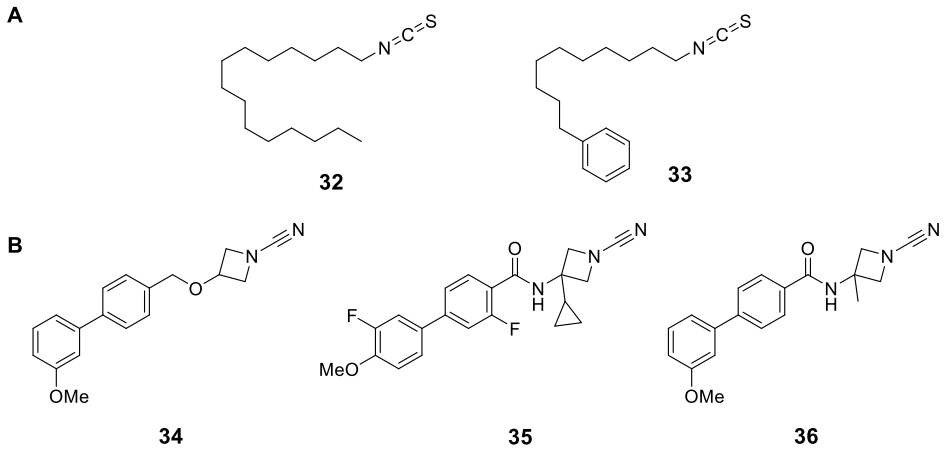

***Figure 19**: A) Isothiocyanate-based NAAA inhibitors. B) Cyanamide-based NAAA inhibitors.*

3.3.Non-covalent inhibitors

The second strategy to achieve NAAA inhibition regarded the identification of structures able to make strong interactions with the active site of the enzyme, without using covalent warhead to improve the time of contact between the inhibitor and the enzyme. These molecules were initially designed on the structure of the substrate, but remarkable results came out from chemical screening.

Starting from the very first approach on NAAA inhibition (compound **6** and **7**) the initial replacement of the polar head, and the followed improvement of the tail, introducing rigid motives led to the discovery of compound **37**, active in model of lung inflammation,[100] and **38** (IC50 = 267 nM on human NAAA).[101]

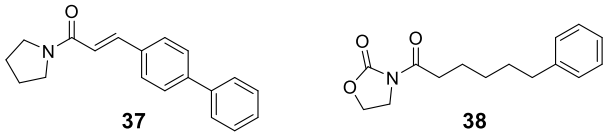

Figure 20: *initial steps in non-covalent NAAA inhibitors development.*

The screening of chemical libraries gave the possibility for the investigation in new structures, like Diacerein **39** (anthraquinone derivative, IC50 = 700 nM),[102] that inhibits NAAA via a non-competitive mechanism. Compound **39**, was also tested in vivo, proving its efficacy in the reduction of inflammatory symptoms in rat model (inflammatory response stimulated by an injection of carrageenan in a paw).

Benzothiazole-piperazine derivatives came out from a second screening, with compound **40**, whose scaffold was the starting point for a SAR study.

ARN19702 (**41**, IC50 = 230 nM on human NAAA) was developed by the replacement of the ortho-methyl group on the phenyl ring with an ethylsulphonyl moiety, and by adding a methyl on the piperazine ring. The structure of **41** make it selective towards a wide range of potential off-targets, stable against cytochrome P450 oxidation, and active by oral administration. Noteworthy, this compound was found to be able to reach the central nervous system in little amount (≈20% brain – blood ratio), increasing levels of PEA and OEA in the brain. Pharmacologycal studies on multiple sclerosis model showed an improvement in neurons inflammation and motor dysfunction.

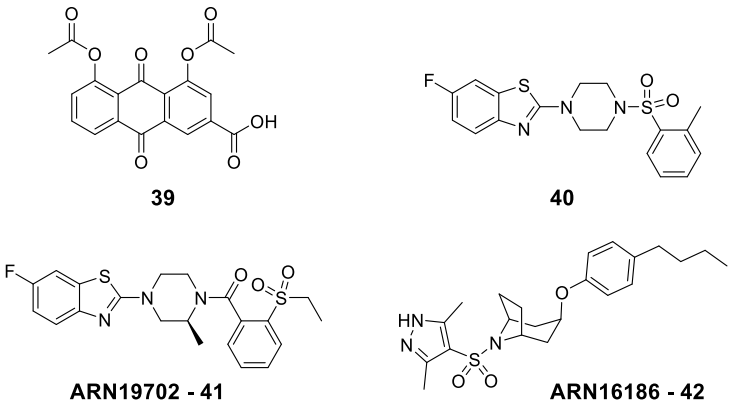

Figure 21: *the structure of Diacerein **39** and compound **40** found to be active on NAAA by a screening investigation. **ARN19702** and **ARN16186** are actually two of the most potent non-covalent NAAA inhibitors.*

A second hit, from the same screening that yielded the starting point for ARN19702, was studied and modified, producing **ARN16186** (**42**), characterized by a 3,4-dimethylpyrazole head linked to a lipophilic tail through an azabyciclo[2,2,2]octane moiety. Information gathered in a published patent affirmed the potency of the inhibitor (IC50 = 23 nM on

human NAAA), the reversible mechanism of action, and the activity in vivo.[103]

4. Synthesis of new potential NAAA inhibitors

4.1.Aim of the work

In the last decade, the interest and efforts put in the investigation of the mechanism of NAAA have significantly grown, leading to the elucidation of the biological role of the enzyme, and the development of many different pharmacological tools to investigate the effects that NAAA activation can cause to the body.

Experimental results suggest that NAAA plays an important role in the development and sustainment of neuroinflammatory disease, like Alzheimer's disease and multiple sclerosis.[104] Efforts made in the direction of the discovery of novel classes of inhibitors led to high-potent compounds, but almost none of them are able to pass the blood-brain barrier, and compounds like ARN19702 can reach the brain but only in little amount.

Starting from these premises, the main objective of this part of the PhD research work was the synthesis of novel NAAA inhibitors, aiming at the identification of a molecule with an increased ability to penetrate the blood-brain barrier and NAAA inhibitory efficacy. To this aim, a nitrile-based cysteine trap group, which is characterized by a lower reactivity compared to isothiocyanate and cyanamide, was selected as an ideal warhead able to react with and covalently modify the catalytic cysteine. Taking advantage of the available X-ray structures, that have disclosed the characteristics of the enzyme biding site, different hydrophobic scaffolds, designed to mimic the acyl chain of PEA or the scaffold of ARN19702 and other known inhibitors, were linked to the nitrile reacting group, in order to increase the selectivity towards NAAA.

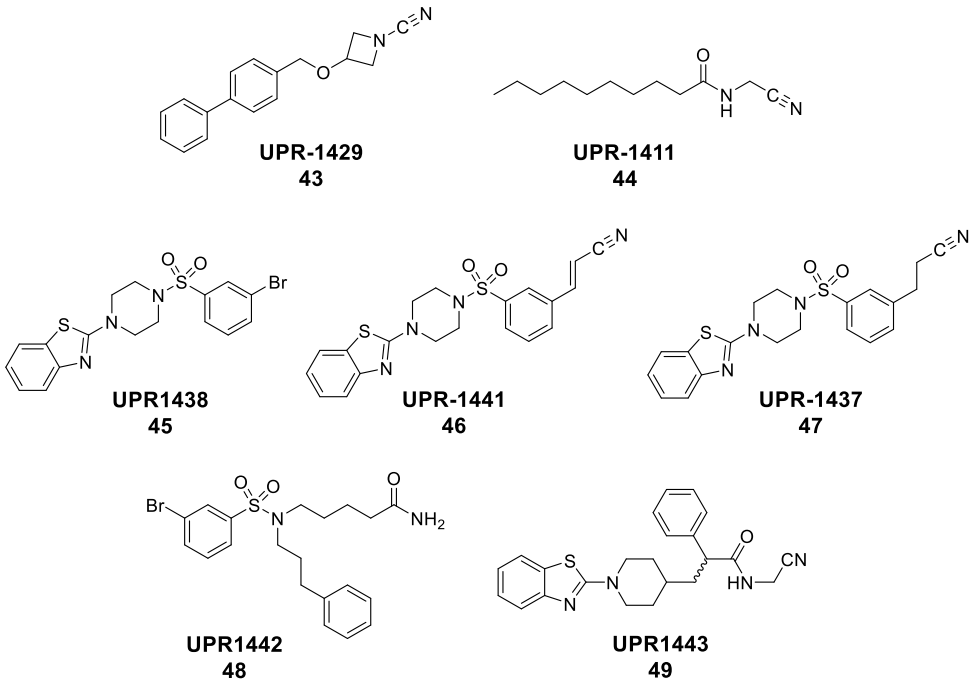

Figure 22: *New compounds designed and synthesized for this project, as inhibitors for NAAA.*

4.2.UPR1429 (43)

UPR1429 (compound **43**) was patented by Makriyannis and coworkers in 2015 (WO2015/179190 A1), along with more than 200 compounds, including compounds **34**, **35** and **36**, all studied as NAAA inhibitors, that were classified based on their IC50. The structure of **UPR1429** is made by the combination of a biphenyl moiety, and a reactive cyanamide warhead, linked one to the other with an ether group. Compound **43** was intended as a benchmark to be compared with our new inhibitors to assess their ability to give potent NAAA inhibition without a strongly reactive warhead. The 4-steps synthetic pathway is described in the patent[98] and it was replicated without any changes, as shown in Scheme 6:

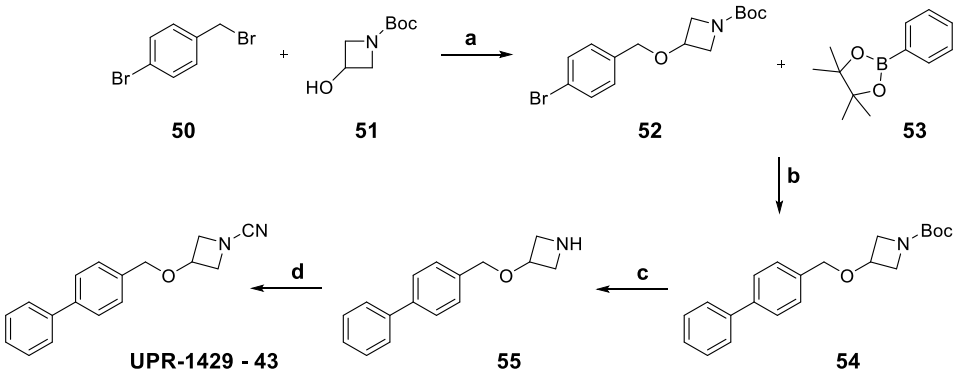

Scheme 6: *Total synthesis of* ***UPR1429****. Reagents and conditions: a) NaH, NaI, DMF, 0°C, yield = 77% b) $PdCl_2(PPh_3)_2$, K_2CO_3, 1,4-dioxane, reflux, yield = 68% c) TFA, DCM, 0°C, Quantitative d) BrCN, Et_3N, DCM, 0°C to rt, overnight, yield = 28%.*

4.3.UPR1411 (**44**)

A first attempt on targeting the catalytic cysteine of NAAA using a less reactive warhead (to avoid unwanted off-target actions) was made with compound **44**, also referred to as **UPR1411**, where the carbonyl group of an ideal substrate of NAAA is substituted with a nitrile moiety, while the acyl portion is maintained. The synthetic pathway for this compound was made up to 3 steps. The first part is the activation of decanoic acid (**56**) with PCl_5, and the fatty acyl chloride (not isolated) was then trapped by N-hydroxysuccinimide to give the OSU-ester **57**. This compound is less reactive then the related acyl chloride and it is able to distinguish between oxygen-nucleophiles (water and alcohols) and nitrogen-nucleophiles (amines), and therefore to react only with amines. In the second step we used the Gabriel synthesis of primary amines to obtain a protected 2-aminoacetonitrile (**60**), by nucleophilic substitution of 2-chloroacetonitile **59** using Phthalimide potassium salt (**58**). The in-situ hydrazinolysis of **60**, followed by the addition of compound **57** yielded **UPR1411**.

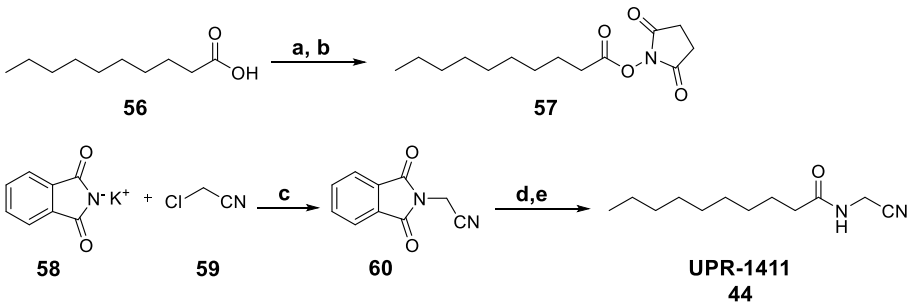

Scheme 7: *Total synthesis of **UPR1411**. Reagents and conditions: a) PCl_5, neat, reflux, 2h b) N-hydroxysuccinimide, Pyridine, 0°C, 1h yield = 80% c) DMF, overnight, 0°C to rt, yield = 58% d) hydrazine monohydrate, ethanol, rt, overnight e) **57**, ethanol, rt, overnight, yield = 42%.*

4.4.UPR1438 (**45**)

Compound **UPR1438** came out from a virtual screening of NAAA-binding compounds. The structure partially reminds of ARN19702, with the retaining of the benzothiazole-piperazine pattern; it lacks the stereocenter on the piperazine and the ethyl-sulfonyl group on the benzene ring. Moreover the amide linking the phenyl ring and the piperazine was replaced by the sulfonamide functionality. The synthetic pathway is convergent, starting from *m*-bromoaniline **61** and 2-bromobenzothiazole **63** to prepare the intermediate **62** and **65**; m-bromoaniline is used to obtain a sulfonyl chloride through the in-situ aryl diazonium salt preparation, followed by a substitution with SO_2 released from the hydrolysis of thionyl chloride, in strong acidic environment and in presence of copper chloride (I) as catalyst. Compound **65** was obtained using "Ullmann-like" coupling conditions: nucleophilic substitution on an aromatic ring using copper iodide (I) for the catalysis. **UPR1438** was finally obtained by the reaction between the free amine of the piperazine ring and the sulfonyl chloride **62** already prepared.

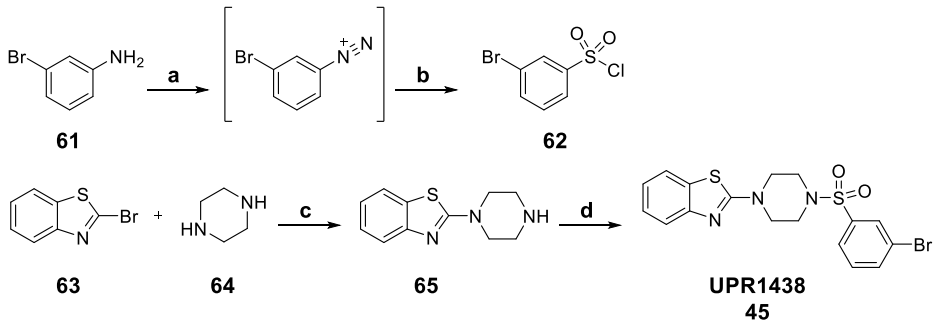

Scheme 8: *Total synthesis of* ***UPR1438****. Reagents and conditions: a) $NaNO_2$, HCl, H_2O, 0°C b) $SOCl_2$,CuCl, H_2O, 0°C, yield = 21% c) CuI, K_2CO_3, DMF, 80°C, yield = 61% d) Et_3N, Pyridine/THF, 0°C, yield = 26%.*

4.5.UPR1440 (**46**) and UPR1437 (**47**)

As shown in schemes 9 and 10, **UPR1438** was used as a starting point for the synthesis of two inhibitors carrying the nitrile warhead, differing the one from the other, by the presence of a conjugated double bond between the phenyl ring and the nitrile. The conversion of **UPR1438** to **UPR1440** was performed with a Heck cross coupling. The product of the reaction was a mixture of the two isomers E and Z; purification with column chromatography provided a sufficient amount of pure **UPR1441** (then recrystallized), while the rest of the product eluted as mixture was used for the synthesis of **UPR1437** (the ratio E/Z for the coupling was not determined).

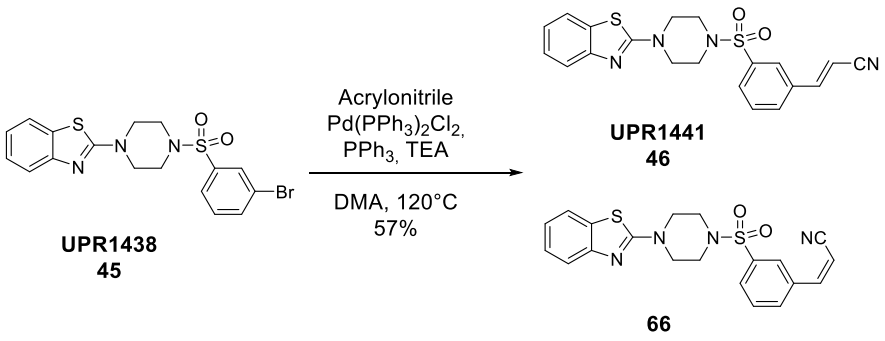

Scheme 9: *Total synthesis of* ***UPR1441****. Total yield for the mixture E+Z = 59 %. Yield for the pure* ***UPR1441*** *= 11%.*

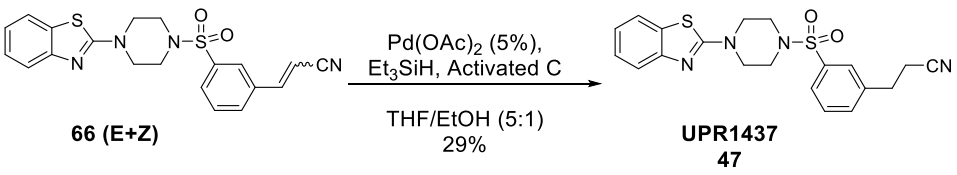

Scheme 10: *Total synthesis of* ***UPR1437****. Reagents and conditions. The target molecule was obtained from the mixture of the two isomers* ***66*** *by the catalytic reduction of the conjugated alkene*

Mixture 66 was converted in the final product **UPR1437** by the reduction of the double bond catalyzed by Palladium diacetate on activated charcoal (5%), using triethylsilane as a source of hydrogen.

4.6.UPR1442 (**48**)

UPR1442 was a first attempt to investigate inhibitory activity changes due to modifications in the lipophilic portion of the compound. The structure is an alteration of compound **UPR1438**, in which the benzothiazole-piperazine moiety is replaced by two chains, while the *m*-bromophenylsulfonyl moiety remains unchanged. Noteworthy, the available X-ray structures of NAAA show the presence of a side-pocket in the narrow hydrophobic channel that accommodates the benzothiazole-piperazine scaffold of **ARN19702**. This cavity, which is partially occupied by the methyl group on the piperazine ring of the co-crystallized inhibitor, is lined by hydrophilic residues which form polar interactions with molecules of water conserved in almost all the X-ray structures. Rational for the design of this compound is to try to make polar interactions in the hydrophilic pocket found in the X-ray structures. For this reason, one of the chains of UPR1442 is functionalized with a primary amide, while the other is completely lipophilic. The synthesis starts with the reduction of 3-phenylpropanal, and the resulting alcohol (**68**) is converted into the related tosil ester (**69**), that is then used to alkylate the piperidin-2-one. Key step of this synthesis is the hydrolysis of the *N*-substituted lactam **70** to obtain compound **71**: the hydrolysis performed with strong basic conditions (NaOH concentrated, reflux) followed by a precipitation of the product in acetone provided the δ-aminoacid, that was then sulfonylated with compound **62** (prepared as shown in scheme 3). The conversion of **72** in **UPR1442** was finally obtained by reaction with pivaloyl chloride to make a mixed anhydride in situ, followed by the addition of ammonium chloride in basic environment.

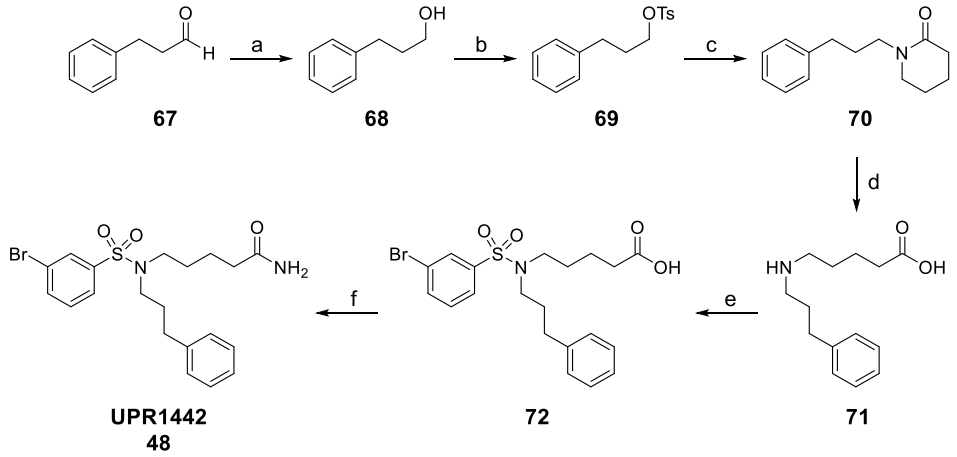

Scheme 11: *Total synthesis of* ***UPR1442****. Reagents and conditions: a) $NaBH_4$, MeOH, 0°C for 30 min, yield = 81% b) Tosyl chloride, Pyridine, rt for 15 min, yield = 76% c) Valerolactam, NaH, NaI (cat.), DMF, 0°C to rt overnight, yield = 64% d) NaOH, H_2O, rt overnight, then 100°C for 48h e)* ***Compound 62****, Et_3N, THF/MeOH, rt for 5h, yield = 34% f) Pivaloyl chloride, Et_3N, dry THF 0°C, 2h, then NH_4Cl, overnight, yield = 14%.*

4.7.UPR1443 (**49**)

The idea behind UPR1443 was to take the scaffold of compound **ARN19702** and to introduce two modifications: a warhead (the nitrile to targeting the catalytic cysteine) and a secondary lipophilic substituent. The synthetic pathway starts from 2-bromobenzo[d]thiazole (**63**) and ethyl isonipecotate (ethyl piperidine-4-carboxylate, compound **73**), that were coupled using the same Ullmann's conditions that were used for compound **65**. Successive steps included the reduction of the ethyl ester to the related alcohol **75** using $LiAlH_4$, and the subsequent conversion into the alkyl iodide **77**. Compound **77** was then alkylated with ethyl phenylacetate (non-stereoselective reaction), and the target molecule **49** was obtained by the coupling reaction of carboxylic acid **79** and 2-aminoacetonitrile performed in presence of 2-(1H-Benzotriazole-1-yl)-1,1,3,3-tetramethylaminium tetra-fluoroborate (TBTU).

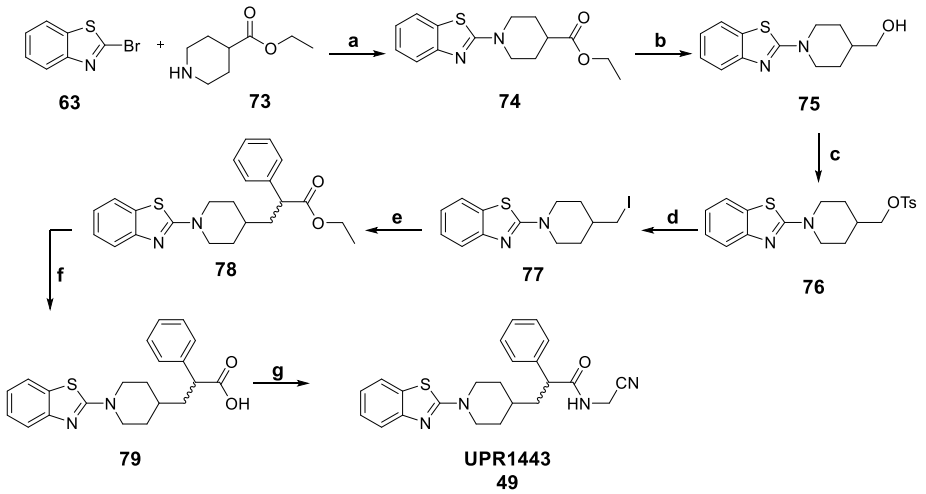

Scheme 12: *Total synthesis of* ***UPR1443****. Reagents and conditions: a)CuI, K_2CO_3, DMF, 75°C for 3.5 h, yield = 87 % b) $LiAlH_4$, dry THF, 0°C for 15 min, yield = > 98 % c) Tosyl chloride,*

2,6-lutidine, DMAP, 40°C for 5 h, yield = 53 % d) NaI, Acetone, reflux for 6h, yield =79 % e) Phenylacetic acid ethyl ester, LiHMDS, dry THF, -50°C, yield = 31 % f) KOH, THF/H_2O, rt for 48 h, yield = 97 %, g) Aminoacetonitrile, TBTU,Et_3N, DMF, 0°C to rt in 20 h, yield = 63 %.

5. Beyond the inhibition: NAAA catalysis mechanism

5.1. Aim of the project

X-ray coordinates for different orthologous NAAA (human, rat and rabbit) were published only in 2018. Most of the efforts in the study of NAAA until that day were aimed at the study of the biological role, especially through the design and the use of inhibitors, while the only molecular characterization was published by Ueda and coworkers.[58] For this reason, the catalytic mechanism of NAAA, and the substrates preferences were not deeply studied.

In this part of this project on NAAA investigation, conduct in the department of Anatomy and Neurobiology at the University of California, Irvine, I developed synthetic procedures for the chemical synthesis of FAEs, and a protocol for the investigation of NAAA substrate affinity. The objectives of this part of the PhD research work were the investigation of the catalytic mechanism of the enzyme and the comprehension of the molecular basis of substrate recognition by NAAA. The experimental results of this project, also supported by the results of molecular modelling studies, provide important information that can be translated to the study of new inhibitors, in order to achieve higher potency and selectivity.

5.2.Synthetic Fatty Acid Ethanolamides

With the specific intent to systematically investigate the effect of modifications to the acyl chain and to the ethanolamide portions of the substrate on the substrate selectivity of NAAA, a library of Fatty Acid Ethanolamides was prepared. Given the easy structure involved, the only synthetic step regarded the condensation of the fatty acid and the ethanolamine, to obtain the related amine.

For all the substrates synthesized in this work two possible protocols were adopted:

- *Acyl substitution:*

  For fatty acids whose chlorides were commercially available, the synthetic strategy involved the direct acyl substitution using ethanolamine. This strategy provided compound with almost quantitative yields in little amount of time, without any particular care; due to the much higher nucleophilicity of the amine compared to the hydroxyl group, no protection was needed for the -OH, and no byproduct was detected in any product obtained with this strategy.

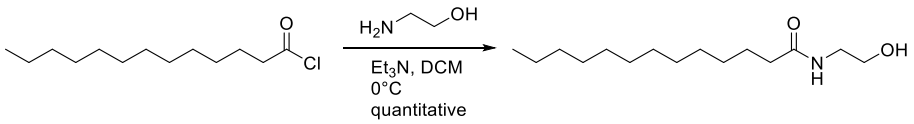

Scheme 13: *Nucleophile acyl substitution on fatty acid chlorides. The reaction allow to obtain quantitative product, in one fast step.*

- *Coupling reaction:*

The amide bond synthesis using coupling agents was the preferred strategy when the related chloride was not commercially available. This strategy, developed for peptide synthesis, allows to prepare amides directly from fatty acids, through a mechanism in which the fatty acid is activated in situ. Among the wide range of coupling agents, 2-(1H-Benzotriazole-1-yl)-1,1,3,3-tetramethylaminium tetrafluoroborate (**TBTU**) was chosen, used together with 1-hydroxybenzotriazole (**HOBt**). Yields obtained following this procedure are lower than the ones from the previous strategy (50-70%).

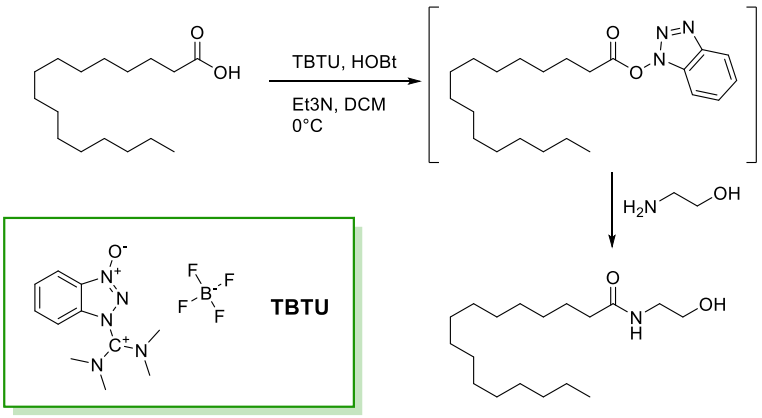

Scheme 14: *synthetic approach with coupling agent TBTU (green label): the reaction is made up by an initial activation of the fatty acid through the formation in situ of the benzotriazolyl-activated ester, followed by the substitution with the desired amine.*

Thanks to these two different strategies, a small library of Fatty Acid Ethanolamides was synthesized (including PEA, Figure 23). Saturated FAEs (PEA derivatives) were synthesized in a length range from tridecanoyl-ethanolamide **80** (13 carbon atoms) to stearoylethanolamide **84** (18 carbon

atoms), while monounsaturated FAEs were prepared in a length range from pentadecenoyl ethanolamide **85** (15 carbon atoms) to eicosenoyl ethanolamide **89** (20 carbon atoms).

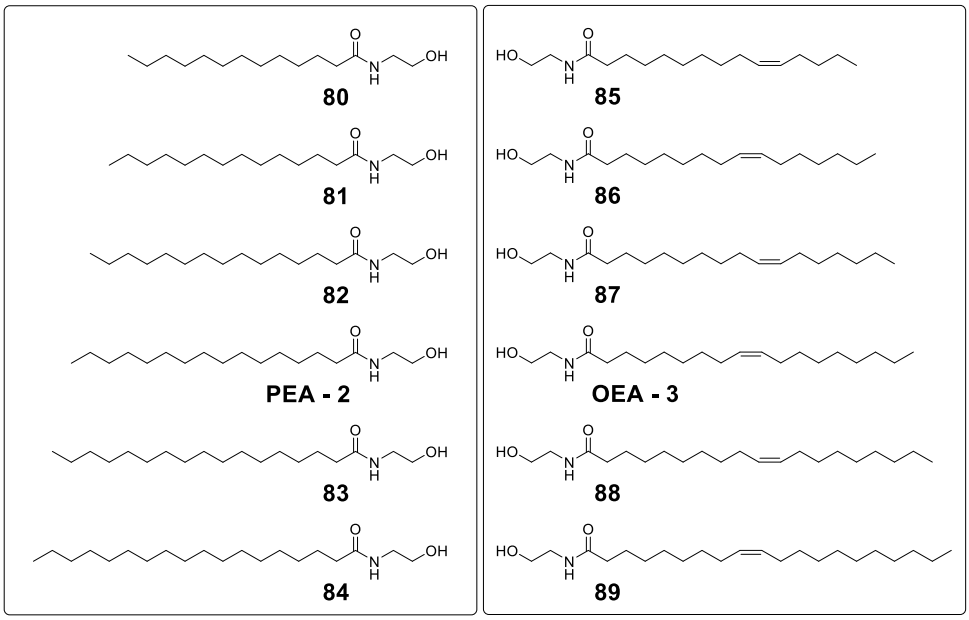

Figure 23: *The library of FAEs synthesized to investigate the role of the acyl chain for the recognition by NAAA: the saturated FAEs (PEA derivatives) on the left, and the monounsaturated FAEs on the right.*

5.3.Substrates kinetic analysis – the length of the chain

The chosen approach for the study of NAAA activity was developed around the quantification of the enzyme hydrolysis products, in order to build the Michaelis-Menten isothermal curve for each substrate. All the substrates in this study were incubated in a concentration range from 1 μM to 200 μM with a lysosomal extract from Heck-293 cells overexpressing rat NAAA. Fatty acid released by the enzyme were extracted from the buffer medium and quantified in LC/MS spectrometry in the presence of a suitable internal standard. Essential kinetic parameters, Michaelis Menten constant (Km) and the maximum reaction rate (Vmax) were extrapolated from the MM curves, and the term of comparison between the substrates was the calculated ratio Vmax/Km.

The study of the hydrolysis kinetics mediated by NAAA was investigated starting by saturated FAEs. As shown in Table 2, modifications of the length of the acyl chain significantly affected the catalytic efficiency. Compounds characterized by a shorter acyl chain than PEA (compounds **80**, **81** and **82**) showed lower Vmax and higher Km, and an almost identical trend resulted from the longer saturated FAEs (**83** and **84**). On the other hand, PEA resulted to be the substrate with the best Vmax/Km ratio, around 5 times higher than **82** (15 carbons) and **83** (17 carbons), and more than 150 times compared to **81**. For compounds **80** and **84**, NAAA activity resulted to be too low to quantify the product.

Compound	Km (μM)	Vmax (μM/s)	Vmax/Km (s^{-1})
80	—	—	< 1.00 x10^{-6}
81	72.86	1.20 x10^{-3}	1.65 x10^{-5}
82	25.46	8.99 x10^{-4}	3.53 x10^{-5}
PEA - 2	19.81	3.43 x10^{-3}	1.73 x10^{-4}
83	6.54	2.45 x10^{-4}	3.75 x10^{-5}
84	—	—	< 1.00 x10^{-6}
85	54.29	6.39 x10^{-4}	1.18 x10^{-5}
86	72.81	9.25 x10^{-4}	1.27 x10^{-5}
87	128.18	7.57 x10^{-3}	5.91 x10^{-5}
OEA - 3	167.28	1.60 x10^{-3}	9.55 x10^{-6}
88	160.95	6.90 x10^{-4}	4.29 x10^{-6}
89	231.70	6.56 x10^{-5}	< 1.00 x10^{-6}

Table 2: *Kinetic parameters for saturated and monounsaturated FAEs involved in this work*

After the results obtained for saturated derivatives, we decided to move on OEA derivatives, to evaluate the effect of an unsaturation in the fatty acid chain on the recognition by the enzyme. OEA derives from oleic acid, a fatty acid from the series of the Δ-9 (a single unsaturation between carbon 9 and carbon 10 in the chain). Because of only natural monounsaturated fatty acid are available with the double bond in the same position, for the non natural the choice was to use compound from the series of the Δ-10 (to put the double bond, located between carbon 10 and carbon 11, as close as possible to the one in the natural fatty acids).

Kinetic parameters for this second series are less precise, because the MM curves didn't reach the plateau for the range of substrate concentration used for the assay.

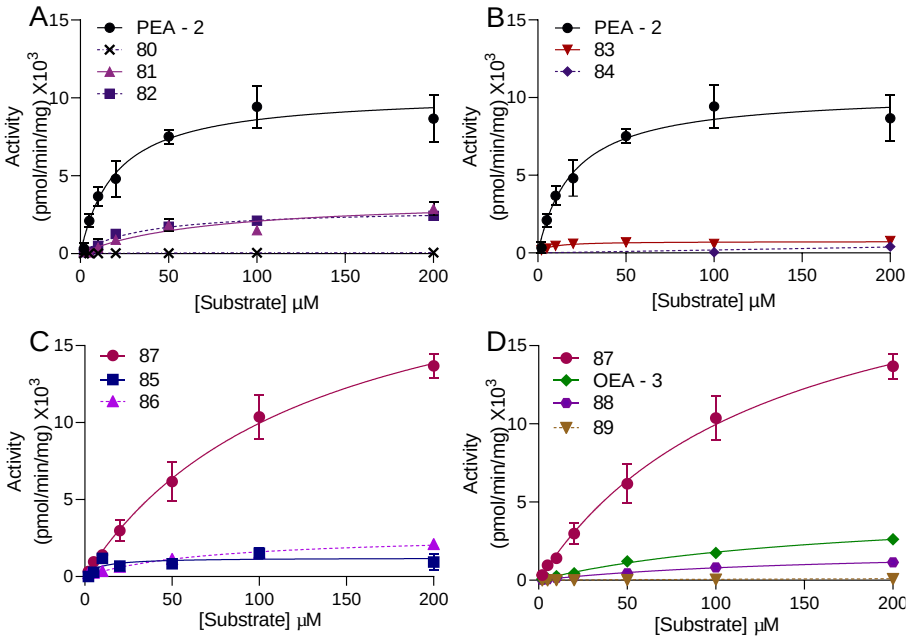

Figure 24: *Michaelis-Menten curves for A) PEA and shorter FAEs B) PEA and longer FAEs C) Compound **59** and shorter FAEs D) Compound **59** and longer FAEs.*

Nevertheless OEA, known to be a substrate not as good as PEA for NAAA, showed a lower Vmax compared not only to PEA, but also to compound **87** ((Z)-*N*-2-(hydroxyethyl)heptadec-10-enamide), that not only demonstrated to be a better substrate than OEA, but it also showed better Vmax/Km ratio than its saturated analogue **83**. General Vmax/Km ratio is lower for this second series compared to PEA derivatives, but the trend is more or less the same, with **87** FAE as best substrate. Notably, the experimental results obtained were in agreement with molecular modelling studies, performed to evaluate the effect of the length of the acyl chain and the presence of an unsaturation on the dynamic stability of the complexes between NAAA and the FAEs considered in this study. More specifically, molecular dynamics simulations revealed that while the interaction between the enzyme and the

natural substrate PEA is characterized by a high stability, other ethanolamides with a non-optimal acyl chain length form unstable complexes with NAAA, impeding the maintenance of interactions that would favor the catalytic process.

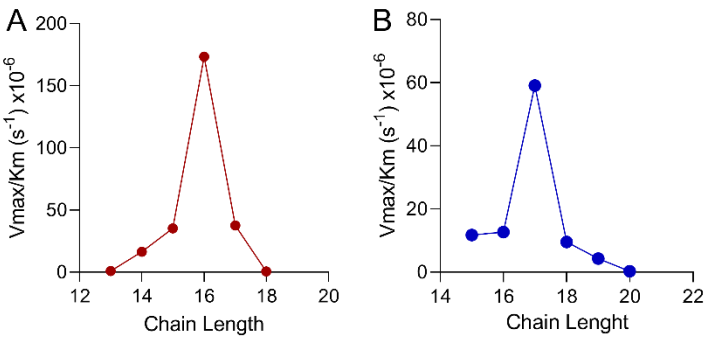

Figure 25: *comparison of the Vmax/Km values for A) PEA and B) OEA derivatives.*

5.4.Substrates kinetic analysis - the hydroxyl group

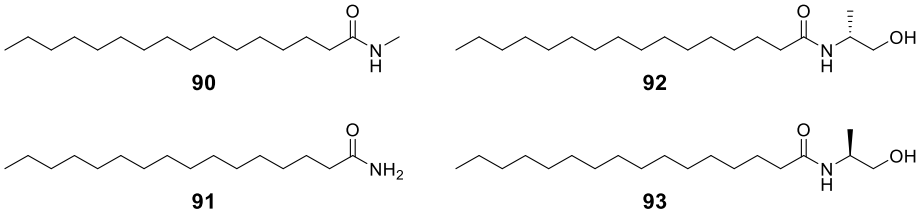

Figure 26: *PEA derivatives designed to investigate the role of the ethanolamine moiety:* ***90*** *and* ***91*** *were used to study the role of the hydroxyl group, while* ***92*** *and* ***93*** *showed the stereoselectivity in NAAA active site.*

To investigate the role of the hydroxyethyl moiety during the catalysis, 4 compounds were prepared from the structure of PEA, by introducing modification on the polar head. For this reason *N*-methylpalmitamide (**90**) and palmitamide (**91**) were prepared to understand in which way the absence of the hydroxyl group could affect the catalysis, by comparison with PEA. At the same time the two enantiomers (R)-*N*-2-hydroxypropyl-palmitamide (**92**) and (S)-*N*-2-hydroxypropylpalmitamide (**93**) were synthesized to investigate the ability of the enzyme to allocate bulkier motives in proximity of the active site, and the possible stereoselectivity between them.

Compound	Km (μM)	Vmax (μM/s)	Vmax/Km (s^{-1})
90	**18.08**	**8.54×10^{-3}**	**4.72×10^{-4}**
91	**18.29**	**5.29×10^{-3}**	**2.89×10^{-4}**
92	**19.32**	**4.69×10^{-3}**	**2.43×10^{-4}**
93	**32.34**	**1.94×10^{-2}**	**5.99×10^{-4}**

Table 3: *Kinetic parameters for compounds 90–93*

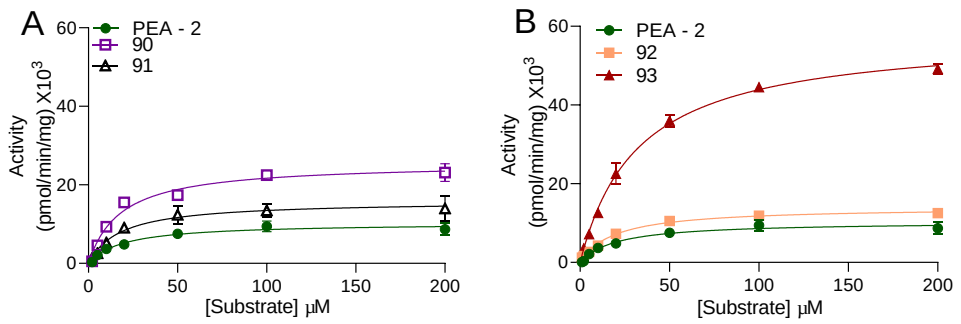

*Figure 27: Michaelis-Menten curves for compounds A) **90** (black triangles) and **91** (purple squares) and B) **92** (orange squares) and **93** (red triangles).*

The Michaelis Menten analysis shows that, compared to PEA, the catalytic efficiency is higher for the more hydrophobic substrate *N*-methylpalmitamide suggesting that the ethanolamine portion plays a minor role during the catalytic process. As shown in figure 27A, while Km remains in the same range, Vmax value is increased by the deletion of the alcoholic group, reaching a value that is 2.5-fold higher for *N*-methylpalmitamide. Importantly, these data have helped to elucidate the catalytic mechanism of NAAA, and support the computational results that show that, similarly to PEA, *N*-methylpalmitamide is efficiently hydrolyzed through a mechanism in which the protonation of the leaving group represents the limiting step of the process.[66]

The introduction of the methyl on the polar head provoked the same effect, but in a different range of values. For the two enantiomers **92** and **93**, the Km resulted to be close to PEA's, while Vmax increased from 1.5-fold (for compound **92**), to 6-fold (for compound **93**). This suggests the idea that in the surroundings of the active residue there is enough space to allocate a branched residue, with a preferred configuration. It is not to exclude a synergistic effect of the alkyl chain, that in the right configuration may be

able to force the hydroxyl group in a preferred configuration that enhances the catalysis ratio (Figure 27B).

6. Development of a hybrid FAAH inhibitor-MT agonist

A side project in which I was involved concerned the preparation of a hybrid compound with a dual biological activity. Compounds **94** and **95** were developed to act as agonist on the melatonin receptors, and as an inhibitor on the enzyme FAAH.

6.1.Glaucoma

Glaucoma is a neuropathic disease of the eye, that displays with an increase of the intraocular pressure, followed by a progressive degeneration of retinal ganglion cells. These effects lead to visual field impairment and blindness as a consequence of optic nerve damage.[105] Glaucoma is usually treated with a daily in-situ administration of multiple drugs, like β-adrenergic antagonists, α2-agonists, prostaglandin analogues, carbonic anhydrase inhibitors, and myotic agents acting on the parasympathetic system.[106] These drugs are usually co-administrated and, for this reason, are available in the market as fixed-combination products. Drugs in fixed combination are preferred to multiple administration of different products, because of their easy way of use, enhancing the patients compliance. An increased adherence to the treatment, as well as the improved satisfaction of the patients, are of critical importance for the success of the therapy, while the lack of continuity in the treatment (usually due to difficulties in following a specific therapeutic plan involving different treatments) leads to a lower treatment effectiveness, responsible for the progression of the disease. Moreover, the simplification of the treatment reduces the exposure

of the eye to irritating agents, and it also may result in a less expensive treatment.[107] On the other hand, the administration of a fixed-combination of drugs is somehow disadvantageous for the patient, due to a less flexible therapy, that cannot be personalized. Interactions between the different drugs in the formulation are also possible, reducing the stability of the formulation and, in the worst case, leading to unexpected adverse effects. For these reasons, the development of a hybrid active compound, able to interact with the different targets that take a part in the regulation of intraocular pressure, would overcome the limitations of other approaches, combining the improved compliance related to the administration of a single formulation and the higher stability which may lack in medications combining different ligands.

6.2.Melatonin and FAAH role in glaucoma

Melatonin (MLT) showed significant effects in lowering the intraocular pressure.[108,109] It is primarily produced by the pineal gland, reaching the highest concentrations at night. Recognized effects are ascribed to melatonin, like in the CNS, where it regulates the circadian rhythms and neuroendocrine processes. In the periphery MLT is related to the regulation of the immune system, glucose balance and cardiovascular homeostasis. Targets of MLT activity in mammals are two G-protein coupled receptors named MT1 and MT2.[110],[111] MLT is locally released in the eye and its receptors are expressed in many areas in the eye, like in the retina, the ciliary body, the cornea and in the sclera.[112] Administration of MLT showed a transient reduction of the intraocular pressure in both normotensive and hypertensive rodents,[113,114] monkeys[115] and humans,[108,116] exerting a

synergistic effect with the adrenergic system, increasing the expression of the α2 receptor, while reducing the expression of the β2 receptors, both responsible for the control of the production and drainage of the aqueous humor within the eye.[117] MLT effects were also confirmed by the activity of synthetic MLT receptor agents,[109] such as agomelatine,[118] 5-MCA-NAT,[114] and IIK7,[115] that showed the same intraocular pressure lowering effects.

As for MLT administration, reduction of intraocular pressure was observed in cannabis users, and after the administration of endogenous or exogenous cannabinoids, such as AEA, D9-THC, or the synthetic CB agonist WIN55212-2.[119],[120] In fact, the enzyme and the receptors responsible for the synthesis, the degradation and the activity of endocannabinoids are expressed in the eye tissues.[121] The effect exerted by topical AEA was counteracted by the simultaneous administration of the CB1 receptor antagonist rimonabant, supporting the idea that CB1 receptor is responsible for the intraocular pressure reduction effect of AEA.[122] However, secondary cannabinoid actions are mediated by the activation of the TRPV1 channel and the orphan receptor GPR55 and by arachidonic acid derivatives.[123] Experimental findings suggest that the endocannabinoid system participates to the control of intraocular pressure by modulating the production and the outflow of aqueous humor. The serine-hydrolase enzyme FAAH, which is the main AEA-degrading enzyme,[124,125] has been described as responsible for the regulation of diurnal variation of IOP. FAAH is expressed with a circadian rhythm, and it is also responsible for the regulation of the levels of *N*-arachidonoyl glycine, that reduces the intraocular pressure through the activation of the GPR18 receptor.[126] Despite the relevance of FAAH, the

effects of FAAH inhibitors on intraocular pressure has never been investigated.

6.3.Dual-activity compounds

The principal limitation of the mainstream treatments for glaucoma were discussed in paragraph 6.1

In this study, we designed and prepared novel dual-acting compounds, behaving both as MT receptor agonists and FAAH inhibitors. The design was made by combining the pharmacophore elements required to activate MT receptors, with those that are essential to achieve FAAH inhibition, exploiting the structural elements of known compounds.

The 15 compounds[127] designed and synthesized were then tested on human MT1 and MT2 receptors to evaluate their binding affinity and intrinsic activity, on rat FAAH for their inhibitory potency and in a rabbit model of ocular hypertension to investigate their intraocular pressure lowering potential.

The most potent derivatives from this study, compound **94** and **95**, showed a higher activity than the benchmark inhibitor dorzolamide (Figure 28). This effect may be due either to the higher lipophilicity of the new derivatives, or to the synergistic effect at the two targets. The combination of melatonin and the FAAH inhibitor (**URB597**) gave the same effect at 60 min, showing no additivity, but maintaining the effect for longer times (120 min). The most active compounds at 120 min showed sub-nanomolar IC50 values on FAAH, suggesting a greater importance of FAAH inhibition activity. In conclusion, the combination of melatoninergic activity with potent FAAH inhibition appeared to have a significant role to achieve persistent intraocular pressure

lowering effect. These compounds are an attractive potential alternative to the traditional therapeutic approach for the treatment of ocular hypertension, offering a promising option for the treatment of glaucoma. This combination may also represent a great choice, thinking about the retinal-protective role described for endocannabinoids,[128] and the neuroprotective role ascribed to melatonin;[109] the reduction of neurodegeneration in the eye, may positively modulate pineal melatonin production that could improve circadian rhythm related functions, thus ameliorating conditions often present in glaucomatous patients such as sleep disorders and depression.[127]

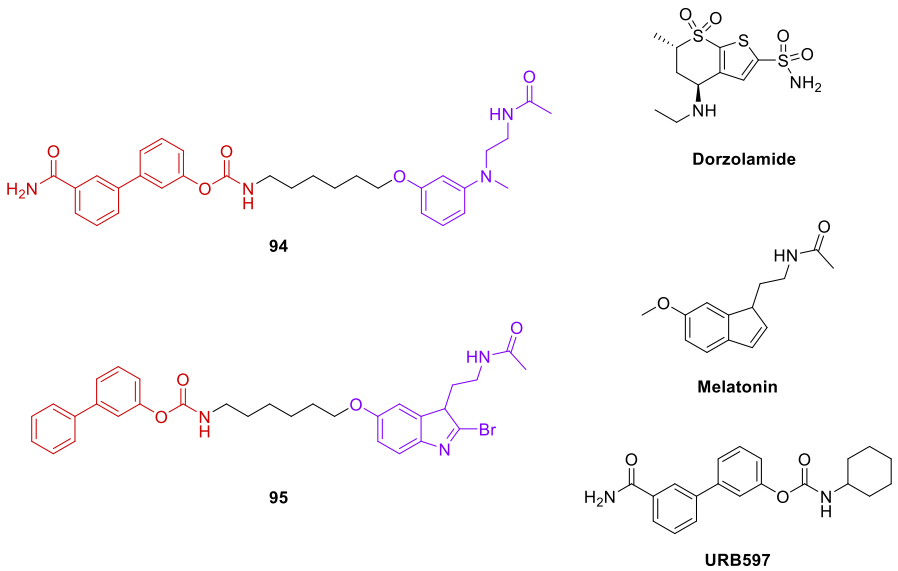

Figure 28: *the structures of compound **94** and **95**,the most potent from this study. The moieties responsible for MT agonism are highlighted in purple, while the fragments that act as FAAH inhibitors are coloured in red. On the right there are the structures of the benchmark compounds for this study. The structures of melatonin and URB597 are clearly recognizable in compound **94** and **95**.*

6.4.Total synthesis of compound **95**

The synthetic approach for the preparation of compound 95 is a convergent pathway that is based on the linkage of the biphenyl ring to the serotonin-like moiety through a hexyl chain.

The first step is the activation of the commercial available [1,1'-biphenyl]-3-ol, using the 4-nitrophenyl chloroformate, in order to obtain the related carbonate **97** (Scheme 15).

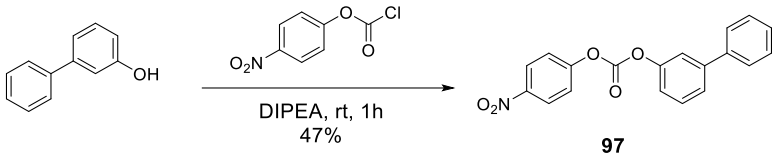

*Scheme 15: Synthesis of compound **97***

N-acetylserotonin is involved in a nucleophilic substitution with the alkyl bromide **98**, yielding the N-Boc derivative **99**. The following modifications are the insertion of a bromine on C2 of the indole ring (**100**) and the cleavage of the protecting group in the terminal amine of the hexyl chain. The free amine is not isolated, but used as crude compound in the final step. The substitution of the 4-nitrophenol with the alkylamine yielded the carbamate **95** (Scheme 16).

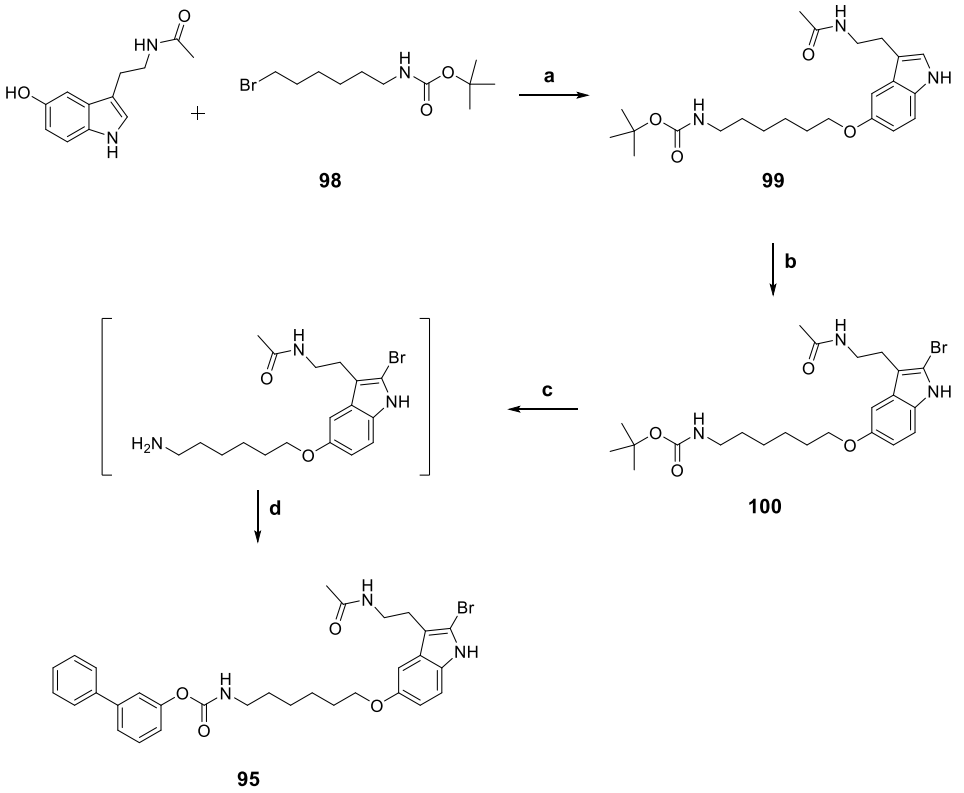

*Scheme 16: Total synthesis of compound **95**. Reagents and conditions: a) K2CO3, dry CH3CN, reflux 1h, then NaI (cat.), reflux 20 h, yield = 59% b) Trimethylphenylammonium tribromide, dry THF, rt for 30 min, yield = 59% c) Trimethylsilyl bromide, dry CH3CN, rt 1h d) Compound **97**, Et3N, dry DCM, dry DMF, 0°C to rt 3h, yield = 83%.*

7. Conclusions

This work was developed around a comprehensive study of the enzyme *N*-acylethanolamine acid amidase, with the development of a new class of potential covalent inhibitors, and the kinetic study of substrate selectivity.

The development of new inhibitors concerned the use of a not-yet tried warhead, the nitrile moiety, in an attempt to covalently bind the catalytic cysteine of this hydrolase. This project was also focused on the design and synthesis of novel inhibitors combining the nitrile reactive group and scaffolds modelled to fit the binding site of NAAA. To this aim, different scaffolds modelled, exploiting not only the SAR of known inhibitors, but also the information obtained from crystallographic studies. All the inhibitors described in this project are now under in-vitro investigation (no results available at the moment).

Besides the design and synthesis of novel potential NAAA inhibitors, a systematic study to elucidate the enzyme substrate selectivity was performed. A total of 16 fatty acid ethanolamides, differing for the chain length, or carrying modifications on the ethanolamine moiety were prepared. These molecules were tested with a fixed amount of rat NAAA, building the relative Michaelis-Menten isothermal curve, and calculating the enzyme fundamental parameters Km and Vmax. These two values were used to rank the substrates, obtaining information about the structural requirements to achieve a better interaction with NAAA. In particular, the length of the substrates appears to be a fundamental parameter: small changes in the chain length led to less recognized substrates, both for saturated and monounsaturated FAEs.

The introduction of a methyl on the ethanolamine moiety, yielded a NAAA hydrolysis rate higher than PEA's, showing a stereoselectivity for the (S)-configuration (Vmax 6-times higher than PEA) over the (R)-enantiomer. In the end, the deletion of the hydroxyl group of PEA led to an increase in NAAA hydrolysis rate, suggesting that the hydroxyl group of the substrate plays a minor role in the NAAA-catalyzed hydrolysis of PEA.

Not directly linked to NAAA investigation, a side project in which I was involved regarded the designed and the synthesis of compounds with dual activity on FAAH and MT receptors. The results of this study show a possible clinical application of compounds involved in the inhibition of FAEs catabolism.

8. Experimental Section

8.1.General Information

All chemicals were used as received, without any further purification, unless stated otherwise. Anhydrous reactions were performed under a steady overpressure of argon or nitrogen delivered through a balloon; flasks for anhydrous reaction were dehydrated in a vacuum oven. Solvents were stored and purified following standard procedures. Thin-layer chromatography (TLC) analysis was conducted on HPTLC aluminum sheets silica gel 60, F254 (Sigma-Aldrich), or Kieselgel 60 F254 (DC-Alufolien, Merck); compounds were visualized by dipping in a solution of p-anisaldehyde (2.5% v/v), prepared as follows: 3.7 mL of p-anisaldehyde were added to 135 mL of absolute ethanol containing 5 mL of concentrated sulfuric acid and 1.5 mL of glacial acetic acid. The staining solution was stored in a jar covered with aluminum foil at 4ºC. 1H NMR spectra for compounds prepared at Università di Parma were recorded on a Bruker 300MHz Avance, or a Bruker 400MHz Avance; 1H NMR spectra for compounds prepared at University of California, Irvine were recorded on a Bruker DRX400 (400 MHz). Chemical shifts (δ scale) are reported in parts per million (ppm), referenced to tetramethylsilane (TMS, 0.00 ppm) or the residual solvent signal. 1H NMR spectra are reported in the following order: number of protons, multiplicity and approximate coupling constant (J value) in Hertz (Hz), and a clear attribution of proton signals is provided. Signal multiplicities were characterized as s (singlet), d (doublet), dd (doublet of doublets), t (triplet), dt (doublet of triplets), q (quartet), quint (quintet) m (multiplet), br (broad signal). Mass spectra were recorded on an Agilent 6410

Triple Quad LC/MS system with an ESI interface. The purity of final compounds prepared in Università di Parma was assessed on a TSQ Quantum Access Max (Thermo Finnigan, USA) equipped with a triple quadrupole; the purity of final compounds prepared in University of California, Irvine was assessed by liquid chromatography/tandem mass spectrometry (LC/MS-MS) using an Agilent 6410 Triple Quad system (Agilent Technologies., Wilmington, DE). Prior to analyses, samples were prepared in methanol at a final concentration of 5 µg/mL. Analytes were separated on an Agilent Zorbax Eclipse XBD C18 column (2.1x50 mm, 1.8 µm particle size) by gradient elution. The flow rate was 0.4 mL/min, and the injected volume was 2.0 µL. Solvent A was water and solvent B was methanol, both additioned of 0.25% v/v acetic acid and 5 mM ammonium acetate. Gradient conditions A: t(0 min): 10% A: 90% B; t(2 min): 5% A: 95% B; t(3 min): 10% A: 90% B. Purity results are presented as tR (min) and relative chemical purity (%). All tested compounds were >95% pure.

tert-butyl 3-((4-bromobenzyl)oxy)azetidine-1-carboxylate (52)[98]

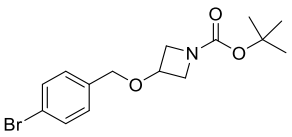

Procedure: to an ice cold (0°C) solution of tert-butyl 3-hydroxyazetidine-1-carboxylate (300 mg, 3.46 mmol), bromobenzyl bromide (866 mg, 3.46 mmol) and a catalytic amount of NaI (26 mg, 0.17 mmol) in DMF, NaH (139 mg, 3.46 mmol) is added portion wise. The mixture is stirred overnight. The mixture is then cooled again, and MeOH is added dropwise; after that the solution is poured into an ammonium chloride solution and extracted with ethyl ether, washed with water and brine, and dried over Na_2SO_4. The crude is purified with column chromatography (PetEt : EtOAc = 4:1 v/v), to obtain 454 mg (77%) of the target compound.

^{1}H-NMR (300 MHz, Chloroform-*d*): 7.46 (d, 2H, *J* = 7.9 Hz), 7.17 (d, 2H, *J* = 8.1 Hz), 4.37 (s, 2H), 4.28 (m, 1H), 4.05 (dd, 2H, *J* = 9.3, 6.4 Hz), 3.85 (dd, 2H, *J* = 9.4, 4.3 Hz), 1.43 (s, 9H).

tert-butyl 3-([1,1'-biphenyl]-4-ylmethoxy)azetidine-1-carboxylate (54)[98]

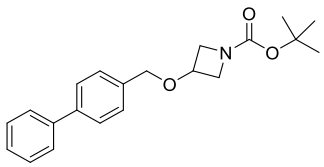

Procedure: in a reaction flask equipped with a silicon septum and a balloon full of argon, tert-butyl 3-((4-bromobenzyl)oxy)azetidine-1-carboxylate (454 mg, 1.33 mmol), phenylboronic acid pinacol ester (414 mg, 2.03 mmol) and K_2CO_3 (712 mg, 5.31 mmol) are dissolved using a mixture of 1,4-dioxane and water (4 : 1 v/v). Tetrakis(triphenylphosphino)palladium(0) (46 mg, 0.13 mmol) is added to the reaction vessel, and the mixture is refluxed. The mixture is then diluted with ethyl acetate, washed with water and brine and dried over Na_2SO_4. The crude product was purified with column chromatography (PetEt : EtOAc = 4 : 1 v/v), to obtain 307 mg of pure compound (68%).

^{1}H-NMR (400 MHz, Chloroform-*d*): 7.57 (m, 4H), 7.37 (m, 5H), 4.47 (s, 2H), 4.32 (m, 1H), 4.07 (dd, 2H, *J* = 9.7, 6.7 Hz), 3.88 (dd, 2H, *J* = 9.8, 4.3 Hz), 1.43 (s, 9H).

3-([1,1'-biphenyl]-4-ylmethoxy)azetidine (55)[98]

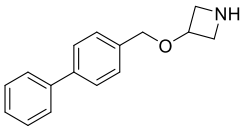

Procedure: trifluoroacetic acid (1.03 g, 9.04 mmol) is added to a flask containing ice-cold tert-butyl 3-([1,1'-biphenyl]-4-ylmethoxy)azetidine-1-carboxylate (307 mg, 0.90 mmol) dissolved in DCM, and the reaction is stirred at room temperature for 6 hours. The mixture was dried under vacuum and rinsed with DCM several times to remove the excess of the TFA, then the crude was purified on silica gel (DCM : EtOAc = 9 : 1, then 100% MeOH saturated with NH_3) to get 216 mg (>98%) of pure product.

^{1}H-NMR (300 MHz, Methanol-*d4*): 7.59 (m, 4H), 7.39 (m, 5H), 4.53 (s, 2H), 4.21 (m, 2H), 4.00 (m, 2H).

3-([1,1'-biphenyl]-4-ylmethoxy)azetidine-1-carbonitrile (UPR1429 - 43)[98]

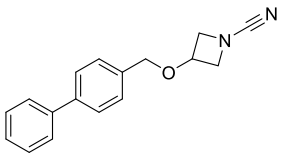

Procedure: 3-([1,1'-biphenyl]-4-ylmethoxy)azetidine (216 mg, 0.90 mmol) is dissolved in DCM, the solution is cooled to 0°C and triethylamine (457 mg, 4.52 mmol) is added. The mixture is stirred for 30 minutes, then cyanogen bromide (192 mg, 1.81 mmol) is added, and the reaction is stirred overnight. The mixture is diluted with EtOAc, washed with saturated $NaHCO_3$, water and brine, and dried over Na_2SO_4. The crude product was purified with column chromatography (PetEt : EtOAc = 3:1 v/v) and recrystallized from heptane to obtain 68 mg of fine white crystals (28%). MS calc.: 264.13, found: 265.09 m/z $[M+H]^+$.

^{1}H-NMR (400 MHz, Chloroform-*d*): 7.59 (m, 4H), 7.45 (m, 2H), 7.37 (m, 3H), 4.49 (s, 2H), 4.42 (m, 1H), 4.24 (dd, 2H, *J* = 8.9, 7.8 Hz), 4.11 (dd, 2H, *J* = 8.9, 5.0 Hz)

2,5-dioxopyrrolidin-1-yl decanoate (57)

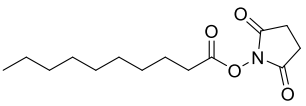

Procedure: decanoic acid (1.213 g, 7.04 mmol) is put in a reaction flask with phosphorous pentachloride (1.460 g, 4.04 mmol) and heated to 170°C for 2 hours. The mixture is dried and washed several times with toluene to remove the $POCl_3$ subproduct. The crude (decanoyl chloride) is dissolved in anhydrous pyridine, and added dropwise to a solution of *N*-hydroxysuccinimide in dry pyridine cooled to 0°C. After 1 hour the reaction is diluted with EtOAc, washed three times with HCl (1M) to remove the pyridine, then saturated $NaHCO_3$, water and brine, and dried over Na_2SO_4. The crude product (1.511 g) is used in the next step without further purification.

^{1}H-NMR (400 MHz, Chloroform-*d*): 2.67 (s, 4H), 2.45 (t, 2H, *J* = 7.4 Hz), 1.59 (quint, 2H, *J* = 7.4 Hz), 1.14 (m, 12H), 0.75 (t, 3H, *J* = 6.5 Hz)

2-(1,3-dioxoisoindolin-2-yl)acetonitrile (60)

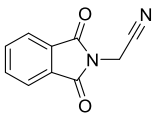

Procedure: phthalimide potassium salt (6.00 g, 32.40 mmol) is suspended in DMF, cooled to 0°C and stirred. Chloroacetonitrile (3.30 g, 43.80 mmol) is added dropwise to the reaction, that is stirred overnight. The reaction mixture is poured into water, forming a white precipitate, that is collected and washed with more water and diethyl ether. The crude product (3.61 g) is used in the next step without any further purification.

^{1}H-NMR (400 MHz, Chloroform-*d*): 7.93 (m, 2H), 7.80 (m, 2H), 4.58 (s, 2H)

***N*-(cyanomethyl)decanamide (UPR-1411 - 44)**

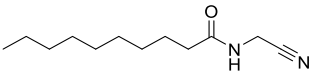

Procedure: 2-(1,3-dioxoisoindolin-2-yl)acetonitrile (481 mg, 2.58 mmol) is suspended in EtOH, and stirred. Hydrazine monohydrate is added to the suspension, and the reaction is stirred overnight. The mixture is filtered to remove the subproduct phthalazine, then 2,5-dioxopyrrolidin-1-yl decanoate (200 mg, 0.83 mmol) is added to the solution and the mixture is stirred overnight. The reaction is diluted with EtOAc, washed with HCl (1M), then saturated $NaHCO_3$, water and brine, and dried over Na_2SO_4. The crude product was purified with column chromatography (gradient from PetEt : EtOAc = 2:1 v/v to PetEt : EtOAc = 45:55 v/v) to obtain 63 mg of target compound (yield = 42%). MS calc.: 210.17, found: 211.11 m/z $[M+H]^+$.

^{1}H-NMR (400 MHz, Chloroform-*d*): 6.13 (s, 1H), 4.19 (d, 2H, *J* = 5.8 Hz), 2.25 (t, 2H, *J* = 7.5 Hz), 1.65 (quint, 2H, *J* = 7.5 Hz), 1.25 (m, 12H), 0.88 (t, 3H, *J* = 6.5 Hz)

3-bromobenzenesulfonyl chloride (62)

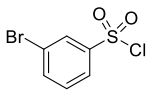

Procedure: Thionyl chloride (9.34 g, 78.51 mmol) is dissolved dropwise in ice-cold water (60 mL), and the mixture is stirred overnight. In a second flask, 3-bromoaniline (3.00 g, 17.44 mol) is suspended in ice-cold concentrated HCl (36%) and $NaNO_2$ (1.81 g, 26.23 mmol) is added to the mixture. CuCl (178 mg, 1.80 mmol) is added to the thionyl chloride, followed by a dropwise addition of the aryldiazonium salt. The mixture is stirred for 2 more hours, than the product is extracted using Et_2O, washed with water and brine, and dried over Na_2SO_4. The crude product is used in the next step without purification.

^{1}H-NMR (400 MHz, Chloroform-*d*): 8.15 (s, 1H), 7.97 (d, 1H, *J* = 7.9 Hz), 7.86 (d, 1H, *J* = 8.0 Hz), 7.52 (t, 1H, *J* = 8.0 Hz).

2-(piperazin-1-yl)benzo[d]thiazole (65)

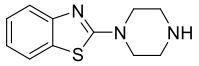

Procedure: to a solution of piperazine (604 mg, 7.01 mmol) in DMF, 2-bromobenzo[d]thiazole (1.00 g, 4.67 mmol), CuI (116 mg, 0.61 mmol) and K_2CO_3 (1.94 g, 14.03 mmol) are added. The mixture is stirred for 2.5 hours at 80°C, than diluted with water and extracted with Et_2O. The organic phased is washed with water and brine, and then dried over Na_2SO_4. The product is purified by column chromatography (DCM : MeOH = 1 : 1 v/v + 1% Triethylamine) to obtain 580 mg of target product (yield = 56%).

^{1}H-NMR (400 MHz, Methanol-*d4*): 7.64 (d, 1H, *J* = 7.8 Hz), 7.48 (d, 1H, *J* = 8.2 Hz), 7.28 (t, 1H, *J* = 7.5 Hz), 7.08 (t, 1H, *J* = 7.3 Hz), 3.60 (t, 4H, *J* = 5.4 Hz), 2.98 (t, 4H, *J* = 5.6 Hz).

2-(4-((3-bromophenyl)sulfonyl)piperazin-1-yl)benzo[d]thiazole (UPR1438 - 45)

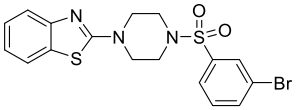

Procedure: 2-(piperazin-1-yl)benzo[d]thiazole (763 mg, 3.48 mmol) is dissolved in an ice cold mixture of dry THF and dry pyridine, and Triethylamine (402 mg, 3.98 mmol) is added to the mixture. 3-bromobenzensulfonyl chloride (635 mg, 2.49 mmol) is dissolved in pyridine, and the solution is added dropwise to the mixture. The reaction is stirred overnight, then diluted with EtOAc, and washed with HCl (1M) several times to remove the pyridine, then water and brine, and dried over Na_2SO_4. The crude product is purified by column chromatography (Pet. Et. : EtOAc = 7 : 3 v/v) and recrystallized from EtOH, to afford 490 mg (45%) of the target compound. MS calc.: 436.99, found: 438.05 m/z $[M+H]^+$.

^{1}H-NMR (400 MHz, Chloroform-*d*): 7.91 (t, 1H, *J* = 1.9 Hz), 7.73 (dt, 1H, *J* = 8.0, 1.3 Hz), 7.69 (dt, 1H, *J* = 7.8, 1.4 Hz), 7.59 (d, 1H, *J* = 7.9 Hz), 7.54 (d, 1H, *J* = 8.1 Hz), 7.42 (t, 1H, *J* = 7.9 Hz), 7.29 (td, 1H, *J* = 7.4, 1.3 Hz), 7.09 (td, 1H, *J* = 7.7, 1.2 Hz), 3.76 (t, 4H, *J* = 5.0 Hz), 3.19 (t, 4H, *J* = 5.2 Hz).

(E)-3-(3-((4-(benzo[d]thiazol-2-yl)piperazin-1-yl)sulfonyl)phenyl)acrylonitrile (UPR1441 - 46)

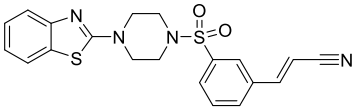

Procedure: UPR1438 (209 mg, 0.48 mmol) is dissolved in dimethylacetamide, followed by triethylamine (97 mg, 0.95 mmol), triphenylphosphine (13 mg, 0.05 mmol) and bis(triphenylphosphine)-palladium dichloride (17 mg, 0.02 mmol). The reaction is stirred at room temperature for 10 minutes, then acrylonitrile (30 mg, 0.57 mmol) is added, and the mixture is stirred at 120°C overnight. The mixture is then allowed to cool down to room temperature, and water is added, resulting in a precipitate. The precipitate is filtered, and the supernatant is extracted using Et_2O. The organic phase is washed with water and brine, dried over Na_2SO_4, and united with the precipitate. The crude product is purified by column chromatography (Pet. Et. : EtOAc = 1 : 1 v/v) to afford 21 mg of pure target compound (E-isomer, yield = 11%) and 95 mg of E- and Z-isomer mixture used for the next step (total conversion = 59%). MS calc.: 410.09, found: 411.12 m/z $[M+H]^+$.

^{1}H-NMR (400 MHz, Dimethylsulfoxide-*d6*): 8.04–7.96 (m, 2H), 7.88–7.66 (m, 4H), 7.43 (d, 1H, *J* = 8.2 Hz), 7.26 (td, 1H, *J* = 7.1, 1.3 Hz), 7.07 (td, 1H, *J* = 7.6, 1.2 Hz), 6.67 (d, 1H, *J* = 16.8 Hz), 3.67 (t, 4H, *J* = 4.8 Hz), 3.10 (t, 4H, *J* = 5.0 Hz).

3-(3-((4-(benzo[d]thiazol-2-yl)piperazin-1-yl)sulfonyl)phenyl)propane-nitrile (UPR1437 - 47)

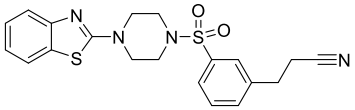

Procedure: Palladium diacetate (2 mg, 0.008 mmol) is dissolved in EtOH, and activated charcoal (20 mg) is added, forming a dark suspension. The E+Z mixture from UPR1440 synthesis (65 mg, 0.158 mmol) is dissolved in a mixture of THF and EtOH, then the dark suspension of Pd/C is added to the stirring solution. Triethylsilane (37 mg, 0.316 mmol) is added dropwise to the mixture. After 2 hours the reaction mixture is filtered over celite, and the resulting solution is dried under vacuum. The crude product is purified by column chromatography (Pet. Et. : EtOAc = 1 : 1 v/v) to afford 25 mg of pure target compound (yield = 38%), recrystallized from EtOH : H2O = 7 : 3 (v/v). MS calc.: 412.10, found: 413.16 m/z $[M+H]^+$.

^{1}H-NMR (400 MHz, Dimethylsulfoxide-*d6*): 7.80–7.57 (m, 5H), 7.44 (d, 1H, *J* = 8.0 Hz), 7.27 (td, 1H, *J* = 7.3, 1.3 Hz), 7.07 (td, 1H, *J* = 7.7, 1.2 Hz), 3.66 (t, 4H, *J* = 5.0 Hz), 3.07 (t, 4H, *J* = 5.1 Hz), 3.01 (t, 2H, *J* = 7.1 Hz), 2.87 (t, 2H, *J* = 6.9 Hz).

3-phenylpropan-1-ol (68)

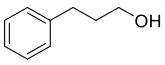

Procedure: 3-phenylpropanal (4.00 g, 29.81 mmol) is dissolved in MeOH, followed by the addition of NaBH4 (337 mg, 8.91 mmol) portion wise. The reaction is stirred for 2 hours, then AcOH (400 μL) is added to quench the reaction. The mixture is diluted with EtOAc, washed with water and brine and dried over Na_2SO_4. The crude is purified by column chromatography (Pet. Et. : EtOAc = 8 : 2 v/v) to afford 3.40 g of pure target compound (yield = 84%).

^{1}H-NMR (400 MHz, Chloroform-*d*): 7.38–7.17 (m, 5H), 3.67 (t, 2H, *J* = 6.4 Hz), 2.73 (t, 2H, *J* = 7.6 Hz), 2.37 (br, 1H), 1.91 (quint, 2H, *J* = 6.8 Hz).

3-phenylpropyl 4-methylbenzenesulfonate (69)

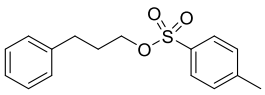

Procedure: 3-phenylpropan-1-ol (3.40 g, 24.94 mmol) is dissolved in pyridine, and tosil chloride (4.76 g, 24.94 mmol) is added to de mixture. The reaction is stirred for 15 minutes, then diluted with Et_2O, and washed with HCl (1M), then saturated $NaHCO_3$, water and brine, and dried over Na_2SO_4. The crude is purified by column chromatography (Pet. Et. : EtOAc = 9 : 1 v/v) to afford 5.87 g of pure target compound (yield = 81%).

^{1}H-NMR (400 MHz, Chloroform-*d*): 7.80 (d, 2H, *J* = 8.3 Hz), 7.35 (d, 2H, *J* = 8.0 Hz), 7.25 (t, 2H, *J* = 7.5 Hz), 7.18 (t, 1H, *J* = 7.2 Hz), 7.07 (d, 2H, *J* = 6.7 Hz), 4.04 (t, 2H, *J* = 6.2 Hz), 2.65 (t, 2H, *J* = 7.4 Hz), 2.46 (s, 3H), 1.96 (quint, 2H, *J* = 6.2 Hz).

1-(3-phenylpropyl)piperidin-2-one (70)

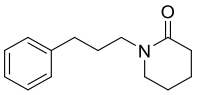

Procedure: in an ice-cold flask under Argon atmosphere, δ-valerolactam (1.62 g, 16.4 mmol) is dissolved in dry DMF, and under vigorous stirring NaH (1.31 g, 32.7 mmol) is added portion wise. After 1 h, 3-phenylpropyl 4-methylbenzenesulfonate (4.75 g, 16.4 mmol) is added to the reaction, that is stirred overnight. A catalytic amount of NaI (123 mg, 0.82 mmol) is added to the mixture and the reaction is stirred overnight. The reaction is quenched by adding MeOH dropwise, followed by water and EtOAc. The organic phase is washed with water several times, then brine and dried over Na2SO4. The crude is purified by column chromatography (Gradient from Pet. Et. : EtOAc 1 : 1 v/v to 100% EtOAc) to afford 2.00 g of pure target compound (yield = 69%).

^{1}H-NMR (300 MHz, Chloroform-*d*): 7.36–7.10 (m, 5H), 3.41 (t, 2H, *J* = 7.4 Hz), 3.28–3.16 (m, 2H), 2.36 (t, 2H, *J* = 7.7 Hz), 2.42–2.27 (m, 2H), 1.88 (quint, 2H, *J* = 7.7 Hz), 1.80–1.65 (m, 4H).

5-((3-phenylpropyl)amino)pentanoic acid (71)

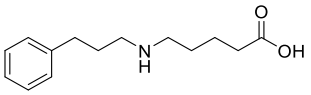

Procedure: NaOH (11.04 g, 0.27 mol) is dissolved in H_2O, then 1-(3-phenylpropyl)piperidin-2-one (2.00 g, 9.20 mmol) is added to the basic solution, and the mixture is stirred under reflux conditions overnight, then the reaction is neutralized with HCl (36%) to quench the excess of NaOH. Acetone is then added to the mixture, causing the formation of a white precipitate, isolated by centrifugation. The crude product (3.13 g) is used in the next step without purification.

^{1}H-NMR (300 MHz, Methanol-*d4*): 7.35–7.09 (m, 5H), 2.70–2.53 (m, 6H), 2.18 (t, 2H, *J* = 7.1 Hz), 1.83 (quint, 2H, *J* = 7.4 Hz), 1.68–1.45 (m, 4H).

5-((3-bromo-N-(3-phenylpropyl)phenyl)sulfonamido)pentanoic acid (72)

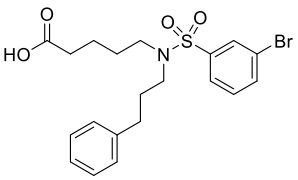

Procedure: 5-((3-phenylpropyl)amino)pentanoic acid (500 mg, 1.943 mmol) is dissolved in an ice-cold mixture of dry THF and pyridine, and Triethylamine (594 mg, 3.886 mmol) is added to the mixture. 3-bromobenzensulfonyl chloride (756 mg, 1.295 mmol) is dissolved in pyridine, and the solution is added dropwise to the mixture. The reaction is stirred for 5 hours, then diluted with ethyl acetate, and washed with HCl (1M) several times to remove the pyridine, then water and brine, and dried over Na2SO4. The crude product is purified by column chromatography (Pet. Et. : EtOAc = 7 : 3 v/v + 1% AcOH) to afford 230 mg of pure target compound (yield = 39%).

^{1}H-NMR (300 MHz, Chloroform-*d*): 9.39 (br, 1H), 7.97–7.90 (m, 1H), 7.70 (dd, H, *J* = 7.9, 1.8 Hz), 7.45–7.10 (m, 6H), 3.29–3.06 (m, 4H), 2.62 (t, 2H, *J* = 7.6 Hz), 2.38 (t, 2H, *J* = 6.7 Hz), 1.87 (quint, 2H, *J* = 7.6 Hz), 1.73–1.49 (m, 4H).

5-((3-bromo-N-(3-phenylpropyl)phenyl)sulfonamido)pentanamide (UPR1442 - 48)

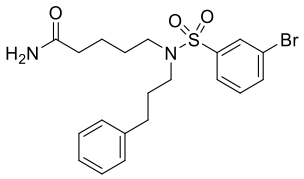

Procedure: 5-((3-bromo-N-(3-phenylpropyl)phenyl)sulfonamido)pentanoic acid (230mg, 0.506 mmol) is dissolved in dry THF, followed by triethylamine (154 mg, 1.519 mmol). Pivaloyl chloride (73 mg, 0.607 mmol) is added to the mixture, and the reaction is stirred for 2 hours. Solid ammonium chloride (54 mg, 1.012 mmol) is then added, and the reaction is stirred overnight. The mixture is diluted with EtOAc, then washed with saturated NaHCO3, water and brine, and dried over Na_2SO_4. The crude compound is purified by column chromatography (Pet. Et. : EtOAc = 7 : 3 v/v + 1% AcOH) to afford 86 mg of target compound (yield = 37%). MS calc.: 452.08, found: 453.11 m/z $[M+H]^+$.

^{1}H-NMR (400 MHz, Methanol-*d4*): 7.89 (s, 1H), 7.77 (d, 1H, *J* = 8.0 Hz), 7.72 (d, 1H, *J* = 7.8 Hz), 7.47 (t, 1H, *J* = 8.0 Hz), 7.26 (t, 2H, *J* = 7.5 Hz) 7.20–7.10 (m, 3H), 3.14 (q, 4H, *J* = 7.7 Hz), 2.57 (t, 2H, *J* = 7.6 Hz), 2.20 (t, 2H, *J* = 6.6 Hz), 1.81 (quint, 2H, *J* = 7.7 Hz), 1.66–1.47 (m, 4H).

Ethyl 1-(benzo[d]thiazol-2-yl)piperidine-4-carboxylate (74)

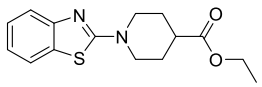

Procedure: to a solution of 2-bromobenzo[d]thiazole (2.00 g, 9.34 mmol) and ethyl isonipecotate (1.47 g, 9.34 mmol) in DMF, K_2CO_3 (2.58 g, 18.68 mmol) and CuI (0.23 g, 1.22 mmol) are sequentially added, and the mixture is stirred at 75°C for 3.5 hours. The reaction is diluted in Et_2O, and washed with water and brine, then the organic phase is dried over Na_2SO_4. The crude product is purified with flash chromatography (eluent mixture: Pet. Et. : EtOAc = 8 : 2 v/v) to obtain 2.365 g of pure product (Yield = 87%).

^{1}H-NMR (400 MHz, Chloroform-*d*): 7.65–7.53 (m, 2H), 7.31 (ddd, 1H, *J* = 8.3, 7.3, 1.3 Hz,), 7.09 (td, 1H, *J* = 7.5, 1.2 Hz), 4.19 (q, 2H, *J* = 7.1 Hz), 4.15–4.07 (m, 2H), 3.32–3.22 (m, 2H), 2.13–2.02 (m, 2H), 1.88 (dtd, 2H, *J* = 13.6, 11.0, 4.2 Hz), 1.29 (t, 4H, *J* = 7.1 Hz).

(1-(benzo[d]thiazol-2-yl)piperidin-4-yl) methanol (75)

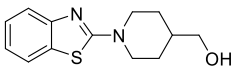

Procedure: under nitrogen atmosphere, ethyl 1-(benzo[d]thiazol-2-yl)piperidine-4-carboxylate (910 mg, 3.13 mmol) is dissolved in dry THF at 0 °C, then a solution of $LiAlH_4$ in dry THF (3.15 mL, 3.13 mmol) is added dropwise, and the mixture is stirred for 15 min. The reaction is quenched by adding a solution of Rochelle's salt, then the mixture is extracted with EtOAc. The organic phase is washed with water and brine, then dried with Na_2SO_4. The crude was purified by column chromatography (eluent mixture: Pet. Et. : EtOAc = 5 : 6 v/v) to obtain 855 mg of pure product (yield > 98%).

^{1}H NMR (400 MHz, Chloroform-*d*): 7.54 (dd, 2H, *J* = 15.2, 7.9 Hz), 7.26 (t, 1H, *J* = 7.7 Hz), 7.04 (t, 1H, *J* = 7.6 Hz), 4.11 (dt, 2H, *J* = 13.5, 3.0 Hz), 3.46 (d, 2H, *J* = 6.2 Hz), 3.06 (td, 2H, *J* = 12.7, 2.8 Hz), 3.01 (s, 1H), 1.81 (dd, 2H, *J* = 13.2, 3.3 Hz), 1.70 (ttt, 1H, *J* = 10.3, 6.5, 3.8 Hz), 1.34 (dd, 1H, *J* = 12.5, 4.4 Hz), 1.32–1.20 (m, 1H).

(1-(benzo[d]thiazol-2-yl)piperidin-4-yl)methyl 4-methylbenzenesulfonate (76)

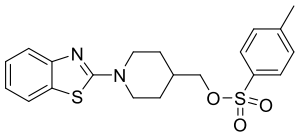

Procedure: (1-(benzo[d]thiazol-2-yl)piperidin-4-yl)methanol (850 mg, 3.423 mmol) is dissolved in 2,6-lutidine, then DMAP (42 mg, 0.342 mmol) is added, followed by tosyl chloride (718 mg, 3.765 mmol). The reaction is heated at 40°C for 5 hours, and then is quenched by adding a 2M solution of citric acid and then extracted with EtOAc. The organic phase is washed with water and brine, and then dried over Na_2SO_4. The crude was purified by column chromatography (eluent mixture: Pet. Et. : EtOAc = 85 : 15 v/v) to obtain 734 mg of pure product (yield = 53%).

^{1}H-NMR (300 MHz Chloroform-*d*): 7.85–7.76 (m, 2H), 7.57 (ddd, 2H, *J* = 17.2, 8.0, 1.2 Hz), 7.37 (d, 2H, *J* = 8.1 Hz), 7.35–7.03 (m, 2H), 4.16 (dt, 2H, *J* = 13.7, 2.7 Hz), 3.91 (d, 2H, *J* = 6.5 Hz), 3.10 (td, 2H, *J* = 12.9, 2.8 Hz), 2.47 (s, 3H), 1.87–1.78 (m, 2H), 2.10–1.91 (m, 1H), 1.45–1.23 (m, 3H).

2-(4-(iodomethyl)piperidin-1-yl)benzo[d]thiazole (77)

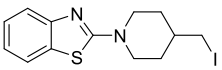

Procedure: (1-(benzo[d]thiazol-2-yl)piperidin-4-yl)methyl4-methylbenzene-sulfonate (730 mg, 1.813 mmol) is suspended in acetonitrile, and then NaI (408 mg, 2.720 mmol) is added. The reaction is heated to the boiling point and stirred for 6 hours. The mixture is diluted with EtOAc, and the organic phase is washed with a saturated solution of sodium thiosulfate ($Na_2S_2O_3$), then water and brine, and the organic phase is dried over Na_2SO_4. The crude was purified by column chromatography (eluent mixture: Pet. Et. : EtOAc = 95 : 5 v/v) to obtain 590 mg of pure product (yield = 75%).

^{1}H-NMR (400 MHz, Chloroform-*d*): 7.59 (dd, 2H, *J* = 19.3, 8.0 Hz), 7.34–7.04 (m, 2H), 4.20 (dt, 2H, *J* = 13.6, 3.1 Hz), 3.20–3.09 (m, 4H), 2.05–1.95 (m, 2H), 1.78 (ttt, 1H, *J* = 10.6, 6.8, 3.7 Hz), 1.40 (qd, 2H, *J* = 12.4, 4.5 Hz).

(±)-Ethyl-3-(1-(benzo[d]thiazol-2-yl)piperidin-4-yl)-2-phenylpropanoate (78)

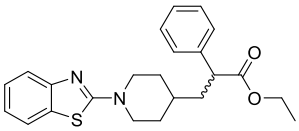

Procedure: under an Argon atmosphere, Phenylacetic acid ethyl ester (523 mg, 3.182 mmol) is dissolved in dry THF, cooled at -50°C, and then a solution of LiHMDS (3.2 mL, 3.182 mmol) in dry THF is added dropwise. The mixture is stirred for 30 minutes, then a solution of 2-(4-(iodomethyl)piperidin-1-yl)benzo[d]thiazole (570 mg, 1.591 mmol) in dry THF is added to the mixture, and the reaction is stirred overnight. The reaction is quenched by adding acetic acid (190 μL), diluted with EtOAc, and washed with water and brine, then dried over Na_2SO_4. The crude was purified by column chromatography (eluent mixture: Toluene : EtOAc = 9 : 1 v/v) to obtain 195 mg of pure product (yield = 31%).

^{1}H-NMR (400 MHz, Chloroform-*d*): 7.57 (dd, 2H, *J* = 19.1, 7.9 Hz), 7.40–7.26 (m, 6H), 7.08 (q, 1H, *J* = 7.8 Hz), 4.15 (dtd, 4H, *J* = 21.6, 7.2, 4.1 Hz), 3.71 (t, 1H, *J* = 7.8 Hz), 3.20–3.01 (m, 2H), 2.16–1.97 (m, 1H), 1.90–1.74 (m, 3H), 1.58–1.40 (m, 1H), 1.44–1.16 (m, 5H).

(±)-3-(1-(benzo[d]thiazol-2-yl)piperidin-4-yl)-2-phenylpropanoic acid (79)

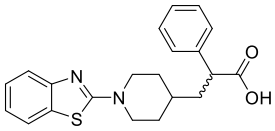

Procedure: ethyl 3-(1-(benzo[d]thiazol-2-yl)piperidin-4-yl)-2-phenylpropanoate (195 mg, 0.495 mmol) is dissolved in an ice-cold mixture of H_2O and THF, then KOH (139 mg, 2.472 mmol) is added. The mixture is heated to 40°C and stirred for 1 hour, then cooled to rt and stirred for 48 hours. The reaction is quenched by adding acetic acid (140 μL), then the mixture is diluted with EtOAc, washed with water and brine, and the organic phase is dried over Na_2SO_4. The crude was purified by column chromatography (eluent mixture: Pet. Et. : EtOAc = 7 : 3 v/v + 0.5% AcOH) to obtain 177 mg of pure product (yield = 97%).

^{1}H-NMR (300 MHz, Chloroform-*d*): 7.63–7.47 (m, 2H), 7.40–7.25 (m, 6H), 7.08 (td, 1H, *J* = 7.5, 1.2 Hz), 4.10 (dt, 2H, *J* = 13.6, 3.1 Hz), 3.74 (t, 1H, *J* = 7.8 Hz), 3.05 (td, 2H, *J* = 12.7, 2.8 Hz), 2.25–2.03 (m, 1H), 1.89–1.68 (m, 3H), 1.44–1.24 (m, 3H).

(±)-3-(1-(benzo[d]thiazol-2-yl)piperidin-4-yl)-N-(cyanomethyl)-2-phenyl-propanamide (UPR1443 - 49)

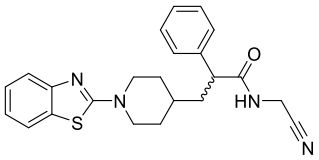

Procedure: to an ice-cold solution of 3-(1-(benzo[d]thiazol-2-yl)piperidin-4-yl)-2-phenylpropanoic acid (30 mg, 0.082 mmol) in DMF, Et3N (38 mL, 0.270 mmol) and TBTU (29 mg, 0.90 mmol) are added sequentially. The mixture is stirred for 30 minutes, then 2-aminoacetonitrile (25.3 mg, 0.164 mmol) is added, and the reaction is let to reach rt. The mixture is stirred for 20 hours, then the mixture is diluted with EtOAc, and the organic phase is washed with water, A saturated solution of $NaHCO_3$ and brine, and then dried over Na_2SO_4. The crude was purified by column chromatography (eluent mixture: Pet. Et. : iPrOH = 9 : 1 v/v) to obtain 21 mg of pure product (yield = 63%). MS calc. = 404.17, found 405.07 $[M+H]^+$; purity >99%.

^{1}H-NMR (300 MHz, Chloroform-*d*): 7.55 (ddd, 2H, *J* = 26.5, 8.0, 1.2 Hz), 7.38 (dddd, 3H, *J* = 11.0, 6.7, 4.5, 2.4 Hz), 7.33–7.23 (m, 4H), 7.07 (td, 1H, *J* = 7.5, 1.2 Hz), 6.16 (t, 1H, *J* = 5.9 Hz), 4.27–3.95 (m, 4H), 3.56 (dd, 1H, *J* = 8.5, 6.9 Hz), 3.09–2.95 (m, 2H), 2.78 (t, 1H, *J* = 7.2 Hz), 2.23–2.04 (m, 1H), 1.89–1.70 (m, 3H).

Fatty Acid Ethanolamides

Procedure A: to a solution of ethanolamine (0.858 mmol) and triethylamine (2.340 mmol) in DCM at 0°C, the desired fatty acid chloride (0.780 mmol) is added dropwise, and a white precipitate is formed immediately. The reaction is stirred for 30 minutes, then diluted with dichloromethane and washed with HCl 1M, then a saturated solution of $NaHCO_3$, and brine. The organic phase is dried over $MgSO_4$, and the crude product is recrystallized from heptane to get the desired FAE (Purity > 95% assessed by LC/MS).

Procedure B: the desired fatty acid (0.585 mmol) is dissolved in dichloromethane and triethylamine (1.755 mmol) in an ice-cold flask. HOBt (0.644 mmol) and TBTU (0.644 mmol) are added sequentially, and the mixture is stirred for 30 minutes, then ethanolamine (0.878 mmol) is added dropwise, forming a white precipitate. The reaction is stirred for 2 more hours then diluted with dichloromethane and washed with HCl 1M, then a saturated solution of $NaHCO_3$, and brine. The organic phase is dried over $MgSO_4$, and the crude product is recrystallized from heptane, or purified by column chromatography (Chloroform : Methanol = 98:2 v/v) to get the desired FAE (Purity > 95% assessed by LC/MS).

***N*-(2-hydroxyethyl)tridecanamide (80)**

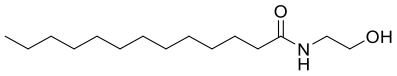

Procedure: A, Quantitative. MS calc.: 257.24, found: 258.3 m/z $[M+H]^+$.

^{1}H-NMR (400 MHz, Chloroform-*d*): 6.17 (br, 1H), 3.71 (t, 2H, *J* = 4.8 Hz), 3.40 (q, 2H, *J* = 5.5 Hz), 3.22 (br, 1H), 2.20 (t, 2H, *J* = 7.6 Hz), 1.63 (quint, 2H, *J* = 7.6 Hz), 1.38–1.14 (m, 18H), 0.88 (t, 3H, *J* = 7.0 Hz).

***N*-(2-hydroxyethyl)tetradecanamide (81)**

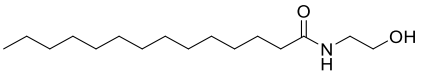

Procedure: A, yield = 98%. MS calc.: 271.25, found: 272.3 m/z $[M+H]^+$.

^{1}H-NMR (400 MHz, Chloroform-*d*): 6.03 (br, 1H), 3.72 (t, 2H, *J* = 5.0 Hz), 3.41 (q, 2H, *J* = 5.4 Hz), 2.91 (br, 1H), 2.20 (t, 2H, *J* = 7.6 Hz), 1.64 (quint, 2H, *J* = 7.7 Hz), 1.39–1.13 (m, 20H), 0.88 (t, 3H, *J* = 7.1 Hz).

***N*-(2-hydroxyethyl)pentadecanamide (82)**

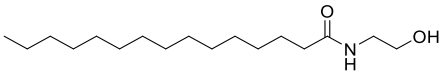

Procedure: A, yield = 95%. MS calc.: 285.27, found: 286.3 m/z $[M+H]^+$.

^{1}H-NMR (400 MHz, Chloroform-*d*): 6.05 (br, 1H), 3.72 (t, 2H, *J* = 4.9 Hz), 3.42 (q, 2H, *J* = 5.3 Hz), 2.96 (t, 1H, *J* = 5.0 Hz), 2.20 (t, 2H, *J* = 7.4 Hz), 1.63 (quint, 2H, *J* = 7.5 Hz), 1.40–1.13 (m, 22H), 0.88 (t, 3H, *J* = 6.9 Hz).

***N*-(2-hydroxyethyl)hexadecanamide (PEA - 2)**

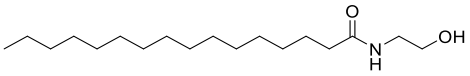

Procedure: B; purified by recrystallization from heptane (yield = 64%). MS calc.: 299.28, found: 300.3 m/z $[M+H]^+$.

^{1}H-NMR (400 MHz, Chloroform-*d*): 5.97 (br, 1H), 3.72 (t, 2H, *J* = 4.9 Hz), 3.42 (q, 2H, *J* = 5.4 Hz), 2.79 (br, 1H), 2.20 (t, 2H, *J* = 7.5 Hz), 1.63 (quint, 2H, *J* = 7.6 Hz), 1.40–1.15 (m, 24H), 0.88 (t, 3H, *J* = 7.0 Hz).

***N*-(2-hydroxyethyl)heptadecanamide (83)**

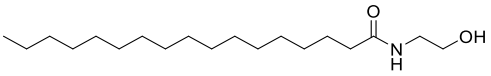

Procedure: A, yield = 92%. MS calc.: 313.30, found: 314.3 m/z $[M+H]^+$.

^{1}H-NMR (400 MHz, Chloroform-*d*): 5.96 (br, 1H), 3.72 (q, 2H, *J* = 4.8 Hz), 3.42 (q, 2H, *J* = 5.4 Hz), 2.75 (t, 1H, *J* = 5.1 Hz), 2.20 (t, 2H, *J* = 7.6 Hz), 1.63 (quint, 2H, *J* = 7.6 Hz), 1.40–1.11 (m, 26H), 0.88 (t, 3H, *J* = 7.0 Hz).

***N*-(2-hydroxyethyl)octadecanamide (84)**

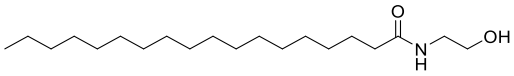

Procedure: A, yield = 98%. MS calc.: 327.31, found: 328.3 m/z $[M+H]^+$.

^{1}H-NMR (400 MHz, Chloroform-*d*): 5.89 (br, 1H), 3.80 - 3.65 (m, 2H), 3.43 (q, 2H, *J* = 5.4 Hz), 2.60 (br, 1H), 2.20 (t, 2H, *J* = 7.5 Hz), 1.63 (quint, 2H, *J* = 7.7 Hz), 1.40–1.12 (m, 28H), 0.88 (t, 3H, *J* = 5.9 Hz).

(Z)-*N*-(2-hydroxyethyl)pentadec-10-enamide (85)

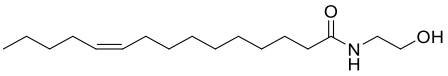

Procedure: B, purified by column chromatography (yield = 53%). MS calc.: 283.25, found: 284.3 m/z $[M+H]^+$.

^{1}H-NMR (400 MHz, Chloroform-*d*): 5.93 (br, 1H), 5.40–5.28 (m, 2H), 3.72 (br, 2H), 3.42 (q, 2H, *J* = 5.4 Hz), 2.67 (br, 1H), 2.20 (t, 2H, *J* = 7.5 Hz), 2.08–1.88 (m, 4H), 1.63 (quint, 2H, *J* = 7.5 Hz), 1.40–1.19 (m, 14H), 0.89 (t, 3H, *J* = 7.0 Hz).

(Z)-*N*-(2-hydroxyethyl)hexadec-9-enamide (86)

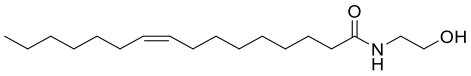

Procedure: B, purified by column chromatography (yield = 49%). MS calc.: 297.27, found: 298.3 m/z $[M+H]^+$.

^{1}H-NMR (400 MHz, Chloroform-*d*): 6.01 (br, 1H), 5.40–5.28 (m, 2H), 3.72 (t, 2H, *J* = 4.9 Hz), 3.42 (q, 2H, *J* = 5.4 Hz), 2.89 (br, 1H), 2.20 (t, 2H, *J* = 7.6 Hz), 2.06–1.93 (m, 4H), 1.63 (quint, 2H, *J* = 7.4 Hz), 1.39–1.17 (m, 16H), 0.88 (t, 3H, *J* = 7.0 Hz).

(Z)-*N*-(2-hydroxyethyl)heptadec-10-enamide (87)

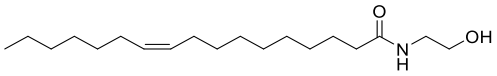

Procedure: B, purified by column chromatography (yield = 58%). MS calc.: 311.28, found: 312.3 m/z $[M+H]^+$.

^{1}H-NMR (400 MHz, Chloroform-*d*): 6.01 (br, 1H), 5.40–5.28 (m, 2H), 3.72 (t, 2H, *J* = 4.9 Hz), 3.41 (q, 2H, *J* = 5.4 Hz), 2.89 (br, 1H), 2.20 (t, 2H, *J* = 7.5 Hz), 2.08–1.91 (m, 4H), 1.63 (quint, 2H, *J* = 7.5 Hz), 1.40–1.15 (m, 18H), 0.88 (t, 3H, *J* = 6.7 Hz).

(Z)-*N*-(2-hydroxyethyl)octadec-9-enamide (OEA - 3)

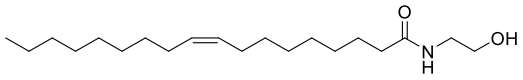

Procedure: B, purified by column chromatography (yield = 61%). MS calc.: 325.30, found: 326.3 m/z $[M+H]^+$.

^{1}H-NMR (400 MHz, Chloroform-*d*): 6.03 (br, 1H), 5.42–5.26 (m, 2H), 3.72 (t, 2H, *J* = 4.9 Hz), 3.41 (q, 2H, *J* = 5.4 Hz), 2.85 (br, 1H), 2.20 (t, 2H, *J* = 7.5 Hz), 2.09–1.90 (m, 4H), 1.63 (quint, 2H, *J* = 7.5 Hz), 1.48–1.06 (m, 20H), 0.88 (t, 3H, *J* = 7.0 Hz).

(Z)-*N*-(2-hydroxyethyl)nonadec-10-enamide (88)

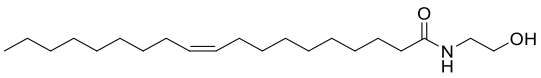

Procedure: B, purified by column chromatography (yield = 33%). MS calc.: 339.31, found: 340.3 m/z $[M+H]^+$.

^{1}H-NMR (400 MHz, Chloroform-*d*): 5.89 (br, 1H), 5.40–5.28 (m, 2H), 3.72 (t, 2H, *J* = 4.7 Hz), 3.42 (q, 2H, *J* = 5.5 Hz), 2.60 (t, 1H, *J* = 4.9), 2.20 (t, 2H, *J* = 7.5 Hz), 2.08–1.91 (m, 4H), 1.63 (quint, 2H, *J* = 7.5 Hz), 1.40–1.20 (m, 22H), 0.88 (t, 3H, *J* = 7.0 Hz).

(Z)-*N*-(2-hydroxyethyl)eicos-9-enamide (89)

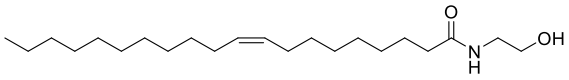

Procedure: B, purified by column chromatography (yield = 41%). MS calc.: 353.33, found: 354.3 m/z $[M+H]^+$.

^{1}H-NMR (400 MHz, Chloroform-*d*): 5.98 (br, 1H), 5.39–5.24 (m, 2H), 3.72 (t, 2H, *J* = 4.8 Hz), 3.42 (q, 2H, *J* = 5.4 Hz), 2.81 (br, 1H), 2.20 (t, 2H, *J* = 7.7 Hz), 2.06–1.91 (m, 4H), 1.63 (quint, 2H, *J* = 7.6 Hz), 1.38–1.18 (m, 24H), 0.88 (t, 3H, *J* = 7.1 Hz).

_N_-methylpalmitamide (90)

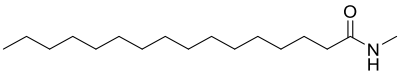

Procedure: to a solution of palmitic acid (210 mg, 0.819 mmol) in cold dichloromethane, triethylamine (249 mg, 2.457 mmol), HOBt (138 mg, 0.901 mmol) and TBTU (289 mg, 0.901 mmol) are added sequentially, and the mixture is stirred for 30 minutes. Then methylamine hydrochloride (166 mg, 2.457 mmol) is added to the reaction, that is stirred for 2 more hours. The mixture is then diluted with DCM and washed with HCl 1M, then saturated $NaHCO_3$, and brine. The organic phase is dried over $MgSO_4$, and the crude product is recrystallized from heptane to get 139 mg of target product (yield = 63%). MS calc.: 269.27, found: 270.3 m/z $[M+H]^+$.

^{1}H-NMR (400 MHz, Chloroform-*d*): 5.39 (br, 1H), (d, 3H, *J* = 4.8 Hz), 2.16 (t, 2H, *J* = 7.5 Hz), 1.62 (quint, 2H, *J* = 7.5 Hz), 1.38–1.15 (m, 24H), 0.88 (t, 3H, *J* = 7.0 Hz).

Palmitamide (91)

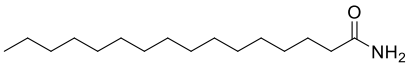

Procedure: to a solution of palmitic acid (198 mg, 0.781 mmol) in cold dichloromethane, triethylamine (237 mg, 2.344 mmol), HOBt (132 mg, 0.859 mmol) and TBTU (276 mg, 0.859 mmol) are added sequentially, and the mixture is stirred for 30 minutes. Then methylamine hydrochloride (125 mg, 2.344 mmol) is added to the reaction, that is stirred for 2 more hours. The mixture is then diluted with DCM and washed with HCl 1M, then saturated $NaHCO_3$, and brine. The organic phase is dried over $MgSO_4$, and the crude product is recrystallized from heptane to get 133 mg of target product (yield = 67%). MS calc.: 255.26, found: 256.3 m/z $[M+H]^+$.

^{1}H-NMR (400 MHz, Chloroform-*d*): 5.35 (br, 2H), 2.22 (t, 2H, *J* = 7.5 Hz), 1.64 (quint, 2H, *J* = 7.5 Hz), 1.40–1.14 (m, 24H), 0.88 (t, 3H, *J* = 7.1 Hz).

(R)-*N*-(1-hydroxypropan-2-yl)palmitamide (92)

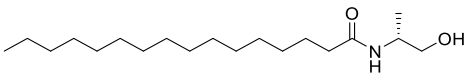

Procedure: to a solution of palmitic acid (153 mg, 0.597 eq) in cold dichloromethane, triethylamine (181 mg, 1.790 mmol), HOBt (100 mg, 0.656 mmol) and TBTU (210 mg, 0.656 mmol) are added sequentially, and the mixture is stirred for 30 minutes. Then (R)-2-amino-1-propanol (67 mg, 0.895 mmol) is added to the reaction, that is stirred for 2 more hours. The mixture is then diluted with DCM and washed with HCl 1M, then saturated $NaHCO_3$, and brine. The organic phase is dried over $MgSO_4$, and the crude product is recrystallized from heptane to get 106 mg of target product (yield = 57%). MS calc.: 313.30, found: 314.3 m/z $[M+H]^+$. $[\alpha]_D^{20}$ = +12.3.

^{1}H-NMR (400 MHz, Chloroform-*d*): 5.54 (br, 1H), 4.07 (qd, 1H, *J* = 6.6, 3.4 Hz), 3.67 (ddd, 1H, *J* = 11.0, 6.2, 3.5 Hz), 3.54 (ddd, 1H, *J* = 11.0, 6.2, 4.8 Hz), 2.75 (dd, 1H, *J* = 6.1, 4.8 Hz), 2.18 (t, 2H, *J* = 7.5 Hz), 1.63 (quint, 2H, *J* = 7.4 Hz), 1.38–1.20 (m, 24H), 1.17 (d, 3H, *J* = 6.8 Hz), 0.88 (t, 3H, *J* = 7.0 Hz).

(S)-*N*-(1-hydroxypropan-2-yl)palmitamide (93)

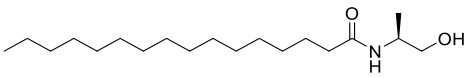

Procedure: to a solution of palmitic acid (170 mg, 0.663 mmol) in cold dichloromethane, triethylamine (201 mg, 1.989 mmol), HOBt (112 mg, 0.729 mmol) and TBTU (234 mg, 0.729 mmol) are added sequentially, and the mixture is stirred for 30 minutes. Then (S)-2-amino-1-propanol (75 mg, 0.994 mmol) is added to the reaction, that is stirred for 2 more hours. The mixture is then diluted with DCM and washed with HCl 1M, then saturated $NaHCO_3$, and brine. The organic phase is dried over $MgSO_4$, and the crude product is recrystallized from heptane to get 100 mg of target product (yield = 48%). MS calc.: 313.30, found: 314.3 m/z $[M+H]^+$. $[\alpha]_D^{20}$ = -12.3.

^{1}H-NMR (400 MHz, Chloroform-*d*): 5.53 (br, 1H), 4.07 (qd, 1H, *J* = 6.7, 3.5 Hz), 3.67 (ddd, 1H, *J* = 11.0, 6.2, 3.5 Hz), 3.54 (ddd, 1H, *J* = 11.0, 6.2, 4.7 Hz), 2.74 (dd, 1H *J* = 6.2, 4.8 Hz), 2.18 (t, 2H *J* = 7.6 Hz), 1.63 (quint, 2H, *J* = 7.4 Hz), 1.38–1.20 (m, 24H), 1.17 (d, 3H, *J* = 6.9 Hz), 0.88 (t, 3H, *J* = 7.0 Hz).

[1,1'-Biphenyl]-3-yl-(4-nitrophenyl)carbonate (97)

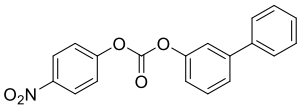

Procedure: to a solution of the commercially available [1,1'-biphenyl]-3-ol (0.14 g, 0.8 mmol) in dry CH_3CN (2.5 mL), under a nitrogen atmosphere, DIPEA (0.15 mL, 0.8 mmol) and a solution of 4-nitrophenyl chloroformate (0.16 g, 0.8 mmol) in dry CH_3CN (4 mL) were added dropwise, and the resulting mixture was stirred at room temperature for 1 h. Upon completion, the mixture was poured into water and extracted with EtOAc. The combined organic phases were washed with brine, dried over Na_2SO_4, and the solvent removed under reduced pressure to give a crude residue that was purified by column chromatography (cyclohexane : EtOAc = 9:1 v/v), to afford 126 mg (yield = 47%) of a white solid product.

^{1}H-NMR (400 MHz, Chloroform-*d*): 7.28–7.29 (m, 1H), 7.37–7.67 (m, 8H), 7.51 (d, 2H, *J* = 9.0 Hz), 8.34 (d, 2H, *J* = 9.0 Hz).

tert-Butyl-(6-{[3-(2-Acetamidoethyl)-1H-indol-5-yl]oxy}hexyl)-carbamate (99)

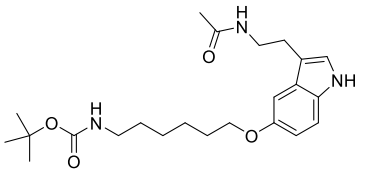

Procedure: *N*-acetyl serotonin (0.10 g, 0.46 mmol) and K_2CO_3 (0.19 g, 1.4 mmol) were dissolved in dry CH_3CN (3 mL) under a nitrogen atmosphere, and the resulting mixture was heated and stirred under reflux for 1 h. Then a solution of the commercially available *N*-Boc derivative **98** (0.13 g, 0.46 mmol) in dry CH_3CN (2 mL) was added to the reaction, followed by a catalytic amount of NaI, and the resulting mixture was refluxed for several 20 h. The reaction was quenched by the addition of water, and the aqueous phase was extracted using EtOAc. The organic phase was dried over Na_2SO_4 and concentrated under vacuum to give a crude residue that was purified by silica gel column chromatography (EtOAc as eluent), to obtain 113 mg (yield = 59%) as an amorphous solid. MS calc.: 417.26, found: 418 m/z $[M+H]^+$.

^{1}H-NMR (400 MHz, Chloroform-*d*): 7.97 (br, 1H), 7.26 (d, 1H, *J* = 8.5 Hz), 7.03 –7.05 (m, 2H), 6.87 (dd, 1H, *J* = 8.5, 2.0 Hz), 5.75 (br, 1H), 4.55 (br, 1H), 4.00 (t, 2H, *J* = 6.5 Hz), 3.59–3.61 (m, 2H), 3.13–3.15 (m, 2H), 2.95 (t, 2H, *J* = 6.5 Hz), 1.96 (s, 3H), 1.78–1.85 (m, 4H), 1.48 (s, 9H), 1.38–1.56 (m, 4H).

tert-Butyl-(6-{[3-(2-Acetamidoethyl)-2-bromo-1H-indol-5-yl]-oxy}hexyl)-carbamate (100).

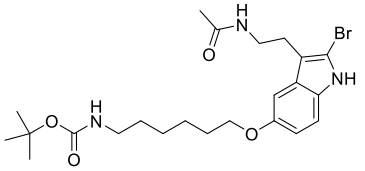

Procedure: to a solution of compound **99** (0.055 g, 0.132 mmol) in dry THF (2.5 mL) under nitrogen atmosphere, trimethyl phenyl ammonium tribromide (0.050 g, 0.132 mmol) was added, and the resulting mixture was stirred at room temperature for 30 min. Upon completion, the solvent was removed under vacuum, and the residue was dissolved in EtOAc. The organic phase was washed with water and brine, and then dried over Na_2SO_4 and concentrated under vacuum pressure to afford a crude residue successively purified by column chromatography (EtOAc : cyclohexane = 6:4 v/v). To obtain 39 mg (yield = 59%) as an oil. MS calc.: 495.17, found: 496 m/z $[M+H]^+$.

^{1}H-NMR (400 MHz, Chloroform-*d*): 8.71 (br, 1H). 7.19 (d, 1H, *J* = 8.5 Hz), 6.94–6.96 (m, 1H), 6.81 (dd, 1H, *J* = 8.5, 2.0 Hz), 5.72 (br, 1H), 4.63 (br, 1H), 3.96 (t, 2H, *J* = 6.5 Hz), 3.51–3.54 (m, 2H), 3.11–3.15 (m, 2H), 2.90 (t, 2H, *J* = 6.5 Hz), 1.94 (s, 3H), 1.76–1.80 (m, 2H), 1.45 (s, 9H), 1.34–1.52 (m, 6H).

[1,1'-Biphenil]-3-yl(6-((3-(2-aminoethyl)-2-bromo-1H-indol-5-yl)oxy)-hexyl)-carbamate (95).

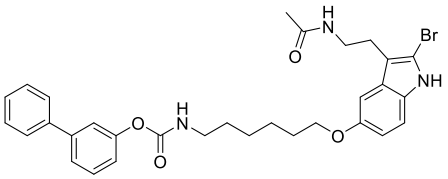

Procedure: trimethylsilyl bromide (48 μL, 0.36 mmol) was added to a solution of compound **100** (0.06 g, 0.12 mmol) in dry CH3CN (1.2 mL), under a nitrogen atmosphere, and the resulting mixture was stirred at room temperature for 1 h. MeOH was added at this point, and the resulting mixture was concentrated under vacuum to obtain the related free amine, used in the next step without further purification. The amine was then dissolved in a mixture of dry DCM (2mL) and DMF (0.2 mL) and Et_3N (0.075 mL, 0.53 mmol). The resulting mixture was added to an ice-cooled solution of carbonate **97** (0.06 g, 0.17 mmol) in dry DCM (1 mL) under a nitrogen atmosphere, and the resulting mixture was stirred for 3 h. Upon completion, the reaction mixture was neutralized by the addition of a saturated solution of NaHCO3 and the aqueous phase was extracted with DCM. The combined organic phases were dried over Na_2SO_4 and concentrated under vacuum to afford a crude residue that was purified by column chromatography (cyclohexane : EtOAc = 7:3 v/v) to afford 59 mg (yield = 83%) of pure product as an amorphous solid. MS calculated for C31H35N3O4Br 591.1811, found: 592.1844 $[M+H]^+$.

^{1}H-NMR (400 MHz, Chloroform-*d*): 8.18 (br, 1H), 7.54–7.57 (m, 2H), 7.40–7.43 (m, 4H), 7.37–7.39 (m, 2H), 7.13 (d, 1H, *J* = 8.5 Hz), 7.11–7.15 (m, 1H),

6.97–6.99 (m, 1H), 6.83 (dd, 1H, *J* = 8.5, 2.0 Hz), 6.18 (br, 1H), 5.27 (br, 1H), 4.01 (t, 2H, *J* = 6.5 Hz), 3.48–3.52 (m, 2H), 3.30–3.31 (m, 2H), 2.89 (t, 2H, *J* = 6.5 Hz), 1.94 (s, 3H), 1.80–1.84 (m, 2H), 1.62–1.67 (m, 2H), 1.44–1.57 (m, 4H).

^{13}C-NMR (100 MHz, Chloroform-*d*): 171.0, 154.8, 153.8, 151.4, 142.6, 140.3, 131.3, 129.6, 128.7, 128.1, 127.6, 127.2, 124.0, 120.4, 120.4, 112.8, 111.9, 111.5, 108.9, 101.2, 68.7, 41.2, 39.6, 29.7, 29.2, 26.5, 25.8, 24.7, 22.9.

8.3.Rat NAAA expression protocol

The encoding sequence of rat NAAA (BC105771) was amplified from the cDNA clone 7930474 (Open Biosystems) using the primer pair: forward primer 5'- CCC**AAGCTT**ATGGGGACCCCAGCCATCCG (Hind-III restriction site is highlighted in bold green); reverse primer sequence 5'-CCG**CTCGAG**TCA-ATGATGATGATGATGATGGCTTGGGTTTCTGATC (Xho-I restriction sites is in bold) also includes a poly-Histidine tag (6x, underlined). The PCR product was cloned into pCDNA 3.1 vector (Invitrogen) using Hind-III and Xho-I restriction enzymes (New England Biolabs). HEK-293 cells (American Type Culture Collection) were cultured at 37°C in an incubator (5% CO2) using complete Dulbecco's modified Eagle's medium (DMEM) containing 10% fetal bovine serum (FBS), 1% penicillin-streptomycin and 1% L-glutamine, and transfected with the rat NAAA(6xHis)-pCDNA3.1 construct using JetPEI transfection reagent (Polyplus), following instructions provided by manufacturer. Stably transfected cells were selected by addition of G418 (1 mg/mL) to the cell culture medium and cell clones were generated by limiting dilution plating. Growing clones were analyzed for NAAA expression by western blot (anti-hASAHL, R&D Systems).

8.4.Lysosomal extract preparation

Cell pellets were resuspended in Tris-HCl buffer (50 mM), pH 7.4, containing sucrose (0.32 M). Samples were sonicated with a Branson digital sonifier 102C, and centrifuged at 800G for 15 min at 4°C. The resulting supernatants were taken and centrifuged at 12,000G for 30 min at 4°C. The pellets were suspended in phosphate-buffered saline (PBS, pH 7.4) and subjected to two freeze/thaw cycles at -80°C. The suspensions were centrifuged at 100,000G for 1 hour at 4°C. Protein concentrations were quantified using BCA analysis, and samples were stored at -80°C until use.

8.5.NAAA activity assay

NAAA overexpression was confirmed by comparison with wild type HEK-293 cells lysosomal extraction. The appropriate incubation time was calculated after a time course assay: 10 aliquots of PEA (1 mM) were incubated in 100 mM Sodium Phosphate Monobasic, 100 mM Sodium Citrate, 0.1% Triton-X 100, 3 mM DTT, pH 4.5 (NAAA assay buffer) with 4 µg of proteins from lysosomal extract at 37°C. Every 10 min (from 0 min to 90 min) one aliquot was quenched by addition of 0.6 mL of a cold mixture of methanol and chloroform (1:1) containing Z-10-heptadecenoic acid as internal standard, and the palmitic acid was quantified by LC/MS. Data were plotted as pmol of palmitic acid as function of reaction time, resulting in a plot that was linear from 0 to 40 minutes.

Substrates were incubated in 100 mM Sodium Phosphate Monobasic, 100 mM Sodium Citrate, 0.1% Triton-X 100, 3 mM DTT, pH 4.5 (NAAA assay buffer) with 4 µg of proteins from lysosomal extract at 37°C for 30 min (triplicate samples). Reactions were terminated by addition of 0.6 mL of a cold mixture of methanol and chloroform (1:1) containing Z-10-heptadecenoic acid (for saturated fatty acids, 12.5 ng/mL, Cayman Chemical, Ann Arbor, MI) or heptadecanoic acid (for monounsaturated fatty acids, 12.5 ng/mL, Nu-Chek Prep, Elysian, MN) as an internal standard. Samples were centrifuged at 3000 rpm for 15 min at 4°C, and the organic phases were transferred into new vials, dried and redissolved in 0.3 mL of a mixture of methanol and chloroform (9 : 1, v/v). Fatty acid quantifications were carried out by LC/MS using an Agilent 6410 Triple Quad LC/MS system. Fatty acids were eluted from a Zorbax Eclipse XBD-C18 column (2.1x50 mm, 1.8 µm pore size, Agilent Technologies) at a flow rate of 0.4 mL/min for 6 min using a

solvent mixture of water (A) and methanol (B), both containing 0.25% acetic acid and 5 mM ammonium acetate (0 min-2 min 90% B, 2 min-3 min 95% B, 3 min-6 min 90% B). Column temperature was set at 40°C. Electrospray ionization was in the negative mode and the capillary voltage was 4 kV. N2 was used as drying gas at a flow rate of 13 L/min and a temperature of 350°C. The $[M-H]^-$ ion was monitored in the selected-ion monitoring (SIM) mode. Calibration curves were generated using commercial heptadecenoic acid (Cayman Chemical) and palmitic acid (Nu-Chek Prep). NAAA activity was calculated as pmol of palmitic acid produced by 1 mg of NAAA in 1 min and plotted as function of substrate concentration. Km and Vmax values were calculated using the Michaelis-Menten function analysis on GraphPad Prism version 8.4.2 (GraphPad Software Inc.).

9. References

1 Devane, W. A.; Hanus, L.; Breuer, A.; Pertwee, R. G.; Stevenson, L. A.; Griffin, G.; Gibson, D.; Mandelbaum, A.; Etinger, A.; Mechoulam, R. **Isolation and structure of a brain constituent that binds to the cannabinoid receptor.** *Science* 1992, 258, 1946-1949.

2 Bachur, N. R.; Masek, K.; Melmon, K. L.; Udenfriend, S. **Fatty acid amides of ethanolamine in mammalian tissues**. *J. Biol. Chem*. 1965, 240, 1019-1024.

3 Schmid, H. H. O.; Schmid, P. C.; Natarajan, V. ***N*-Acylated glycerolphospholipids and their derivatives**. *Prog. Lipid Res*. 1990, 29, 1-43.

4 Calignano, A.; La Rana, G.; Giuffrida, A.; Piomelli, D. **Control of pain initiation by endogenous cannabinoids**. *Nature* 1998, 394, 277-281.

5 Calignano, A.; La Rana, G.; Piomelli, D. **Antinociceptive activity of the endogenous fatty acid amide, palmitylethanolamide**. *Eur. J. Pharmacol*. 2001, 419, 191-198.

6 Rodríguez de Fonseca, F.; Navarro, M; Gómez, R.; Escuredo, L.; Nava, F.; Fu, J.; Murillo-Rodríguez, E.; Giuffrida, A.; LoVerme, J.; Gaetani, S.; Kathuria, S.; Gall, C.; Piomelli, D. **An anorexic lipid mediator regulated by feeding**. *Nature* 2001, 414(6860), 209-212.

7 Nielsen, M. J.; Petersen, G., Astrup, A., Hansen, H. S. **Food intake is inhibited by oral oleoylethanolamide**. *Lipid Res*. 2004, 45(6), 1027-1029.

8 Oveisi, F.; Gaetani, S.; Eng, K. T.; Piomelli, D. **Oleoylethanolamide inhibits food intake in free-feeding rats after oral administration**. *Pharmacol Res*. 2004, 49(5), 461-466.

9 Sasso, O.; Pontis, S.; Armirotti, A.; Cardinali, G.; Kovacs, D.; Migliore, M.; Summa, M.; Moreno-Sanz, G.; Picardo, M.; Piomelli, D. **Endogenous N-acyl taurines regulate skin wound healing**. *Proc. Natl. Acad. Sci. U. S. A.* 2016, 113, 4397-4406.

10 Waluk, D. D.; Vielfort, K.; Derakhshan, S.; Aro, H.; Hunt, M. C. ***N*-Acyl taurines trigger insulin secretion by increasing calcium flux in pancreatic β-cells**. *Biochem. Bioph. Res. Co*. 2013, 1, 54-59.

11 Grevengoed, T. J.; Trammell, S. A. J.; McKinney, M. K.; Petersen, N.; Cardone, R. L.; Jens, S; Svenningsen, J. S.; Ogasawara, D.; Nexøe-Larsen, C. C.; Knop, F. K.; Schwartz, T. W.; Kibbey, R. G.; Cravatt, B. F.; Gillum, M. P. ***N*-acyl taurines are endogenous lipid messengers that improve glucose homeostasis**. *Proc. Natl. Acad. Sci. U. S. A.* 2019, 116(49), 24770-24778.

12 Al Suleimani, Y. M.; Al Mahruqi, A. S. **The endogenous lipid N-arachidonoyl glycine is hypotensive and nitric oxide-cGMP-dependent vasorelaxant**. *Eur J Pharmacol* 2017, 794, 209-215.

13 Bondarenko, A. I.; Drachuk, K.; Panasiuk, O.; Sagach, V.; Deak, A. T.; Malli, R.; Graier, W. F. ***N*-Arachidonoyl glycine suppresses Na^+/Ca^{2+} exchanger-mediated Ca^{2+} entry into endothelial cells and activates BK(Ca) channels independently of GPCRs**. *Br. J. Pharmacol*. 2013, 169(4), 933-948.

14 Cazade, M.; Nuss, C. E.; Bidaud, I.; Renger, J. J.; Uebele, V. N.; Lory, P.; Chemin, J. **Cross-Modulation and Molecular Interaction at the Cav3.3 Protein between the Endogenous Lipids and the T-Type Calcium Channel Antagonist TTA-A2**. *Mol. Pharm*. 2014, 85(2), 218-225.

15 Jaggar, S. I.; Sellaturay, S.; Rice, A. S. **The endogenous cannabinoid anandamide, but not the CB2 ligand palmitoylethanolamide, prevents the viscero-visceral hyper-reflexia associated with inflammation of the rat urinary bladder**. *Neurosci. Lett.* 1998, 253(2), 123-126.

16 Jaggar, S. I.; Hasnie, F. S.; Sellaturay, S.; Rice, A. S. **The anti-hyperalgesic actions of the cannabinoid anandamide and the putative CB2 receptor agonist palmitoylethanolamide in visceral and somatic inflammatory pain**. *Pain* 1998, 76(1-2), 189-199.

17 Onaivi, E. S.; Chakrabarti, A.; Gwebu, E. T.; Chaudhuri, G. **Neurobehavioral effects of *Δ*9-THC and cannabinoid (CB1) receptor gene expression in mice**. *Behav. Brain Res.* 1996, 72, 115-125.

18 Matsuda, L. A.; Lolait, S. J.; Brownstein, M. J.; Young, A. C.; Bonner, T. I. **Structure of a Cannabinoid Receptor and Functional Expression of the Cloned cDNA**. *Nature* 1990, 346, 561-564.

19 Munro, S.; Thomas, K. L.; Abu-Shaar, M. **Molecular Characterization of a Peripheral Receptor for Cannabinoids**. *Nature* 1993, 365, 61-65.

20 Porter, A. C.; Felder, C. C. **The Endocannabinoid Nervous System: Unique Opportunities for Therapeutic Intervention**. *Pharmacol. Ther.* 2001, 90, 45-60.

21 Cavuoto, P.; McAinch, A. J.; Hatzinikolas, G.; Janovská, A.; Game, P.; Wittert, G. A. **The expression of receptors for endocannabinoids in human and rodent skeletal muscle**. *Biochem. Bioph. Res. Co.* 2007, 364(1), 105-110.

22 Esposito, I.; Proto, M. C.; Gazzerro, P.; Laezza, C.; Miele, C.; Alberobello, A. T.; D'Esposito, V.; Beguinot, F.; Formisano, P.; Bifulco, M. **The cannabinoid CB1 receptor antagonist rimonabant stimulates 2-deoxyglucose uptake in skeletal muscle cells by regulating the expression of phosphatidylinositol-3-kinase**. *Mol. Pharmacol.* 2008, 74(6), 1678-1686.

23 Bouaboula, M.; Rinaldi, M.; Carayon, P.; Carillon, C.; Delpech, B.; Shire, D.; Le Fur, G.; Casellas, P. **Cannabinoid-receptor expression in human leukocytes**. *Eur. J. Biochem.* 1993, 214(1), 173-180.

24 Galiègue, S.; Mary, S.; Marchand, J.; Dussossoy, D.; Carrière, D.; Carayon, P.; Bouaboula, M.; Shire, D.; Le Fur, G.; Casellas, P. **Expression of central and peripheral cannabinoid receptors in human immune tissues and leukocyte subpopulations**. *Eur. J. Biochem.* 1995, 232(1), 54-61.

25 Van Sickle, M. D.; Duncan, M.; Kingsley, P. J.; Mouihate, A.; Urbani, P.; Mackie, K.; Stella, N.; Makriyannis, A.; Piomelli, D.; Davison, J. S.; Marnett, L. J.; Di Marzo, V.; Pittman, Q. J.; Patel, K. D.; Sharkey, K. A. **Identification and functional characterization of brainstem cannabinoid CB2 receptors**. *Science* 2005, 310(5746), 329-332.

26 Sugiura, T.; Waku, K. **Cannabinoid receptors and their endogenous ligands**. *J. Biochem.* 2002, 132(1), 7-12.

27 Liu, W. M.; Duan, E. K.; Cao, Y. J. **Effects of anandamide on embryo implantation in the mouse**. *Life Sci*. 2002, 71(14), 1623-1632.

28 Dennedy, M. C.; Friel, A. M.; Houlihan, D. D.; Broderick, V. M.; Smith, T.; Morrison, J. J. **Cannabinoids and the human uterus during pregnancy**. *Am. J. Obstet. Gynecol*. 2004, 190(1), 2-9.

29 Russo, R.; Loverme, J.; La Rana, G.; Compton, T. R.; Parrott, J.; Duranti, A.; Tontini, A.; Mor, M.; Tarzia, G.; Calignano, A.; Piomelli, D. **The fatty acid amide hydrolase inhibitor URB597 (cyclohexylcarbamic acid 3'-carbamoylbiphenyl-3-yl ester) reduces neuropathic pain after oral administration in mice**. *J. Pharmacol. Exp. Ther.* 2007, 322(1), 236-242.

30 Clapper, J. R.; Moreno-Sanz, G.; Russo, R.; Guijarro, A.; Vacondio, F.; Duranti, A.; Tontini, A.; Sanchini, S.; Sciolino, N. R.; Spradley, J. M.; Hohmann, A. G.; Calignano, A.; Mor, M.; Tarzia, G.; Piomelli, D. **Anandamide suppresses pain initiation through a peripheral endocannabinoid mechanism**. *Nat. Neurosci*. 2010, 13(10), 1265-1270.

31 Kuehl, F. A., Jr.; Jacob, T. A.; Ganley, O. H.; Ormond, R. E.; Meisinger, M. A. P. **The identification of N-(2-ydroxyethyl)palmitamide as a naturally occurring anti-inflammatory agent**. *J. Am. Chem. Soc.* 1957, 79, 5577-5578.

32 Ganley, O. H.; Robinson, H. J. **Antianaphylactic and antiserotonin activity of a compound obtained from egg yolk, peanut oil and soybean lecithin**. *J. Allergy 1959*, 30, 415-419.

33 Bachur, N. R.; Masek, K.; Melmon, K. L.; Udenfriend, S. **Fatty acid amides of ethanolamine in mammalian tissues**. *J. Biol. Chem.* 1965, 240, 1019-1024.

34 Benvenuti, F.; Lattanzi, F.; De Gori, A.; Tarli, P. **Activity of some derivatives of palmitoylethanolamide on carragenine-induced edema in the rat paw**. *Boll. Soc. Ital. Biol. Sper.* 1968, 44, 809-813.

35 Perlík, F.; Rasková, H.; Elis, J. **Anti-inflammatory properties of *N*-(2-hydroxyethyl)palmitamide**. *Acta Physiol. Acad. Sci. Hung.* 1971, 39, 395-400.

36 Perlík, F.; Krejcí, J.; Elis, J.; Pekárek, J.; Svejcar, J. **The effect of *N*-(2-hydroxyethyl)-palmitamide on delayed hypersensitivity in guinea pig**. *Experientia* 1973, 29, 67-68.

37 Masek, K.; Perlík, F.; Klíma, J.; Kahlich, R. **Prophylactic efficacy of *N*-2-hydroxyethyl palmitamide (impulsin) in acute respiratory tract infections.** *Eur. J. Clin. Pharmacol*. 1974, 7, 415-419.

38 Kahlich, R.; Klíma, J.; Cihla, F.; Franková, V.; Mašek, K.; Rosický, M.; Matousek, F.; Bruthans, J. **Studies on prophylactic efficacy of *N*-2-hydroxyethyl palmitamide (Impulsin) in acute respiratory infections. Serologically controlled field trials.** *J. Hyg. Epidemiol. Microbiol. Immunol.* 1979, 23, 11-24.

39 Skaper, S. D.; Buriani, A.; Dal Toso, R.; Petrelli, L.; Romanello, S.; Facci, L.; Leon, A. **The ALIAmide palmitoylethanolamide and cannabinoids, but not anandamide, are protective in a delayed post glutamate paradigm of excitotoxic death in cerebellar granule neurons.** *Proc. Natl. Acad. Sci. U. S. A.* 1996, 93, 3984-3989.

40 O' Sullivan, S. E.; Kendall, D. A. **Cannabinoid activation of peroxisome proliferator-activated receptors: potential for modulation of inflammatory disease.** *Immunobiology* 2010, 215, 611-616.

41 Lo Verme, J.; Fu, J.; Astarita, G.; La Rana, G.; Russo, R.; Calignano, A.; Piomelli, D. **The nuclear receptor peroxisome proliferator-activated receptor-alpha mediates the anti-inflammatory actions of palmitoylethanolamide**. *Mol. Pharmacol.* 2005, 67, 15-19.

42 Lo Verme, J.; La Rana, G.; Russo, R.; Calignano, A.; Piomelli, D. **The search for the palmitoylethanolamide receptor.** *Life Sci.* 2005, 77, 1685-1698.

43 Lo Verme, J.; Russo, R.; La Rana, G.; Fu, J.; Farthing, J.; Mattace-Raso, G.; Meli, R.; Hohmann, A.; Calignano, A.; Piomelli, D. **Rapid broad-spectrum analgesia through activation of peroxisome proliferator-activated receptor-alpha.** *J. Pharmacol. Exp. Ther.* 2006, 319, 1051-1061.

44 Pontis, S.; Ribeiro, A.; Sasso, O.; Piomelli, D. **Macrophage-derived lipid agonists of PPAR-α as intrinsic controllers of inflammation.** *Crit. Rev. Biochem. Mol. Biol.* 2016, 51, 7-14.

45 Zheng, B.; Liao, Z.; Locascio, J. J.; Lesniak, K. A.; Roderick, S. S.; Watt, M. L.; Eklund, A. C.; Zhang-James, Y.; Kim, P. D.; Hauser, M. A.; Grünblatt, E.; Moran, L. B.; Mandel, S. A.; Riederer, P.; Miller, R. M.; Federoff, H. J.; Wüllner, U.; Papapetropoulos, S.; Youdim, M. B.; Cantuti-Castelvetri, I.; Young, A. B.; Vance, J. M.; Davis, R. L.; Hedreen, J. C.; Adler, C. H.; Beach, T. G.; Graeber, M. B.; Middleton, F. A.; Rochet, J. C.; Scherzer, C. R. Global PD Gene Expression (GPEX) Consortium. **PGC-1α, a potential therapeutic target for early intervention in Parkinson's disease.** *Sci. Transl. Med.* 2010, 2, 52ra73.

46 Glass, C. K.; Ogawa S. **Combinatorial roles of nuclear receptors in inflammation and immunity.** *Nat Rev Immunol* 2006, 6 (1), 44-55.

47 Pointer, M. E.; Daynes R. A. **Peroxisome Proliferator-activated Receptor α Activation Modulates Cellular Redox Status, Represses Nuclear Factor-κB Signaling, and Reduces Inflammatory Cytokine Production in Aging.** *J. Biol. Chem.* 1998, 273 (49), 32833-32841.

48 Zhu, C.; Solorzano, C.; Sahar, S.; Realini, N.; Fung, E.; Sassone-Corsi, P.; Piomelli, D. **Proinflammatory stimuli control *N*-acylphosphatidylethanolamine-specific phospholipase-D expression in macrophages**. *Mol. Pharmacol.* 2011, 79, 786-792.

49 Korbecki, J.; Bajdak-Rusinek, K. **The effect of palmitic acid on inflammatory response in macrophages: an overview of molecular mechanisms.** *Inflamm. Res.* 2019, 68 (11), 915-932.

50 Ogura, Y.; Parsons, W. H.; Kamat, S. S.; Cravatt, B. F. **A calcium dependent acyltransferase that produces *N*-acyl phosphatidylethanolamines.** *Nat. Chem. Biol.* 2016, 12, 669-671.

51 Piomelli, D.; Sasso, O. **Peripheral gating of pain signals by endogenous lipid mediators.** *Nat. Neurosci.* 2014, 17, 164-174.

52 Okamoto, Y.; Morishita, J.; Tsuboi, K.; Tonai, T.; Ueda, N. **Molecular characterization of a phospholipase D generating anandamide and its congeners**. *J. Biol. Chem.* 2004, 279, 5298-5305.

53 Wang, J.; Okamoto, Y.; Morishita, J.; Tsuboi, K.; Miyatake, A.; Ueda, N. **Functional analysis of the purified anandamide-generating phospholipase D as a member of the metallo-beta-lactamase family.** *J. Biol. Chem.* 2006, 281, 12325-12335.

54 Tsuboi, K.; Uyama, T.; Okamoto, Y.; Ueda, N. **Endocannabinoids and related *N*-acylethanolamines: biological activities and metabolism.** *Inflammation Regener.* 2018, 38, 28.

55 Brannigan, J. A.; Dodson, G.; Duggleby, H. J.; Moody, P. C.; Smith, J. L.; Tomchick, D. R.; Murzin, A. G. **A protein catalytic framework with an *N*-terminal nucleophile is capable of self-activation.** *Nature* 1995, 378, 416-419.

56 Oinonen, C.; Rouvinen, J. **Structural comparison of Ntn hydrolases.** *Protein Sci.* 2000, 9, 2329-2337.

57 Gebai, A.; Gorelik, A.; Li, Z.; Illes, K.; Nagar, B. **Structural basis for the activation of acid ceramidase.** *Nat. Commun.* 2018, 9, 1621.

58 Tsuboi, K.; Sun, Y. X.; Okamoto, Y.; Araki, N.; Tonai, T.; Ueda, N. **Molecular characterization of *N*-acylethanolamine-hydrolyzing acid amidase, a novel member of the choloylglycine hydrolase family with structural and functional similarity to acid ceramidase.** *J. Biol. Chem.* 2005, 280, 11082-11092.

59 Gorelik, A.; Gebai, A.; Illes, K.; Piomelli, D.; Nagar, B. **Molecular mechanism of activation of the immunoregulatory amidase NAAA.** *Proc. Natl. Acad. Sci. U. S. A.* 2018, 115, E10032-E10040.

60 Sun, Y. X.; Tsuboi, K.; Zhao, L. Y.; Okamoto, Y.; Lambert, D. M.; Ueda, N. **Involvement of *N*-acylethanolamine-hydrolyzing acid amidase in the degradation of anandamide and other *N*-acylethanolamines in macrophages.** *Biochim. Biophys. Acta, Mol. Cell Biol. Lipids* 2005, 1736, 211-220.

61 Tsuboi, K.; Zhao, L. Y.; Okamoto, Y.; Araki, N.; Ueno, M.; Sakamoto, H.; Ueda, N. **Predominant expression of lysosomal *N*-acylethanolamine-hydrolyzing acid amidase in macrophages revealed by immunochemical studies.** *Biochim. Biophys. Acta, Mol. Cell Biol. Lipids* 2007, 1771, 623-632.

62 Mellman, I.; Fuchs, R.; Helenius, A. **Acidification of the endocytic and exocytic pathways.** *Annu. Rev. Biochem.* 1986, 55, 663-700.

63 Zhao, L. Y.; Tsuboi, K.; Okamoto, Y.; Nagahata, S.; Ueda, N. **Proteolytic activation and glycosylation of *N*-acylethanolamine-hydrolyzing acid amidase, a lysosomal enzyme involved in the endocannabinoid metabolism.** *Biochim. Biophys. Acta, Mol. Cell Biol. Lipids* 2007, 1771, 1397-1405.

[64] Piomelli, D.; Scalvini, L.; Fotio, Y.; Lodola, A.; Spadoni, G.; Tarzia, G.; Mor, M. ***N*-Acylethanolamine Acid Amidase (NAAA): Structure, Function, and Inhibition.** *J. Med. Chem.* 2020, 63, 7475-7490.

65 Tai, T.; Tsuboi, K.; Uyama, T.; Masuda, K.; Cravatt, B. F.; Houchi, H.; Ueda, N. **Endogenous molecules stimulating *N*-acylethanolamine-hydrolyzing acid amidase (NAAA).** *ACS Chem. Neurosci.* 2012, 3, 379-385.

66 Scalvini, S.; Ghidini, A.; Lodola, A.; Callegari, D.; Rivara, S.; Piomelli, D.; Mor, M. **N-Acylethanolamine Acid Amidase (NAAA): Mechanism of Palmitoylethanolamide Hydrolysis Revealed by Mechanistic Simulations.** *ACS Catal.* 2020, 10(20), 11797–11813.

67 Désarnaud, F.; Cadas, H.; Piomelli, D. **Anandamide amidohydrolase activity in rat brain microsomes. Identification and partial characterization.** *J. Biol. Chem.* 1995, 270, 6030-6035.

68 Ueda, N.; Kurahashi, Y.; Yamamoto, S.; Tokunaga, T. **Partial purification and characterization of the porcine brain enzyme hydrolyzing and synthesizing anandamide.** *J. Biol. Chem.* 1995, 270, 23823-23827.

69 Hillard, C. J.; Wilkison, D. M.; Edgemond, W. S.; Campbell, W. B. **Characterization of the kinetics and distribution of *N*-arachidonylethanolamine (anandamide) hydrolysis by rat brain.** *Biochim. Biophys. Acta, Lipids Lipid Metab*. 1995, 1257, 249-256.

70 Ueda, N.; Kurahashi, Y.; Yamamoto, S.; Tokunaga, T. **Partial purification and characterization of the porcine brain enzyme hydrolyzing and synthesizing anandamide**. *J. Biol. Chem.* 1995, 270, 23823–23827.

71 Kailash, R.; Tripathi, P. **A perspective review on fatty acid amide hydrolase (FAAH) inhibitors as potential therapeutic agents.** *Eur. J. Med. Chem.* 2020, 188, 111953.

72 Migliore, M.; Pontis, S.; Fuentes de Arriba, A. L.; Realini, N.; Torrente, E.; Armirotti, A.; Romeo, E.; Di Martino, S.; Russo, D.; Pizzirani, D.; Summa, M.; Lanfranco, M.; Ottonello, G.; Busquet, P.; Jung, K. M.; Garcia-Guzman, M.; Heim, R.; Scarpelli, R.; Piomelli, D. **Second-generation non-covalent NAAA inhibitors are protective in a model of multiple sclerosis.** *Angew. Chem. Int. Ed.* 2016, 55, 11193-11197.

73 Tsuboi, K.; Hilligsmann, C.; Vandevoorde, S.; Lambert, D. M.; Ueda, N. ***N*-Cyclohexanecarbonylpentadecylamine: a selective inhibitor of the acid amidase hydrolysing *N*-acylethanolamines, as a tool to distinguish acid amidase from fatty acid amide hydrolase.** *Biochem. J.* 2004, 379, 99-106.

74 Yamano, Y.; Tsuboi, K.; Hozaki, Y.; Takahashi, K.; Jin, X. H.; Ueda, N.; Wada, A. **Lipophilic amines as potent inhibitors of *N*-acylethanolamine-hydrolyzing acid amidase.** *Bioorg. Med. Chem.* 2012, 20, 3658-3665.

75 Saturnino, C.; Petrosino, S.; Ligresti, A.; Palladino, C.; De Martino, G.; Bisogno, T.; Di Marzo, V. **Synthesis and biological evaluation of new**

potential inhibitors of *N*-acylethanolamine hydrolyzing acid amidase. *Bioorg. Med. Chem. Lett.* 2010, 20, 1210-1213.

76 Vago, R.; Bettiga, A.; Salonia, A.; Ciuffreda, P.; Ottria, R. **Development of new inhibitors for *N*-acylethanolamine-hydrolyzing acid amidase as promising tool against bladder cancer.** *Bioorg. Med. Chem.* 2017, 25, 1242-1249.

77 Rossocha, M.; Schultz-Heienbrok, R.; von Moeller, H.; Coleman, J. P.; Saenger, W. **Conjugated bile acid hydrolase is a tetrameric N-terminal thiol hydrolase with specific recognition of its cholyl but not of its tauryl product.** *Biochemistry* 2005, 44, 5739–5748.

78 Solorzano, C.; Zhu, C.; Battista, N.; Astarita, G.; Lodola, A.; Rivara, S.; Mor, M.; Russo, R.; Maccarrone, M.; Antonietti, F.; Duranti, A.; Tontini, A.; Cuzzocrea, S.; Tarzia, G.; Piomelli, D. **Selective *N*-acylethanolamine-hydrolyzing acid amidase inhibition reveals a key role for endogenous palmitoylethanolamide in inflammation.** *Proc. Natl. Acad. Sci. U. S. A.* 2009, 106, 20966-20971.

79 Solorzano, C.; Antonietti, F.; Duranti, A.; Tontini, A.; Rivara, S.; Lodola, A.; Vacondio, F.; Tarzia, G.; Piomelli, D.; Mor, M. **Synthesis and structure-activity relationships of *N*-(2-oxo-3-oxetanyl)amides as *N*-acylethanolamine-hydrolyzing acid amidase inhibitors.** *J. Med. Chem.* 2010, 53, 5770-5781.

80 Greenspan, M. D.; Bull, H. G.; Yudkovitz, J. B.; Hanf, D. P.; Alberts, A. W. **Inhibition of 3-hydroxy-3-methylglutaryl-CoA synthase and cholesterol biosynthesis by beta-lactone inhibitors and binding of these inhibitors to the enzyme.** *Biochem. J.* 1993, 289, 889-895.

81 Lall, M. S.; Karvellas, C.; Vederas, J. C. **Beta-lactones as a new class of cysteine proteinase inhibitors: inhibition of hepatitis A virus 3C proteinase by *N*-Cbz-serine beta-lactone.** *Org. Lett.* 1999, 1, 803-806.

82 Pojer, F.; Ferrer, J. L.; Richard, S. B.; Nagegowda, D. A.; Chye, M. L.; Bach, T. J.; Noel, J. P. **Structural basis for the design of potent and species-specific inhibitors of 3-hydroxy-3-methylglutaryl CoA synthases.** *Proc. Natl. Acad. Sci. U. S. A*. 2006, 103, 11491-11496.

83 Armirotti, A.; Romeo, E.; Ponzano, S.; Mengatto, L.; Dionisi, M.; Karacsonyi, C.; Bertozzi, F.; Garau, G.; Tarozzo, G.; Reggiani, A.; Bandiera, T.; Tarzia, G.; Mor, M.; Piomelli, D. **β-Lactones inhibit *N*-acylethanolamine acid amidase by S-acylation of the catalytic *N*-terminal cysteine.** *ACS Med. Chem. Lett*. 2012, 3, 422-426.

84 Duranti, A.; Tontini, A.; Antonietti, F.; Vacondio, F.; Fioni, A.; Silva, C.; Lodola, A.; Rivara, S.; Solorzano, C.; Piomelli, D.; Tarzia, G.; Mor, M. ***N*-(2-Oxo-3-oxetanyl)carbamic acid esters as *N*-acylethanolamine acid amidase inhibitors: synthesis and structure-activity and structure-property relationships.** *J. Med. Chem.* 2012, 55, 4824-4836.

85 Ponzano, S.; Bertozzi, F.; Mengatto, L.; Dionisi, M.; Armirotti, A.; Romeo, E.; Berteotti, A.; Fiorelli, C.; Tarozzo, G.; Reggiani, A.; Duranti, A.; Tarzia, G.; Mor, M.; Cavalli, A.; Piomelli, D.; Bandiera, T. **Synthesis and structure-activity relationship (SAR) of 2-methyl-4-oxo-3-oxetanylcarbamic acid esters, a class of potent *N*-acylethanolamine acid amidase (NAAA) inhibitors.** *J. Med. Chem.* 2013, 56, 6917-6934.

86 Khasabova, I. A.; Xiong, Y.; Coicou, L. G.; Piomelli, D.; Seybold, V. **Peroxisome proliferator-activated receptor α mediates acute effects of palmitoylethanolamide on sensory neurons.** *J. Neurosci.* 2012, 32, 12735-12743.

87 Sasso, O.; Moreno-Sanz, G.; Martucci, C.; Realini, N.; Dionisi, M.; Mengatto, L.; Duranti, A.; Tarozzo, G.; Tarzia, G.; Mor, M.; Bertorelli, R.; Reggiani, A.; Piomelli, D. **Antinociceptive effects of the *N*-acylethanolamine acid amidase inhibitor ARN077 in rodent pain models.** *Pain* 2013, 154, 350-360.

88 Sasso, O.; Summa, M.; Armirotti, A.; Pontis, S.; De Mei, C.; Piomelli, D. **The *N*-acylethanolamine acid amidase inhibitor ARN077 suppresses inflammation and pruritus in a mouse model of allergic dermatitis.** *J. Invest. Dermatol.* 2018, 138, 562-569.

89 Fiasella, A.; Nuzzi, A.; Summa, M.; Armirotti, A.; Tarozzo, G.; Tarzia, G.; Mor, M.; Bertozzi, F.; Bandiera, T.; Piomelli, D. **3-Aminoazetidin-2-one derivatives as *N*-acylethanolamine acid amidase (NAAA) inhibitors suitable for systemic administration.** *ChemMed-Chem* 2014, 9, 1602-1614.

90 Ribeiro, A.; Pontis, S.; Mengatto, L.; Armirotti, A.; Chiurchiù, V.; Capurro, V.; Fiasella, A.; Nuzzi, A.; Romeo, E.; Moreno-Sanz, G.; Maccarrone, M.; Reggiani, A.; Tarzia, G.; Mor, M.; Bertozzi, F.; Bandiera, T.; Piomelli, D. **A potent systemically active *N*-acylethanolamine acid amidase inhibitor that suppresses inflammation and human macrophage activation.** *ACS Chem. Biol.* 2015, 10, 1838-1846.

91 Nuzzi, A.; Fiasella, A.; Ortega, J. A.; Pagliuca, C.; Ponzano, S.; Pizzirani, D.; Bertozzi, S. M.; Ottonello, G.; Tarozzo, G.; Reggiani, A.; Bandiera, T.; Bertozzi, F.; Piomelli, D. **Potent α-amino-β-lactam carbamic acid ester as NAAA inhibitors. Synthesis and structure-activity relationship (SAR) studies.** *Eur. J. Med. Chem.* 2016, 111, 138-159.

92 Petracca, R.; Ponzano, S.; Bertozzi, S. M.; Sasso, O.; Piomelli, D.; Bandiera, T.; Bertozzi, F. **Progress in the development of β-lactams as *N*-acylethanolamine acid amidase (NAAA) inhibitors: synthesis and SAR study of new, potent *N*-O-substituted derivatives.** *Eur. J. Med. Chem.* 2017, 126, 561-575.

93 Romeo, E.; Ponzano, S.; Armirotti, A.; Summa, M.; Bertozzi, F.; Garau, G.; Bandiera, T.; Piomelli, D. **Activity-based probe for *N*-acylethanolamine acid amidase.** *ACS Chem. Biol.* 2015, 10, 2057-2064.

94 Romeo, E.; Pontis, S.; Ponzano, S.; Bonezzi, F.; Migliore, M.; Di Martino, S.; Summa, M.; Piomelli, D. **Preparation and in vivo use of an activity-based**

probe for -acylethanolamine acid amidase. *J. Visualized Exp.* 2016, 117, e54652.

95 Bottemanne, P.; Muccioli, G. G.; Alhouayek, M. ***N*-acylethanolamine hydrolyzing acid amidase inhibition: tools and potential therapeutic opportunities.** *Drug Discovery Today* 2018, 23, 1520-1529.

96 Alhouayek, M.; Bottemanne, P.; Subramanian, K. V.; Lambert, D. M.; Makriyannis, A.; Cani, P. D.; Muccioli, G. G. ***N*-Acylethanolamine-hydrolyzing acid amidase inhibition increases colon *N*-palmitoylethanolamine levels and counteracts murine colitis.** *FASEB J.* 2015, 29, 650-661.

97 Falgueyret, J. P.; Oballa, R. M.; Okamoto, O.; Wesolowski, G.; Aubin, Y.; Rydzewski, R. M.; Prasit, P.; Riendeau, D.; Rodan, S. B.; Percival, M. D. **Novel, nonpeptidic cyanamides as potent and reversible inhibitors of human cathepsins K and L.** *J. Med. Chem.* 2001, 44, 94-104.

98 Malamas, M.; Makriyannis, A.; Subramian, K. V.; Whitten, K. M. ***N*-Acylethanolamine Hydrolyzing Acid Amidase (NAAA) Inhibitors and Their Use Thereof.** *WO2015179190A1*, 2015.

99 Malamas, M. S.; Farah, S. I.; Lamani, M.; Pelekoudas, D. N.; Perry, N. T.; Rajarshi, G.; Miyabe, C. Y.; Chandrashekhar, H.; West, J.; Pavlopoulos, S.; Makriyannis, A. **Design and synthesis of cyanamides as potent and selective *N*-acylethanolamine acid amidase inhibitors.** *Bioorg. Med. Chem.* 2020, 28, 115195.

100 Zhou, P.; Xiang, L.; Yang, Y.; Wu, Y.; Hu, T.; Liu, X.; Lin, F.; Xiu, Y.; Wu, K.; Lu, C.; Ren, J.; Qiu, Y.; Li, Y. ***N*-Acylethanolamine acid amidase (NAAA) inhibitor F215 as a novel therapeutic agent for osteoarthritis.** *Pharmacol. Res.* 2019, 145, 104264.

101 Yang, L.; Li, L.; Chen, L.; Li, Y.; Chen, H.; Li, Y.; Ji, G.; Lin, D.; Liu, Z.; Qiu, Y. **Potential analgesic effects of a novel *N*-acylethanolamine acid amidase inhibitor F96 through PPAR-α.** *Sci. Rep.* 2015, 5, 13565.

102 Petrosino, S.; Ahmad, A.; Marcolongo, G.; Esposito, E.; Allarà, M.; Verde, R.; Cuzzocrea, S.; Di Marzo, V. **Diacerein is a potent and selective inhibitor of palmitoylethanolamide inactivation with analgesic activity in a rat model of acute inflammatory pain.** *Pharmacol. Res.* 2015, 91, 9-14.

103 Bertozzi, F.; Bandiera, T. **Modulation of *N*-Acylethanolamine-Hydrolysing Acid Amidase (NAAA) for Disease Treatment.** *US20190135802A1*, 2019.

104 Pontis, S.; Palese, F.; Summa, M; Realini, N.; Lanfranco, M.; De Mei, C.; Piomelli, D. ***N*-Acylethanolamine Acid Amidase contributes to disease progression in a mouse model of multiple sclerosis.** *Pharmacol. Res.* 2020, 160, 105064.

105 Jonas, J. B.; Aung, T.; Bourne, R. R.; Bron, A. M.; Ritch, R.; PandaJonas, S. **Glaucoma.** *Lancet* 2017, 390, 2183−2193

106 Dikopf, M. S.; Vajaranant, T. S.; Edward, D. P. **Topical treatment of glaucoma: established and emerging pharmacology.** *Expert Opin. Pharmacother.* 2017, 18, 885−898.

107 Hollo, G.; Topouzis, F.; Fechtner, R. D. **Fixed combination intraocular pressure-lowering therapy for glaucoma and ocular hypertension: advantages in clinical practice.** *Expert Opin. Pharmacother.* 2014, 15, 1737−1747.

108 Samples, J. R.; Krause, G.; Lewy, A. J. **Effect of melatonin on intraocular pressure.** *Curr. Eye Res.* 1988, 7, 649−653.

109 Crooke, A.; Colligris, B.; Pintor, J. **Update in glaucoma medicinal chemistry: emerging evidence for the importance of melatonin analogues.** *Curr. Med. Chem.* 2012, 19, 3508−3522.

110 Jockers, R.; Delagrange, P.; Dubocovich, M. L.; Markus, R. P.; Renault, N.; Tosini, G.; Cecon, E.; Zlotos, D. P. **Update on melatonin receptors: IUPHAR review 20.** *Br. J. Pharmacol.* 2016, 173, 2702−2725.

111 Zlotos, D. P.; Jockers, R.; Cecon, E.; Rivara, S.; Witt-Enderby, P. A. **MT1 and MT2 melatonin receptors: ligands, models, oligomers, and therapeutic potential.** *J. Med. Chem.* 2014, 57, 3161−3185.

112 Alarma-Estrany, P.; Pintor, J. **Melatonin receptors in the eye: location, second messengers and role in ocular physiology.** *Pharmacol. Ther.* 2007, 113, 507−522.

113 Martínez-Á guila, A.; Fonseca, B.; Perez de Lara, M. J.; Pintor, J. **Effect of melatonin and 5-methoxycarbonylamino-N-acetyltryptamine on the intraocular pressure of normal and glaucomatous mice.** *J. Pharmacol. Exp. Ther.* 2016, 357, 293−299.

114 Alarma-Estrany, P.; Crooke, A.; Mediero, A.; Pelaez, T.; Pintor, J. **Sympathetic nervous system modulates the ocular hypotensive action of MT2-melatonin receptors in normotensive rabbits.** *J. Pineal Res.* 2008, 45, 468−475.

115 Serle, J. B.; Wang, R. F.; Peterson, W. M.; Plourde, R.; Yerxa, B. R. **Effect of 5-MCA-NAT, a putative melatonin MT3 receptor agonist, on intraocular pressure in glaucomatous monkey eyes.** *J. Glaucoma* 2004, 13, 385−388.

116 Ismail, S. A.; Mowafi, H. A. **Melatonin provides anxiolysis, enhances analgesia, decreases intraocular pressure, and promotes better operating conditions during cataract surgery under topical anesthesia.** *Anesth. Analg.* 2009, 108, 1146−1151.

117 Crooke, A.; Huete-Toral, F.; Martínez-Á guila, A.; Martín-Gil, A.; Pintor, J. **Melatonin and its analog 5-methoxycarbonylamino-Nacetyltryptamine potentiate adrenergic receptor-mediated ocular hypotensive effects in rabbits: significance for combination therapy in glaucoma.** *J. Pharmacol. Exp. Ther.* 2013, 346, 138−145.

118 Martínez-Á guila, A.; Fonseca, B.; Bergua, A.; Pintor, J. **Melatonin analogue agomelatine reduces rabbit's intraocular pressure in**

normotensive and hypertensive conditions. *Eur. J. Pharmacol.* 2013, 701, 213−217.

119 Hepler, R. S.; Frank, I. R. **Marihuana smoking and intraocular pressure.** *JAMA* 1971, 217, 1392−1392.

120 Porcella, A.; Maxia, C.; Gessa, G. L.; Pani, L. **The synthetic cannabinoid WIN55212−2 decreases the intraocular pressure in human glaucoma resistant to conventional therapies.** *Eur. J. Neurosci.* 2001, 13, 409−412.

121 Panahi, Y.; Manayi, A.; Nikan, M.; Vazirian, M. **The arguments for and against cannabinoids application in glaucomatous retinopathy.** *Biomed. Pharmacother.* 2017, 86, 620−627.

122 Laine, K.; Jarvinen, K.; Pate, D. W.; Urtti, A.; Jarvinen, T. **Effect of the enzyme inhibitor, phenylmethylsulfonyl fluoride, on the IOP profiles of topical anandamides.** *Invest. Ophthalmol. Vis. Sci.* 2002, 43, 393−397.

123 Cairns, E. A.; Baldridge, W. H.; Kelly, M. E. M. **The endocannabinoid system as a therapeutic target in glaucoma.** *Neural Plast.* 2016, 2016, 9364091.

124 Piomelli, D. **The molecular logic of endocannabinoid signaling**. *Nat. Rev. Neurosci.* 2003, 4, 873−884.

125 Labar, G.; Michaux, C. **Fatty acid amide hydrolase: from characterization to therapeutics.** *Chem. Biodiversity* 2007, 4, 1882−1902.

126 Miller, S.; Leishman, E.; Oehler, O.; Daily, L.; Murataeva, N.; Wager-Miller, J.; Bradshaw, H.; Straiker, A. **Evidence for a GPR18 role in diurnal regulation of intraocular pressure.** *Invest. Ophthalmol. Visual Sci.* 2016, 57, 6419−6426.

127 Spadoni, G.; Bedini, A.; Furiassi, L.; Mari, M.; Mor, M., Scalvini, L.; Lodola, A.; Ghidini, A.; Lucini, V.; Dugnani, S.; Scaglione, F.; Piomelli, D.; Jung, K. M.; Supuran, C. T.; Lucarini, L.; Durante, M.; Sgambellone, S.; Masini, E.; Rivara

S. **Identification of Bivalent Ligands with Melatonin Receptor Agonist and Fatty Acid Amide Hydrolase (FAAH) Inhibitory Activity That Exhibit Ocular Hypotensive Effect in the Rabbit.** *J. Med. Chem.* 2018, 61, 7902–7916

128 Nucci, C.; Bari, M.; Spano, A.; Corasaniti, M.; Bagetta, G.; Maccarrone, M.; Morrone, L. A. **Potential roles of (endo)cannabinoids in the treatment of glaucoma: from intraocular pressure control to neuroprotection.** *Prog. Brain Res.* 2008, 173, 451−464.